**Proceeding of conference
"Development of the Science, Technologies and Techniques
for the Manufacture, Packaging, Storage and Distribution
of Foods"**

CONTENS

ACTIVE PACKAGING IN FOOD AND PHARMACEUTICAL INDUSTRY

V. G. Lasheva, S.A. Kotlarova

University of Chemical Technology and Metallurgy

Abstract: *Packages with active materials are packages with intentionally embedded components that would release or absorb substances into / or packaged products or their environment.*
Packages with active materials are developed with the goal of extending shelf life for food and increasing the period of time that the food is high quality.
Bulgarian producers to be competitive in the European market, one way of this is to bet on active packaging, which can extend shelf life, maintain or improve the quality of packaging materials.
From essential in the production of active packaging is to design functional materials that contain the active ingredient in its structure, which to act or to be released in a controlled manner.

Keywords: packaging, packages with active materials, food and pharmaceutical industry, nanotechnology

I. Introduction

Although traditional packaging covers the basic needs of food containment, society is becoming increasingly complex and innovative packaging is the result of consumers' demand for packaging that is more advanced and creative than what is currently offered. Active packaging and intelligent packaging are the result of innovating thinking in packaging. Active packaging is an extension of the protection function of a package and is common loused to protect against oxygen and moisture. Intelligent packaging can be defined as "packaging that contains an external or internal indicator to provide information about aspects of the history of package and/or the quality of the food". Intelligent packaging is an extension of the communication function of traditional packaging [1].

Bulgarian producers to be competitive in the European market, one way of this is to bet on active packaging, which can extend shelf life, maintain or improve the quality of packaging materials.

The packages with active materials are packages with intentionally embedded components that would release or absorb substances into / or packaged products or their environment.

Active Packaging: Packaging Gets Active

The definitions set out in the Ordinance 1935/2004/ EU and in the Ordinance450/2009/EU had considered active materials and manufactures such as "materials and products", which are intended to extend the shelf life, but also for maintaining or improving condition of packaged food" [2].

Active packaging systems are developed with the goal of extending shelf life for foods and increasing the period of time that the food is high quality. Active packaging technologies include some physical, chemical, or biological action which changes interactions between a package, product, and/or headspace of the package in order to get a desired outcome [3]. The most common active systems scavenge Oxygen from the package or the product and Mayeven be activated by an outside source Such as UV light. Active packaging typically is founding two types of systems; sachets and Pads which are placed inside of packages, and active ingredients that are incorporated directly into packaging materials [4].

II. Application of active packaging in the chemical and pharmaceutical industry

Market expansion by pharmaceutical products is forcing manufacturers to seek competitive and innovative packaging materials, which are compared and innovative materials, to more informed consumers in nowadays.

Most important in this type of industry is a characteristics of the pharmaceutical product. For example, should take into account whether it is sensitive to light or moisture [5].

Primary packaging (packaging that located close to the pharmaceutical product) is a subject to strict control. The productive process of the package should be carried out in clean rooms and controlled temperature and humidity. Furthermore, there must be built and functioning system of

quality control at every stage of the process. For each packing material must be available specification that contains the following elements: description of the packaging material, indication sampling, requirement for acceptance limit, storage conditions, transport packaging and labeling [6].

Actavis Bulgaria e part of the global Actavis Inc. Actavis is the highest selling pharmaceutical company in Bulgaria. In the factory they make tests for the medicinal product Atsefein tablets in a new kind of packaging material - Formpack foil OPA /Aluminium/ PE + Desiccant, company Amcor Flexible Sigen GmbH.

The film is a many layer, supply, resistant to moisture, untransparent with metallic color on the outside, blue colored polish with polyethylene and desiccant inside.

Desiccant: $CaO + H_2O \rightarrow Ca(OH)_2$
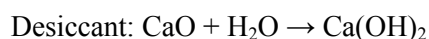
The foil exhibits resistance to heat and capacity is independent of the level of humidity.
Polyethylene (PE) and the drying layer are joined by a coextrusion.
CaO and PE are encased in full mineral desiccant – PE (main batch). The main batch was coated in aluminum foil by co-extrusion.
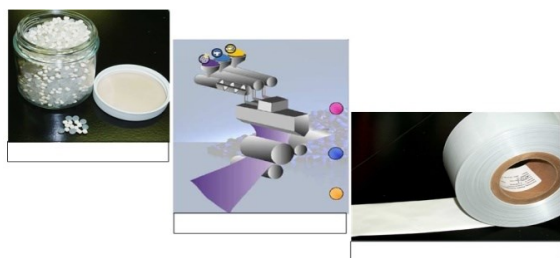
PE + CaO   Coextrusion   Coated Al foil

Figure1. *Coextrusion of the PE and desiccant*

PA	25μm
Adh.+Primer	5.1g
Al soft	45μm
Primer	1g
HDPE	3g
PE+CaO 50%	38g
HDPE	9g
PA	25μm
Adh.+Primer	5.1g
Al soft	45μm
Primer	1g
HDPE	3g
PE+CaO 50%	38g
HDPE	9g
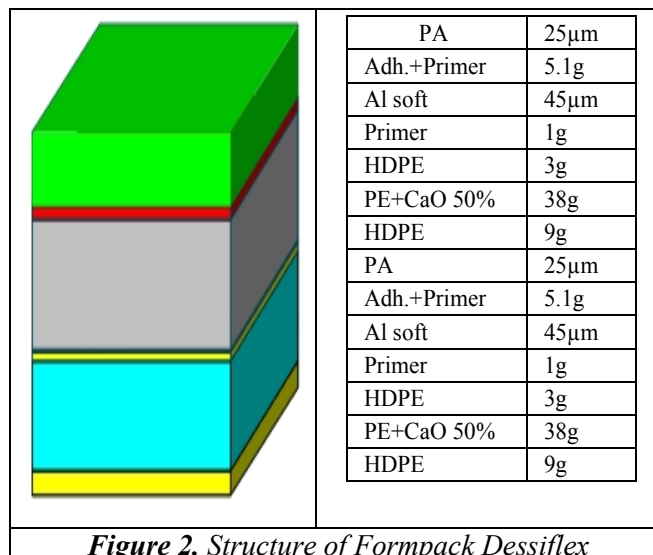
Figure 2. *Structure of Formpack Dessiflex*

Polyethylene sealing layer is multi-layer to: improve the ability of forming, allow better storage, avoid direct contact of the product with the layer that contains the color of a pigments and a drying part and to arrange a high-power adhesion.

The advantage of the foil is the following:

✓ eliminates the need of separate bag for desiccant or agent;
✓ reducing package size and simplifies the packaging process;
✓ desiccant is located near the product, but desiccant is not in direct contact to it;
✓ each separate unit is an individually protected;
✓ the shelf life of the product can be extended [7].

III. Application of nanotechnology in packaging materials

Nano packaging have the greatest application in the food products, the baked goods and the meat products. Nano packaging dominates in sectors of sodas and bottled water at liquid foods. Today, commercial applications of the nano packaging is apply at oxygen absorbers in packages with sliced meat, ready-to-eat meats and beer.

The part of the dehumidifier in fresh meat and fish are made of nanomaterials. They are also used for the capture of the molecules of the ethylene in the packaging of fruit and vegetables [8].

The silver nanoparticles are another type of this technology. Silver has known with its antibacterial properties.

In its modern form, silver nanoparticles have become in a promising antimicrobial materials with a variety of applications, because they can disrupt the bacterial cells by destroying enzymes of the food.

Researchers from the Institute of Nanotechnology and Advanced Materials at the University of Bar-Ilan in Israel have reported the development of a new method for the infliction of silver nanoparticles on paper by using a sonochemical technology [9].

The new method uses ultrasound or high frequency sound waves, which secure the particles to the paper. The sheet was immersed in a solution. Solution contains colloidal silver, and then the sheet is treated with ultrasound. As a result, the paper prepared erasable layer of silver. As a result, the paper has prepared erasable layer of silver [10].

Antimicrobial films have the potential to extend the shelf life of some foods and they can also provide an additional advantage for food safety in a certain circumstances [9].

IV. Conclusions

Active packaging systems are developed with the goal of extending shelf life for foods and increasing the period of time that the food is high quality.

Active materials and products, which are in contact with the product, are defined as materials and products. They are intended to extend shelf life, maintain or improve the quality of packaging materials, and in some cases to improve the state of the packaged product.

Active materials contains intentionally embedded components that could release or absorb substances into / or from packaged products or from the environment which they are placed.

The main advantage of active packaging consists in the fact that additives in packaging or packaging material does not lead to changes of food or pharmaceutical products.

Nanotechnology offers enormous opportunities for development that are associated with the packaging of foods which can benefit the both consumers and industry.

Silver nanoparticles can be used in the packing material which can be a promising way to improve the quality of the package.

V. References

1. Anonymous, *Smart packaging: coming a store near you. Food Engineering & Ingredients.* 2007, 32:20, 2.
2. *"*Packages with active materials*", The Package Printing Converting Magazine*,2007,4, pp 35-39.
3. Иванова В., Бенчева С., Тодорова Д., *Ръководство по химия, технология и свойства на хартията.* (2009).
4. De Jong A., Boumans, H., Slaghek, T., Van Veen, J., Rijk, R. and Van Zandvoort, M., *Active and intelligent packaging for food: is it the future?. Food Additives & Contaminants*,2005 Part A.,22,975-979.
5. A.Brody, Packeges become more active and more intelligent,58, 2004, № 1.
6. Technical Specifications – Actavis.
7. Company documentation of Amcor.
8. Crumnikal M., Lius J., *Perspectives in nanotechnology*, John Wallace and Sons, 1992
9. Gottesman R., et al, "*Sonochemical coating of paper by microbicidal silver nanoparticles*, Langmuir 2011, 27(2), 720-726.
10. Boeva R.-Spiridonova, E. Petkova, N. Georgieva, L. Yotova, I. Spiridonov, "*Utilization of a chemical-mechanical pulp with improved properties from poplar wood in the composition of packing papers*", BioResources, 2007,2(1), pp. 34 –40.

ADIABATIC DYNAMINA OF COOLING MASHING THROUGH CREATION OF VACUUM IN THE FERMENTATION APPARATUS

O.O. Boiko, V.A. Piddubnyi, A. O. Chagayda

Department of Technical Mechanics and Packaging Machinery, National University of Food Technologies, 68 Volodymyrska str., 01601, Kyiv, Ukraine, e-mail: boikooo@gmail.com

Abstract. *The use of technology for reducing pressure in fermentation of carbonaceous material enables partially remove ethanol from the material flow, simultaneously adiabatic cooling mashing in fermentation unit. The intensity of these processes with respect to the mashing almost unexplored .*

The content of water vapor and ethanol vapor in the gas-steam phase that is removed from the fermentation medium depends on the pressure above the phase separation in the machine. Theoretical calculations show that the dependence of this process on the pressure, are missed. In trials carried calculation of gas-steamed bubbles formed in the bulk material flow, the total surface area of the bubbles and the intensity of heat and mass transfer on the surface mass transfer. Determination of these parameters is important in the development of devices for removing alcohol from the mash by adiabatic boiling.

Key Words: adiabatic cooling mashing, alcohol, carbon dioxide, fermentation

I. Introduction

Transformation of the material flow of sugar as part of the solution corresponding to equation Gay-Lussac, and they are the result of the transformation of life of yeast. Thus one mole of glucose (180 g) with fermentation produced 92 g of ethanol and 88 g of CO_2. The accumulation of carbon dioxide in solution occurs to a certain limit , which corresponds to the solubility of the gas in the wort at a certain pressure. Formed during alcoholic fermentation gas after reaching this limit stands wort.

The lifetime occurrence of gas bubbles to hit at up-liquid space should be divided into two periods. First period - an increase of bubbles on the surface where it originated. It is characterized by a gradual increase in its size at the site of formation. Second period - the ascent, which is characterized by the growth of the bubble by reducing the hydrostatic pressure in the fluid surrounding the gas bubble.

After the occurrence of gas bubble grows in size due to its diffusion of dissolved gases, and evaporation of the liquid phase volume . After reaching a critical size bubble breaks away from the surface on which it arose, and expires and is removed from the solution at up-liquid space.

When surfacing vapor- gas bubbles in the bulk liquid in the bubble volume evaporates molecules of ethanol, water and diffusion of molecules of carbon dioxide. To determine amount of these substances and the end of the size it is necessary to determine the surface area and mass transfer while the process.

II. Materials and methods

During the study used mathematical modeling techniques and general physical laws (Mendeleev - Clapeyron law, Gay-Lussac, Henry and others). Among the generalizations and assumptions used are as follows : all gas-steamed bubbles appear on the surface of solid particles and the walls of the container, the number of bubbles formed directly proportional to the concentration of simple hydrocarbons per unit volume, gas-steamed bubble when surfacing is spherical.

Temperature indicators in fermentation processes relating to both microbiological, physical and chemical effects. They may be such that the optimal approach to the processes best stabilize the temperature by cooling the environment and in accordance with the law of Van-Hoff influencing osmotic pressure, reflected by:

$$\pi = cRT,$$

(1)

where: c - molyalnist solution; R - universal gas constant; T - absolute temperature environment.

III. Results and discussion

Features of steam bubbles at lower pressure in the fermentation unit. The initial stage of the formation of gas bubbles can be characterized by two parameters: the number of embryos created and the minimum radius.

The number of embryos bubbles N^1, which is formed in a unit volume of fluid can be determined from the equation, derived by Russian scientist Zeldovich [1]:

$$N^1 = \frac{bK_D}{R_{\min}^4} \left(\frac{8\pi\sigma_{l-g}}{kT} \right)^{1/2},$$

(2)

where b - coefficient of proportionality, taking into account the properties of the liquid; K_D - analog diffusion coefficient; Rmin - minimum radius of the gas bubble; σ_{l-g} - surface tension at the interface liquid-gas; k - Boltzmann constant; T - absolute temperature.

Total number of embryos bubbles N, which is formed in the volume of mashing, provided equal distribution centers of blistering:

$$N = V N^1 = \frac{b V K_D}{R_{min}^4} \left(\frac{8\pi\sigma_{l-g}}{kT} \right)^{\frac{1}{2}}, \qquad (3)$$

where: V - volume of mashing that is in the fermentation unit.

Critical bubble radius R_{min} can be defined by the equation formulated by Frenkel and Klassen [1]:

$$R_{min} = \frac{2\sigma_{l-g}}{k\Delta C}, \qquad (4)$$

where: σ_{l-g} - surface tension at the interface liquid-gas; k - constant of Henry; ΔC - supersaturation of the solution gas.

In the fermentation of yeast sugar substitute hydrocarbon saturation mash the gas phase is a result of carbon dioxide as a byproduct of alcoholic fermentation. Supersaturation mashing carbon dioxide, the infinitesimal time interval can be considered equal to the amount of carbon dioxide that the yeast will allocate for that period of time in a single volume of liquid

$$\Delta C = \frac{\partial Q_{CO_2}}{V \partial \tau}, \qquad (5)$$

where: ∂Q_{CO_2} - the amount of carbon dioxide that would release at the time $\partial \tau$.

Analyzing formula (3) - (5) we can conclude that the pressure drop at up-liquid space would reduce the number of bubbles generated per unit volume of fluid.

Changing the radius of the gas bubble is due to saturation of its internal space with carbon dioxide, water vapor and alcohol. Accordingly, while the existence of bubbles on the surface will depend on the intensity of the process of fermentation and its density. After reaching a critical diameter of the vapor bubble is its separation from the surface and surfacing.

The diameter of the gas bubbles at the time of separation from the surface on which it occurred can be determined by the following relationship:

$$D_n = 0,018\theta \left(\frac{\sigma_{l-g}}{\rho_l - \rho_g} \right)^{\frac{1}{2}}, \qquad (6)$$

where: θ - angle boundary between the bubble and the surface heating. For steel tanks and dense environment, this setting will be between 35-40 º (0,611-0,698 rad); ρ_r - density solution (mashing); ρ_r - density of the gas phase.

At the stage of the gas bubbles density gas phase should take the density of carbon dioxide at the appropriate pressure. In the future, when the density of the gas phase will have a mean density of a mixture of carbon dioxide vapors of ethanol and water relevant concentrations.

In finding the average radius of the gas bubbles R_{avr} will use the assumption that the intensity of growth does not change over time. Under this assumption R_{avr} can be defined by the formula:

$$R_{avr} = \frac{R_{min} + 0,5 D_n}{2} = \frac{\sigma_{l-g}}{k\Delta C} + 0,009\theta \left(\frac{\sigma_{l-g}}{\rho_l - \rho_g} \right)^{\frac{1}{2}}. \qquad (7)$$

By reducing the pressure in the fermentation apparatus solubility of carbon dioxide is directly proportional to the decrease. From (4) it is evident that it would reduce the average radius of the bubble. At the same time, a reduction in pressure by the formula (6) does not lead to a change in the diameter of the bubble , which is separated from the surface on which it originated. This suggests that the pressure drop at up-liquid space will increase the lifetime of the gas bubbles. This, in turn, suggesting an increase in the concentration of ethanol in the gas space bubbles by increasing the time course of the evaporation process.

The change in the diameter of the bubbles surfacing. When surfacing gas bubble begins to increase its capacity by reducing the hydrostatic pressure of the fluid that surrounds it. Under the law Mendeleev - Clapeyron product of gas pressure

on him in the middle of the bubble volume at constant temperature is constant, and when the volume of gas bubbles surfacing it will increase by addiction

$$V_{bubl}^{pr} P_{bubl}^{pr} = V_n P_n, \qquad (8)$$

where: V_n and P_n - volume and excessive pressure in the gas bubble at the time of separation from the surface where it originated.

The pressure in the middle of the gas bubbles can be determined by dependence:

$$P_{bubl} = P_{out} + \frac{2\sigma_{l-g}}{R_{bubl}}, \qquad (9)$$

where: $P_{зовн}$ - outside overpressure gas bubbles.

After determining the amount of bubbles through its radius formula (6), and the pressure in it according to equation (9) we have:

$$\frac{4}{3}\pi R_{bubl}^3\left(P_{out}+\frac{2\sigma_{l-g}}{R_{bubl}}\right)=\frac{4}{3}\pi\left(0,5D_n\right)^3\left(\rho g h_f+\frac{2\sigma_{l-g}}{0,5D_n}\right), \qquad (10)$$

$$P_{out}R_{bubl}^2+2\sigma_{l-g}R_{bubl}^2=0,125D_n^3\left(\rho g h_f+\frac{4\sigma_{l-g}}{D_n}\right), \qquad (11)$$

where: h_f - the depth at which gas bubbles formed; ρ - density of the mashing.

From equation (11) we can determine the radius of the bubble at the moment of achieving surface. At this point $P_{out}=0$, because we have:

$$R_{bubl}=\sqrt{\frac{0,125D_n^3\left(\rho g h_f+\frac{4\sigma_{l-g}}{D_n}\right)}{2\sigma_{l-g}}}. \qquad (12)$$

Assuming a uniform distribution centers of blistering by volume capacity mean radius of bubbles during ascent, will be:

$$R_{bubl}=\sqrt{\frac{0,0625D_n^3\left(0,5\rho g H_{mash}+\frac{4\sigma_{l-g}}{D_n}\right)}{\sigma_{l-g}}}, \qquad (13)$$

where: H_{mash} - the mashing level in reservoir .

Rate of rise of gas bubbles in an infinite volume of liquid. After tearing off the gas bubbles from the surface, it begins to run . Time floating bubbles will depend on the depth of its occurrence H_{mash} and rate of ascent v_∞. According to formula (5) the number of gas bubbles formed is inversely proportional to the solution supersaturation of carbon dioxide. At first sight this great can be considered equivalent to the intensity of hydrocarbon fermentation yeast cells. If mixing

mashing in the fermentation apparatus in accordance with the intensity can be considered as the last value uniformly distributed throughout the volume of the container.

Speed floating bubbles will grow indefinitely, but only to a certain limit - the maximum speed of bubbles floating separate v_∞. From the literature it is known that to achieve this speed will occur immediately, so we can assume that the rate of ascent v_∞ does not depend on time, but only on the geometrical parameters of the bubbles and physics-chemical parameters of the environment. The dependence of v_∞ on the physical and mechanical properties of the liquid has been experimentally confirmed by another American physicist Peebles and German chemist Haber. Thus, it can be quite accurately described by the equation derived Stokes virgin soil. This equation can be written as following:

$$v_\infty=\frac{1}{18}\frac{D_n^2 g(\rho_g-\rho_l)}{\mu_f}, \qquad (14)$$

where: D_n - the diameter of the gas bubbles at the time of separation from the surface where it originated; μ_f - viscosity of the wort.

Due to the formula (6) we see that the value of a single bubble velocity v_∞ has the form:

$$v_\infty=\frac{1}{18}\frac{\left(0,018\theta\left(\frac{\sigma_{l-g}}{\rho_l-\rho_g}\right)^{1/2}\right)^2 g(\rho_l-\rho_g)}{\mu_f}=1,8\cdot10^{-5}\frac{\theta^2\sigma_{l-g}g}{\mu_f}. \qquad (15)$$

Taking an average depth of occurrence of bubbles - half of the mashing in the office, while surfacing will be:

$$\tau_{fl}=\frac{0,5H_{mash}}{v_\infty}=\frac{0,9\cdot10^5 H_{mash}\mu_f}{\theta^2\sigma_{l-g}g}. \qquad (16)$$

The number of bubbles that float:

$$N_{fl}=\frac{NV_{ap}}{\tau_{fl}}=\frac{\frac{bV^2K_D}{R_{min}^4}\left(\frac{8\pi\sigma_{l-g}}{kT}\right)^{1/2}}{\frac{H_{mash}}{2v_\infty}}. \qquad (17)$$

Substituting the expression (17) R_{min} and simplifying the resulting value of the expression, we have

$$N_{fl}=\frac{v_\infty bV^2K_D k^4\Delta C^4}{H_{mash}\sigma_{l-g}^4}\left(\frac{\pi\sigma_{l-g}}{8kT}\right)^{1/2}. \qquad (18)$$

The value V_{avr}^1 can be found using the following expression

$$V_{avr}^1=\frac{4}{3}\pi\left(R_{avr}^{fl}\right)^3=\frac{4}{3}\pi\left(\frac{0,5D_n+R_{bubl}}{2}\right)^3. \qquad (19)$$

The total area of the outer surface of phase separation for bubbles that float is determined by the following formula:

$$S_{bubl}^{avr}=S_{avr}^1 N_{fl}; \qquad (20)$$

$$S_{avr}^1=4\pi\left(R_{avr}^{fl}\right)^2=2\pi\left(0,5D_n+R_{bubl}\right)^2. \qquad (21)$$

Energy and mass flow of the mashing to the gas bubbles. Diffusion of the gas phase and water-alcohol vapor in the bubbles causes their growth.

Evaporation of ethyl alcohol and water may be limited by two factors - energy potential and the partial pressure of the substance in the bulk gas bubbles by Henry's law.

Since the rate of evaporation of matter in a closed space defined by the equation of American chemist and physicist Danish Langmuir-Knudsen [2]

$$K_{vap}^1 = \alpha \left(p_{part}^{sat} - p_{part}^{curr} \right) \sqrt{\frac{M_{vap}}{2\pi RT}},\qquad(22)$$

where: α - coefficient of evaporation that takes into account the purity of the solution and evaporation conditions; p_{part}^{sat} - partial pressure of the saturation vapor pressure of the substance at P_{bubl} and temperature T; p_{part}^{curr} - the current value of the partial pressure in the bulk gas bubbles; M_{vap} – molecular weight of a substance that evaporates.

$$\alpha = \left(\frac{p_{solv}^0}{p_{vap}^0} \right) \sqrt{\frac{M_{vap}}{M_{solv}}},\qquad(23)$$

where: p_{solv}^0 та p_{vap}^0 - vapor pressure of pure solvent and a substance that evaporates at a temperature T; M_{solv} - molecular weight of the solvent.

In determining the intensity of evaporation of ethanol in the amount of gas bubbles under water solvent is taken, and in finding the intensity of evaporation of ethyl alcohol.

When using formulas (22) and (23) it is necessary to know the partial pressure of vapor bubbles in the bulk. This value is variable. On the one hand the constant evaporation of substances will increase the partial vapor pressure of zero at the time of the bubble to a certain value. On the other hand the constant diffusion of carbon dioxide in the gas space of the bubbles and the corresponding increase in the size of the bubbles will reduce the partial vapor pressure of ethanol and water. It is therefore advisable to talk about the size K_{vap}^1 as a variable in time.

The mass of each component vapor that evaporates can be determined by the following formula:

$$m_{vap} = \frac{\partial K_{vap}^1}{\partial \tau} S_{bubl}^{all}.\qquad(24)$$

The total heat flow from the mash to the gas space bubbles follows the relationship:

$$Q_{gr} = N_{all} q_{gr} = (N + N_{fl}) \frac{r \rho_g R_{bubl}}{\tau_0}.\qquad(25)$$

On the other hand the density of heat flow which corresponds to the heat capacity at time τ_0 is transferred through the boundary phase separation (liquid / gas bubble) with molecules of substances that evaporate. Hence we can write:

$$Q_{zp} = r_{H_2O} m_{H_2O}^{vap} + r_{C_2H_5OH} m_{C_2H_5OH}^{vap}.\qquad(26)$$

where: r_{H_2O} та $r_{C_2H_5OH}$ - latent heat of vaporization of water and ethanol at a temperature T.

Using equations (24) and (26) we can determine the mass of ethanol and water that evaporates during fermentation of carbohydrates in the fermentation unit. After separation of carbon dioxide from the vapors of ethanol and water ratio $m_{C_2H_5OH}^{vap} / m_{H_2O}^{vap}$ it will determine feasibility of feeding water-alcohol solution into the distillation separation.

IV. Conclusions

The analysis of the intensity of the gas phase removal of mashing during fermentation and influence in the process of reducing the pressure in the fermentation unit. Displaying capabilities that allow us to estimate the geometrical parameters of gas bubbles, the time of their existence, the volume of gas phase, which is removed during the time τ; total surface area of mass and energy exchange. Also bred dependence for determining the mass of ethanol and water are removed from the mashing while reducing pressure in fermentation unit.

References

[1] Bogdanov O.S. Fiziko-himicheskie osnovy. Moskov. Nauka. 1983. 264 p.
[2] Cianfrini C., Corcione M., Habib E., Quintino A. Energy performance of air-conditioning systems using an indirect evaporative cooling combined with a cooling/reheating treatment. *Energy and Buildings*, 69, Pp 490-497.
[3] Cianfrini C. et all. Energy performance of air-conditioning systems using an indirect evaporative cooling combined with a cooling/reheating treatment. *Energy and Buildings*, 69, Issue null, pp. 490-497.
[4] Diepen P.J., et all. Melt crystallization by controlled evaporative cooling. The caprolactam–water system in batch operation. *Chemical Engineering Science*, 55, Issue 18, Pp 3575-3584.
[5] Hanby V.I., Smith S.Th. Simulation of the future performance of low-energy evaporative cooling systems using UKCP09 climate projections. *Building and Environment*, 55, Pp 110-116.
[6] Lazzarin R. M. Introduction of a simple diagram-based method for analyzing evaporative cooling. *Applied Thermal Engineering*, 27, Issue 11, Pp 2011-2025.
[7] Semenchenko B.A. Fizicheskaja meteorologija. Moskov. Aspekt-Press. 2002. 415 p.

ANALYSIS AND SYNTHESIS OF AN ELECTROHYDRAULIC CLOSED LOOP CONTROL SYSTEM FOR DRIVE OF AN ELECTROGENERATOR DEVICE

I. Angelov, N. Stanchev

Abstract . *The article presents research and development of electro-hydraulic closed loop control system to power generators for production of electric current trough a renewable source of energy - energy recovery wave. Discussed are the syntheses of the structure of the hydraulic system. Basic design parameters are calculated and made the choice of the hydraulic machines and components and control electronic devices.*

Keywords: hydraulic motor, hydraulic cylinder, generator, wave, energy, valve.

Introduction

Utilization of wave energy is determined constructively by sponsor of this project "Vogel" Ltd., as a T-shaped pendulum, culminating with a special weight form that is partially submerged in the sea (Fig.1). To the T-shaped part are attached, respectively, two hydraulic cylinders, for operating in the pumping mode, in combination with specially constructed for this purpose, hydraulic valves.
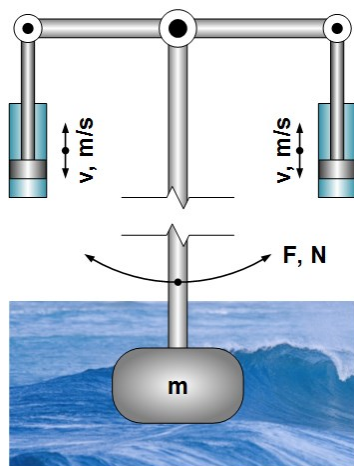
Fig. 1

The whole system consists of nine pendulums located on free-floating platform that are working part of the system - the T-shaped pendulums with applied hydraulic cylinders, control part - a set of hydraulic control elements, and power part - hydraulic motors, that convert hydraulic energy generated by the kinetic energy of sea waves into mechanical energy to power generating devices [1].

The main objective of this work is to do an energy analysis of the developed hydraulic drive system for generating installation developed in three different design variations.

The principle of operation of the operating part of the system can be described based on Figure 1, wherein the wave energy is absorbed by a mass of **m**

and a specific shape, and then is converted into hydraulic energy, such as a reciprocating movement of the hydraulic cylinders.

1. Hydraulic draft of the system – different variants

The main hydraulic system parameters are set based on the terms of reference of the manager of the project as follows:

- Drive three or four electric generator groups with output power P = 25 kW;
- Possibility for electric generator groups to work in parallel or separately;
- Maintaining a constant rotational speed, respectively, for n = 500 rpm and n = 1000 rpm;
- Required drive torque executive, M500 = 240 Nm, M1000 = 475 Nm;

After analysis of the results [1] by the authors and by the manager of the project are defined as basic operating parameters of the system:

- Maximum available flow in the system for the movement of a pendulum and thus a pair of hydraulic cylinders, q_{max} = 75 l / min;
- Maximum working pressure in the system, p_{max} = 17,5 MPa;

On this basis, defines the basic design parameters of the components that construct the different variants of the hydraulic system. The corresponding hydraulic components and their operating and design parameters are presented in Table 1.

In order to optimally efficient technical solution are developed three variations to power generator sets. On Fig. 2 is shown a hydraulic diagram of **Variant 1** for drive through volume displacement control of the speed of the hydraulic actuator with speed n = 1000 rpm. The system consists of three main independent of one another circulation circuits, and for the supply of hydraulic power to each circuit are separated three pendulums in one group with two hydraulic cylinders of each pendulum. The hydraulic

cylinders are designed constructively with built respectively suction and high pressure check valve, which aims at simplifying the design and reducing the dimensions of the cylinder.
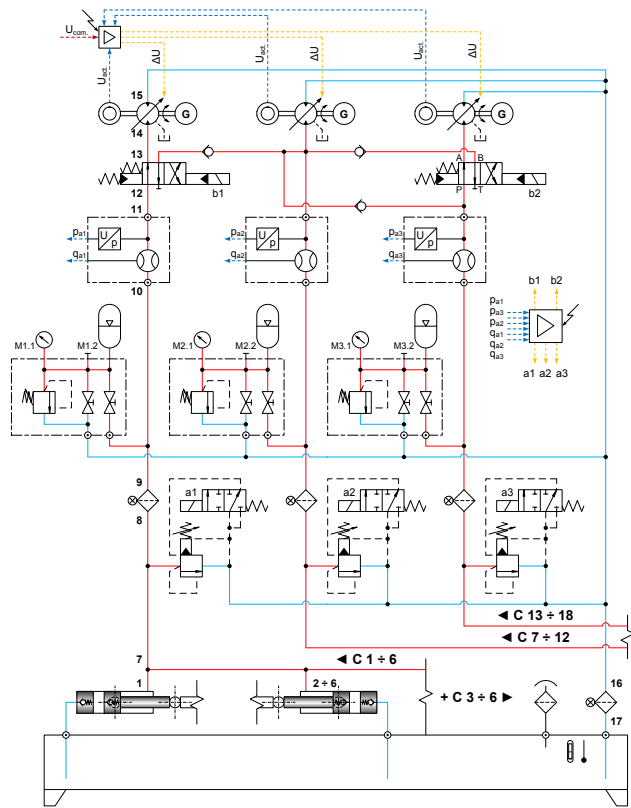
Fig.2 *Hydraulic system circuit – Variant 1*

Three circulation circuits are identical. Each circulation circuit is fed by a total of six hydraulic cylinders, a hydraulic working fluid feeding into a common high pressure line, in which is mounted a pilot operated pressure relief valve in parallel. The system also included a pressure filter and accumulator block located in parallel to the high pressure line. The operating parameters of the system - the flow rate **q** and pressure Δ**p** are measured by a flow meter, in which is also mounted a pressure sensor.

Variable hydraulic motor with electro-proportional control and mounted directly to it Speed sensor converts hydraulic energy derived from the movement of hydraulic cylinders into mechanical energy to drive an electric generator with output power P = 25 kW. Management of the three-motor system is performed by a specialized electronic device - multi-controller.

On Fig. 2 are shown some additional hydraulic components involved in the hydraulic drive – pilot operated directional valves and check valves. Developed and separate electronic control device for

controlling the operating modes of the system depending on the intensity of the sea motion.
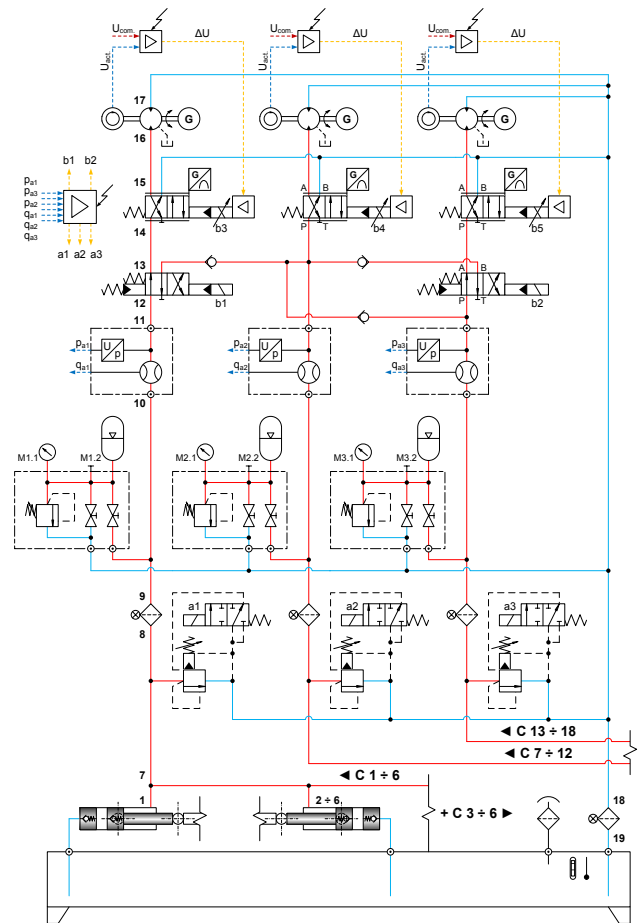
Fig.3 *Hydraulic system circuit – Variant 2*

Fig. 3 presents the hydraulic diagram of **Variant 2** for hydraulic drive with throttle control of the speed of the hydraulic rotary actuator with speed n = 500 rpm. In this proposed solution differences appear only in the fact that the hydraulic actuators are non-variable orbital hydraulic motors with built-in speed sensors and as regulating device are added additional hydraulic pilot operated valves with electro-proportional control. To regulate the speed of the motors are designed three separate closed loop control circuits by electronic controls. The principle of operation of the system is similar to that of the first variant, except for autonomous speed control of hydraulic motor through three separated closed loop control systems, while there is scope for gradual and steeples acceleration of electro-generator groups due to the selected schematic distribution of proportional directional valves.
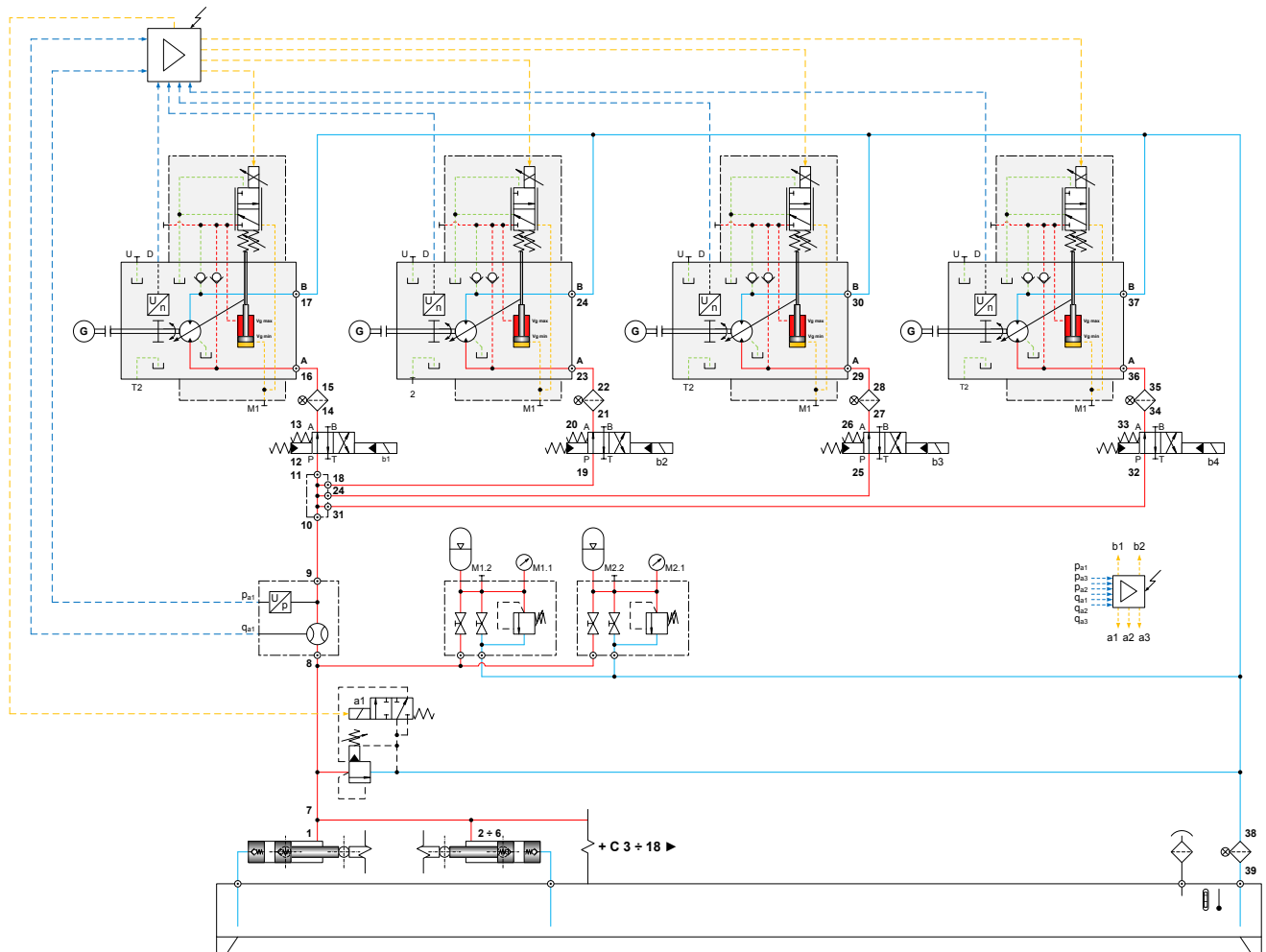
Fig. 4 *Hydraulic system circuit– Variant 3*

Fig. 4 presents the hydraulic circuit of **Variant 3** of the drive system, again with volume displacement control of the speed of the hydraulic actuator with speed n = 1000 rpm. By this solution is added one additional generator group with power P = 25 kW, so the total power output of the facility becomes P_{all} = 100 kW.

The main difference between the system in question and the previous two, the system is structured by a single circulation loop, i.e. the hydraulic actuators work in parallel simultaneously .

The hydraulic actuators are again variable hydraulic motors with integrated speed sensors and electro-proportional control. The operating parameters of the system - the flow rate and pressure are measured by a flow meter disposed in the pressure line, which is also mounted a pressure sensor.

Such decision may be highlighted as a priority work of the hydro motors in parallel in a single circulation loop. Due to the operation of all hydraulic cylinders simultaneously in a circulation loop, flow supplied to the actuators is with minimal unevenness. This contributes to the achievement of optimum frequency control of the rotational speed of the variable hydro motors.

In Table 1 are shown the main hydraulic components with their basic parameters and quantities for each of the tree variants of the system.

Table 1

Hydraulic component, parameters	Variant 1 Qty	Variant 2 Qty	Variant 3 Qty
Hydraulic cylinder, *D x d x H = 70 x 45 x 65, mm*	18	18	18
Pressure reslief valve, *p_{max} = 31,5 MPa*	3	3	1
Accumulator group, *V_0 = 50 l*	3	3	2
Flowmeter, *q_{max} = 300 l/min, p_{max} = 40 MPa*	3	3	-
Flowmeter, *q_{max} = 1000 l/min, p_{max} = 40 MPa*	-	-	1
Directional valve 4/2, *NG25*	2	2	4
Proportional directional valve 4/2, NG16, *q_{max} = 220 l/min*	-	3	-
Hydraulic non variable motor, *Vg = 315 cm^3, p_{max} = 25 MPa*	-	3	-
Hydraulic variable motor, *Vg = 140 cm^3, p_{max} = 35 MPa*	3	-	-
Hydraulic variable motor, *Vg = 160 cm^3, p_{max} = 35 MPa*	-	-	4

2. Energy analysis of the proposed solutions

Energy analysis of the proposed three solutions is presented as loss of nominal power of the input of the system, trough by presents the effectiveness of each of the systems as the Structure efficiency.

In established flow stream pressure losses (linear losses) in pipes due to the resistance of the pipe wall friction is calculated by the formula:

$$\Delta p_{Li} = R_{Li}.q, \text{MPa} \qquad (1)$$

Where:

$$R_{Li} = \frac{128.\rho.\nu.l}{\pi.d^4}, \frac{\text{Pa.s}}{\text{m}^3} \qquad (2)$$

ρ – Density of the working fluid;
ρ = 900 kg/m^3;
ν – Kinematic viscosity;
ν = 41,4.10^{-6} m^2/s;
d – Diameter of the cross-sectional area of the pipeline, m;
l – Length of the pipeline, m;

Hydraulic losses due the local resistances. In established flow stream at the locations of the pipeline connections, bends, branches, and other there is a pressure loss of local resistances. The local resistance is derived from both the tangential stresses which are exerted on the walls of the fluid motion, and the vortex generating, wherein the kinetic energy of the fluid passes into the inner one of the heat resulting from friction. Pressure losses in local resistances of hydraulic systems are perceived to be calculated by the formula:

$$\Delta p_{Lo} = R_{Lo}.q^2, \text{MPa} \qquad (3)$$

Where:

$$R_{Lo} = \xi \frac{\rho}{2S^2}, \frac{\text{Pa.s}^2}{\text{m}^6} \qquad (4)$$

ξ – Coefficient of local resistance;
ξ = 1,6;
ρ – Density of the working fluid;
ρ = 900 kg/m^3;
S – Cross-sectional area of the local resistance;

Pressure losses in the flow of fluid through the individual hydraulic elements are defined by the graphical analysis of the real static characteristics, which are presented in the technical documentation from the manufacturer for the device.

Pressure losses in the system can be represented as a power loss, using the following mathematical relationship:

$$P_{Loss} = \frac{q.\Delta p}{60}, \text{kW} \qquad (5)$$

Where:
q – Flow rate, l/min;
Δp – Pressure drop, MPa;

Table 2 shows the calculation of the hydraulic losses in the first version of the system with throttle speed control of the hydraulic actuators at maximum flow, in which realizes the set rotational speed of the adjustable hydraulic motor to drive the electric generator. Analogously losses are calculated at the maximum and minimum flow rate in all three cases. With maximum power losses in the Variant 1 are P_{Loss} = 5,4 kW, in Variant 2 - P_{Loss} = 1,6 kW and in Variant 3 - P_{Loss} = 6,7 kW.

Table 2

Section	L	d	q	q	R_{Li}	R_{Lo}	Δp	Δp
-	m	m	l/min	m³/s	Pa.s/m³	Pa.s²/m⁶	Pa	MPa
1-7	2	0,019	37,5	0,000625	23297995	8856983326	18021,01	0,018021
2-7	2	0,019	37,5	0,000625	23297995	8856983326	18021,01	0,018021
3-7	2	0,019	37,5	0,000625	23297995	8856983326	18021,01	0,018021
4-7	2	0,019	37,5	0,000625	23297995	8856983326	18021,01	0,018021
5-7	2	0,019	37,5	0,000625	23297995	8856983326	18021,01	0,018021
6-7	2	0,019	37,5	0,000625	23297995	8856983326	18021,01	0,018021
7-8	11	0,04	225	0,00375	6523124	450879267	30802,21	0,0308022
8-9	Filter							0,1
9-10	2	0,04	225	0,00375	1186023	450879267	10788,07	0,0107881
10-11	Flow m.							0,06
11-12	1,5	0,04	225	0,00375	889517	450879267	9676,178	0,0096762
12-13	Valve							0,04
13-14	1,5	0,04	225	0,00375	889517	450879267	9676,178	0,0096762
14-15	P. Valve							1
15-16	1,5	0,04	225	0,00375	889517	450879267	9676,178	0,0096762
17-18	5	0,06	675	0,01125	585690,2	89062571,3	17861	0,017861
18-19	Filter							0,05
Total pressure losses:								**1,44661**
Total energy losses In kW:								**0,542477**

3. Comparative analysis and effectiveness of the proposed solutions

Figures 5, 6 and 7 are shown graphically in scale hydraulic losses at a minimum and maximum flow, corresponding to variants 1, 2 and 3. Graphs illustrate visually how much the available inlet pressure of the system is lost to overcome the hydraulic resistance of the examined specific hydraulic systems.
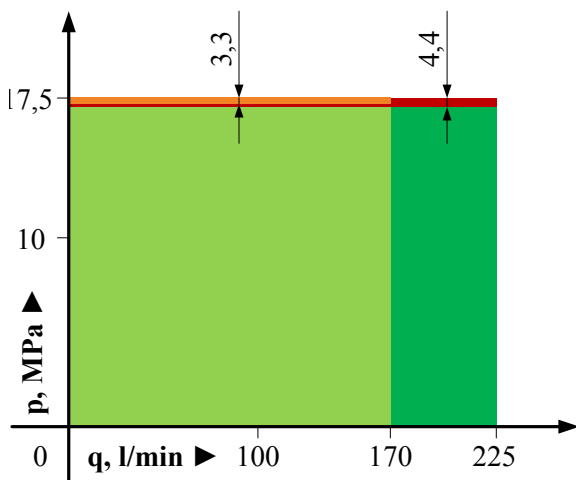
Fig.5. *Hydraulic losses, Variant 1*
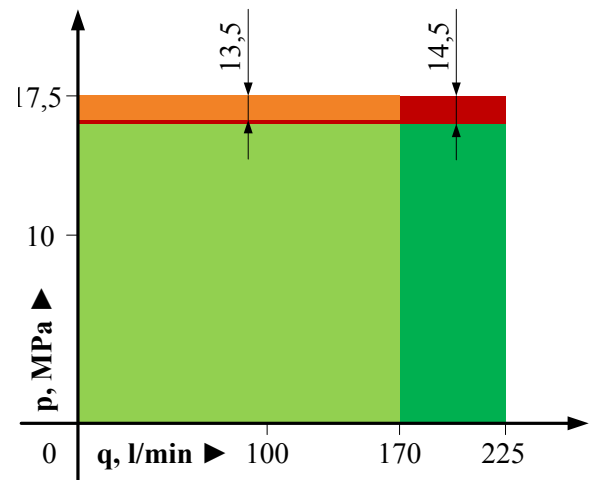
Fig.6. *Hydraulic losses, Variant 2*

The calculations were applied to the same work regimes and the same design parameters for the three circuit solutions. This gives grounds for comparison to the performance of each system. The so-called efficiency is determined based on the nominal power of the used hydraulic machines and components in the relevant circuit solutions, taking into account losses and calculated by the formula:

$$\eta_{Eff.} = \frac{P_{Nom.} \cdot P_{Loss}}{P_{Nom.}} \cdot 100\% \quad (6)$$

Where:

$\eta_{Eff.}$ – Effectiveness;

$P_{Nom.}$ – Nominal output power;

P_{Loss} – Loosed power;

Analysis of the results shows that the three proposed options the efficiency is different. The highest efficiency is in variant 1 with volume adjustment, and the lowest is in variant 3.
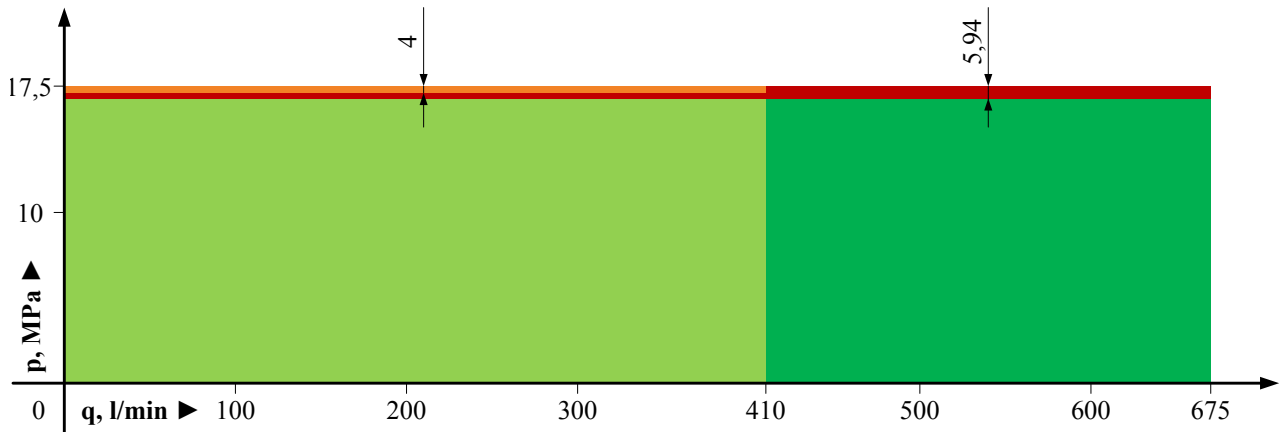
Fig.7 *Hydraulic losses, Variant 3*

4. Conclusion

1. Regardless of the comparison of the different options, if so specified energy efficiency refers to the maximum output power obtained at the suitable option from this perspective proves the performance of the system as Variant 1 or Variant 3.

2. Energy efficiency results shown in Fig. 8 show that the difference between Variant 2 and Variant 3 is minimal (within 1%), which imposes additional economic analysis, and here it should be noted that variant 3 rated power output is $P_{all} = 100$ kW, while variant 1 is $P_{all} = 75$ kW.

3. Final choice of Variant of the hydraulic system can be made only after a thorough technical-economy analysis of the three variants mainly depends on the effectiveness which is shown on Fig.8
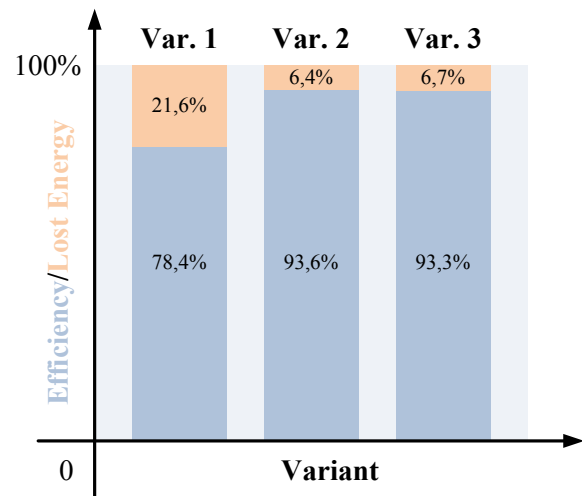
Fig. 8 *Effectiveness of the Variants*

References

[1] Il. Iv. Angelov, N. I. Stanchev, "Analisys and Synthesis of an Electrohydraulic Closed Loop Control System for Drive of an Electrogenerator Device" – Sozopol 2013.

[2] Bogdan I. Draganov, Automatic control, "Technique" - Sofia 1980.

[3] Michail D. Komitovski, Elements of hydraulic and pneumatic, "Technique" - Sofia 1985.

[4] H. Exner, R. Freitag, Dr. – Ing, H. Geis, R. Lang, J. Oppolzer, P. Schwab, E. Sumpf, U. Ostendorff, M. Reik, Hydraulics. Basic Principles and Components– The hydraulic Trainer, Volume 1, Bosch Rexroth AG 2003.

ANALYSIS OF TURKEY AS A RAW MATERIAL FOR USE IN THE DEVELOPMENT OF THE FORMULATION OF MEAT PRODUCTS

N.V. Budnik[1], M.V. Korovina[2], I.I. Gagach[2]

[1]*Poltava University of Economics and Trade*
[2]*Kyiv National University of Food Technologies*

Absreact: *A poultry market monitoring and chemical analysis of meat turkeys major operators in Ukraine. Comparative characteristics of turkey meat from broiler chicken meat, dairy beef and lamb and development on the meat based special products. A comparative analysis of the fatty acid composition of different types of poultry meat to develop new products and expand their range.*

Keywords: turkey, market, muscle, diet product, sausages

Characteristic of modern society sedentary lifestyle, poor nutrition with increasing amounts of refined foods, constant psychological stress lead to increased atherosclerotic changes in the vessel walls of the heart and brain, early heart attacks and strokes, obesity [1].

Hence the obvious need to develop an integrated model of prevention of chronic fatigue, as the adoption of a number of drugs for the treatment usually contraindicated production so special direction is relevant. In the future, we are going to food by prescription: what to eat, when, how much, in what combination with maximum health benefits [1].

Scientists of the department "Technology of meat and meat products" NUFT collaboration with the laboratory of the Institute of Gerontology gerodietetiki im. D.F.Chebotarova NAMS of Ukraine" is addressing the issue of healthy balanced diet of people in older age groups. In this direction, some progress in the area of health foods and in the field of special diets, using an integrated approach in the development of "health technology" required for the cultivation, processing, storage and subsequent sale of products.

Principles of healthy eating is:
- Compliance with dietary energy supply energy costs human;
- The adequacy of the chemical composition of the diet of the physiological needs of the body for nutrients and their balance each other ;
- Compliance with the chemical structures of the food enzyme systems of the body ;
- Regulated diet ;
- Increase in the production of meat products

with reduced fat content , as well as products of organic production. [1]

The aim is to monitor the market meat poultry and turkey meat chemical analysis of the main operators in Ukraine. Comparative characteristics of turkey meat from broiler chicken meat, dairy beef and lamb and development based on specific meat products.

At present, the products containing poultry have become the most popular subject of innovation around the world, because the market needs innovation. In order to satisfy the consumer need to expand the range and create original form products with different fillings expand distribution and promote events, exhibitions, tasting [3].

By products include poultry products and meat products, recipes are included poultry, even if it is not a major component. Among the producers of poultry in Ukraine broad demand only products from chicken. Primarily this is due to their cost, which is lower compared with products from other species of birds, despite the fact that turkey meat is a dietary, simpler and cheaper, and it is growing chickens in industrial environments. Poultry is one of the most mechanized and automated sub-sectors of agriculture, production of which is most suitable for better nutrition [4].

According to the FAO global meat production in 2013 increased by 2 % and was 251,22 million tons by poultry 88,982 million tons of the total number of poultry produced up to 86 % - chickens. The structure of gross agricultural output Ukraine poultry generates 15 % of total production, and over 42% of animal

products. Industrial breeding turkeys as a branch of poultry meat is an important source of the increase in meat production and diversification. Share turkey meat production is 7,9 % of poultry production. [3]

Turkey meat consumption per capita per year is in Israel – 12,0 kg in the United States – 8,0 kg in Europe – 4,0 kg , including in Poland – 4,5 kg, of about 1 kg in Ukraine - 0,2 kg [3].

Nature and Climate of Ukraine, its well-developed grain farming creates all conditions for growing turkeys. In the U.S., Holland, France, Hungary, the Czech Republic for the manufacture of semi-finished products use 30 to 50% of the poultry of the total number of all meat [3].

Today on the shelves of major chains in Ukraine represent products from turkey meat packed chilled products in a modified gas atmosphere , vacuum packed products.

The main market operators in turkey meat production in Ukraine are: "Ukrainian food group "Invest"(Chernivtsi); Ltd. "Plemptahoradhosp" Brovarskyi"(Kiev region.) PP "Shark" (Kyiv region). LLC "Lord" - is part of the agricultural holding "Gals-Agro" (Kiev region.) Open AP "Sumy bacon" (Sumy region.) OJSC "Agricultural firm" Welfare Carpathians"; Firm «Shakhtar» (Donetsk region.) OJSC "Agricultural firm" Hrelye - Broshukova "(Ukrainian-French company (Rivne region). OJSC "Zolotonoshamya'so" (Cherkasy region).

Return turkey meat production in Ukraine, as a rule, commercial secrets, but given that the cost of feed per 1 kg increase in body weight in turkeys in 1.3-1.5 times higher than in broilers, and the same proportion higher selling price of meat turkeys, turkey meat production profitability is not inferior to the production of broiler meat [3].

Table 1 *Physico-chemical characteristics of meat*

Type of raw material	Mass fraction, %				pH	Aw	VZZ, % of meat	VUZ, % to total moisture	Energy value, kcal / kJ
	protein	moisture, W	fat	ash					
File turkey	21,5	72,74	3,41	1,91	5,95	0,992	70,95	93,25	116,5/488
Thigh turkey	21,0	72,09	4,93	1,52	6,2	0,991	70,6	92,4	128/538
Fillet of broiler chickens	20,75	75,84	1,85	1,55	6,2	0,993	65,82	90,76	89/370
Thigh of broiler chickens	20,36	74,97	3,55	1,12	6,4	0,992	63,58	92,81	92/383
Muscle tissue turkey "PP Shark"	20,66	73,27	4,59	1,44	6,61	0,995	70,5	92,2	
Muscle tissue turkey "Ltd Brovarskyi"	18,37	74,17	5,89	1,53	6,35	0,993	72,8	94,5	
Muscle tissue turkey "OOO Dobrobut Prikarpatya"	22,57	70,39	5,16	1,94	6,4	0,994	70,1	98,7	
Muscle tissue turkey " OJSC Zolotonosha of meat"	21,4	73,79	3,52	1,25	6,03	0,993	72,5	94,65	
Milk veal	21,82	75,4	1,46	1,3	6,0	0,993	71,3	92,7	96,4/401
Young lamb	17,2	67,9	14,1	1,18	6,22	0,992	70,9	92,8	467,8

From the table it is clear that the physical-chemical parameters turkey meat is not very different from dietary and environmentally friendly veal meat and protein content (22,0 %) higher than all other types of raw meat.

Water-holding capacity of turkey meat is also quite high (70,1-72,5 % meat), indicating good functional and technological properties and the feasibility of its use for industrial processing.

From a technological point of view, the more water is bound, the more it is to be processed. So, the best way to heat treatment is considered the meat of an adult bird, as characterized by a greater ability to bind water in comparison with the young.

In muscle tissue water is present both in the cells and in the extracellular space. Parts of it are able to move from the cell into the extracellular space, and the ability to transition is the criterion for the separation and connectedness to the free water.

Part of the muscle tissue in the carcass 1 and category 2 is within 44-47 %, and the skin with subcutaneous fat is 13-22 %. In turkey meat protein and fat ratio close to optimal . On the content of nutrients in practice little different from beef , but there's relatively little connective tissue due to the less defective proteins (collagen and elastin) than beef and pork , which significantly affects the juiciness, texture and nutritional value of the finished product.

Connective tissue of poultry meat has less strength than beef and pork , so much faster hydrolyzed by heat treatment. Meat absorbed by the human body by 93%. It contains proteins (15-22 %), fat (5-39 %) , mineral salts, extractives, vitamins, A, D, PP . Poultry muscle tissue is denser and close-grained . Less connective tissue , it is tender and fluffy. Poultry fat melts easily , since it contains a lot of oleic acid. The melting point of the fat chick 23 - 380s , turkeys 31 - 32^0C . . When cooked fat melts and infiltrates the muscle tissue , meat is juicy, improving its taste.Turkey meat - a unique diet product that combines the properties of chicken, veal and lamb, rich in vitamins and also low in calories, it low cholesterol. Meat turkeys in great demand in the U.S., where it is used as a delicious product , but in this country still as popular meat chickens and broilers.

In red muscle contains more protein, fat, cholesterol, phosphatides, ascorbic acid in white muscle carnosine more glycogen , adenosine phosphate. Vbelyh muscle myoglobin contains 0,05-0,08 % , red centuries it several times more. Body fat in poultry are under the skin , on nutrennih organs and between muscle bundles. At complex processing will be allocated lump meat sc more valuable parts of carcasses (chest , hips, rear quarter with skin and beztinikiroyu) that Used for production of semi-finished sausage, food products and canned meat one piece.

Total protein content in meat is not fully characterizes its nutritional value, as near complete proteins in the remaining meat and go defective. Therefore, the biological value of meat is determined by its amino acid composition.

Table 2 *The amino acid composition of proteins meat turkeys, broiler chicken , veal and lamb (g 100 g meat)*

Amino acids	The composition of amino acids in a protein						
	Turkey "Ltd Brovarsky"	Turkey "PP Shark"	Turkey "OOO Dobrobut Prikarpatya"	Turkey cross BUT-9	Tsiplyata broiler cross-HNS 500	Milk veal	Young lamb
1	2	3	4	5	6	7	8
Essential amino acids							
Lysine	1,726	1,689	1,636	1,43	0,86	0,72	1,42
1	2	3	4	5	6	7	8
Valine	0,706	0,752	0,930	0,90	0,77	1,90	0,612
Leucine	1,444	1,345	1,587	1,78	1,10	2,01	1,332
Isoleucine	0,602	0,655	0,963	0,91	0,58	1,86	0,533
Methionine	0,650	0,726	0,497	0,11	0,13	0,74	0,511
Phenylalanine	0,765	0,747	0,803	0,70	0,68	1,72	0,660
Threonine	0,875	0,811	0,875	0,80	0,55	0,79	0,681
Arginine	1,403	1,347	1,168	1,62	1,23	0,59	1,301
Histidine	0,625	0,656	0,540	0,60	0,79	0,61	0,538
Sum of essential amino acids	4,996	5,615	5,870	6,66	4,34	5,15	5,075
Nonessential amino acids							
Alanine	1,095	1,046	1,218	1,41	1,38	0,85	1,025
Aspartic acid	1,453	1,229	2,007	2,11	1,22	1,85	1,078
Glutaminic acid	3,376	3,032	3,280	4,34	2,28	2,77	2,858
Glycine	0,836	0,815	1,137	1,01	0,80	0,35	1,167
Proline	0,615	0,627	0,831	0,46	0,55	1,32	0,638
Serine	0,819	0,747	0,735	0,50	0,47	0,64	0,641
Tyrosine	0,693	0,669	0,616	0,50	0,57	0,72	0,544
Cystine	0,100	0,186	0,121	0,18	0,18	0,74	0,189
Sum of essential amino acids	12,78	12,082	18,94	19,36	14,1	20,18	15,728

In turkey meat compared to broiler meat higher levels of amino acids such as cepin, valine, tpeonin, isoleucine, lysine, methionine, leucine and glutamic acid. Amino acid content, which depends on the formation of the organoleptic properties of meat products (alanine, glutamic acid, methionine, threonine), turkey meat is dominated by veal and lamb (5,615-6,66) versus 5,15 and 5,075, respectively, per 100 grams of meat.

Important role in assessing the nutritional value of foods plays lipid composition of meat . Lipids poultry are carriers of energy, their biological value determined by the content of polyunsaturated fatty acids and fat-soluble vitamins. Fats provide the intestinal absorption of fat-soluble vitamins. Important role they play in shaping the flavor of meat. Poultry fat having a melting point below 400^0C, which makes good emulsifying them in the digestive tract and digestion. The content of unsaturated fatty acids in meat turkeys almost twice as much saturated, this trend has continued in respect of poly unsaturated essential fatty acids.

Table 3 *Fatty acid composition of meat*

Fat	The content of essential fatty acids, %			Relations characterizing the biological value of fats				
	MNFA	PNFA	NFA	MNFA: PNFA: NFA	PNFA: NFA	C18:2 : C18:1	C18:2 : C18:3	ω 6: ω 3
Ideally	33,30	33,30	33,30	1:1:1	0,2-0,4	<0,25	<0,7	4:1
Turkey	37,55	30,60	29,95	1:0,7:0,7	0,82	0,45	7,37	14,5:1
Gallinaceous	49,81	17,78	32,41	1:0,4:0,7	0,56	0,38	17	23:1
Duck's	49,14	20,54	24,42	1:0,4:0,5	0,83	0,23	2,47	18:1
Anserine	51,11	21,67	25,86	1:0,4:0,5	0,84	0,29	4,76	16:1

We carried out a comparative analysis of the fatty acid composition of different types of poultry meat to develop new products and expand their range . The table shows that none of the conventionally used lipid components is not ideal . Closest to the ideal to be fat turkey (37,6:30,6:29,95) that provides a basis to develop a computer simulation model samples sausage recipes given fatty acid composition and biological value.

The greatest changes in the chemical composition of meat associated with quantitative and qualitative composition of the lipids, the data show that turkey meat is highly valuable and healthy food products, which is especially important for those patients with obesity, hypertension, diabetes.

References

1. Бесенен Д. Г. Избыточный вес и ожирение. Профилактика, диагностика и лечение.- М: ЗАО «Издательство БИНОМ», 2004,-240 с.
2. Гурвич М. М. Большая энциклопедия фитотерапии.- М: Эксмо, 2008.-768 с.
3. Мойса В. Ю. Мясо индейки и продукты из него./Мойса В. Ю.// Птица и птицепродукты,-2006.-№4.-с.49-50
4. Фёдоров М. Методологические подходы к разработке продуктов питания с повышенной биологической активностью./Фёдоров М.// Международный сельскохозяйственный журнал.-2003.- №1.- с. 33-35

APPLICATION of DIGITAL DRY OFFSET PRINTING with DIRECT IMAGING for PACKAGING

R. D. Sardjeva, V. A. Angelov

Technical University Sofia, br. Plovdiv
sardjeva@mail.bg

Abstract. *The market for print media still remains large and attractive since a high proportion of the ever growing advertising expenditure flows into print media communication and the demand for combination of print and electronic media for packaging worldwide is increasing. In commercial sheet-fed offset printing there is a visible trend for all print products to apply special types of substrates and hence to improve continuously printing quality, achieving a highest position in the graphic arts industry.*

Digital dry offset with direct imaging of information inside the printing machine is one of those impulses in the information and communication sector which provided a positive impact for the whole graphic arts industry. It is a relative new printing technology, named also CtPress or Direct Imaging (DI). The use of computer-to-press systems now is already widespread and is undergoing continuous development (for example Presstek DI). In order to achieve a smooth flow of digital data from prepress to press, the integration networking and digitalization of all processing steps is essential, all which are available in DI systems. Printing process here is being increasingly controlled and adjusted electronically, which leads to consistent high quality and greater productivity.

For all printing companies which need to deliver fast turn, high quality color in the range of 500 to 20,000 sheets at the lowest cost per page, they can use digital dry offset with direct imaging inside the printing machine using the current generation of DI presses. The great advantage of this technology is improved product quality, achieving even so called photographic quality. DI technology now offers a high flexibility in the processing of a large variety of substrates, which is very important for variable packaging products.

Key words: digital dry offset, direct imaging, packaging, paper, quality

I.Introduction

Packaging providers are eager for new solutions. The massive transition in global demographics, consumer preferences, and product branding affect every segment of the packaging industry – flexible packaging, labels, plastics, as well as folding cartons. The market will always require high quality, fast speeds, low cost substrates, and mainstream production efficiency.

Current digital technologies struggle to meet the standards of printing quality criteria. Digital solution is undeniably critical as run lengths (grow shorter), turnaround times get faster, just-in-time production rises.

Nowadays the trend for permanent high printing quality of food packaging is a strong and dominates in current printing development. Factors defined problem-less printing process and quality as, type of technology, inks, substrates and their mutual influences, are the
topic of this study. *The purpose is to definite what are possibilities of digital waterless offset printing with direct imaging (DI) of information inside the printing machine, in the field of color packaging production.*

There is an increasing focus on environmental issues in the commercial printing industry and customers are demanding products that

reduce their environmental footprint. Generally DI presses are waterless, highly automated, and available in 4- to 6-colour models. DI presses provide a fast return on investment and enable easy entry into the profitable digital offset printing market. A large diversity of substrates is optional in this technology. Here can be used different types of papers and cardboards, chemical papers, coated glossy and matt papers, aqueous coating is optional on them, self-adhesive papers, plastics, low grade of mechanical papers like newsprint and so on.

For the purpose of this study is used digital sheet-fed dry offset printing machine with direct imaging, produced by Heidelberg GmbH - Quickmaster DI 46-4. Printing process here is characterized as CtPress digital sheet-fed waterless offset process. This is a perfect digital (DI) offset printing machine, proper for the short run series of four color production including packaging and using printing-on-demand scheme. This digital offset machine achieves enlargement of dry offset method applying direct imaging inside the printing machine.

Quickmaster DI is an example of satellite configuration with integrated four plate and four offset rollers, running around common pressure cylinder which has four time bigger diameter and consequently inks applying. [1].(Fig. 1)

Quickmaster DI 46-4 is on the base of dry offset principles associated them with requirements of

Toray analogue waterless offset plates.[1] This machine is equipped with 12 chill zones into the inks system and with integrated imaging system of 16 thermal laser diodes for each color.

PEARLdry polyester roll substrate here are printing "plates" which can be placed on the plate cylinder fully automatically. These are process free plates, known for yielding dramatic environmental and economic benefits for customers without sacrificing quality and output. This kind of plates removes the need for the plate processor, which requires chemicals, water and energy while generating waste.

Temperature control is essential for dry offset and here is realized by cool water for the whole four printing sections including zonal cooling. But for the runs of 5 000 copies there is no need of cooling at all.

Laser heads in the imaging system expose information on the PEARLdry roller on the surface of plate cylinder inside the machine. As a result due to ablation process is available evaporation (destruction) of silicon layer on the plates. Then the plate surface is cleaned by the towel damped with cleaning solution and special device is responsible for sucking the silicon powder. Printing plate is inked by forming 12 zones, which can be adjusted manually or automatically by the blades on doctor-roller like in conventional printing machine.

Heidelberg Quickmaster DI 46-4 has a extremely short starting time, of around 10-15 min, including plate changing and exposure time, washing and register adjusting. This type of DI technology offers additional opportunities to use varnish and other methods for having luxurious products.

Compared to digital electro-photographic dry toner printers, QM-DI 46-4 is an ideal for optimal runs of 10 000 copies, but with excellent printing quality, more often named photographic quality. The flexibility towards substrates and ease of service all these are advantages, incomparable with other digital printing machine. More over this machine can be used as a proofing system for high-qualitative high runs products, produced by conventional printing machines.

II. Experimental

For the purpose of this study have been done complex of tests – first of all have to be generated test file, then printing and measuring several fixed parameters, responsible for the whole printing quality and total result.
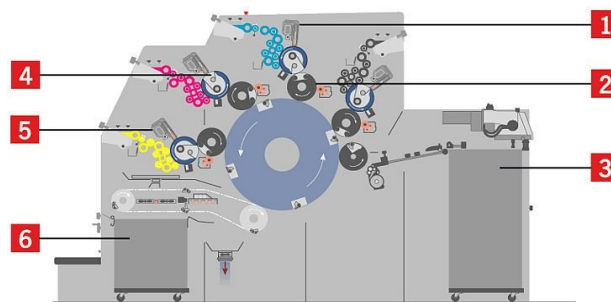
Figure 1. *Heidelberg QM DI-46, sheet-fed digital offset printing machine (1-exposure system, 2-offset roller, 3- paper system, 4- plate cylinder, 5-inks system, 6-output device)*

Test file was generated by the help of spectrophotometer i1Profiler, which offers ICC application, optimized on the real halftone illustrations, using process colors (CMYK), black, white and different PANTONE colors or other spot colors.

Table 1. *Heidelberg QM DI-46*

№	Technical data	
1.	Max size	460 mm x 340 mm
2.	Max print surface	450 mm x 330 mm
3.	Max sheet thichness	0,1mm – 0,4mm
4.	Speed of printing	10 000 листа/ час
5.	Register	0,02mm
6.	Exposure resolution	1270 dpi; 2540 dpi
7.	Exposure time	7 min–1270 dpi 14 min-2540dpi
8.	Additional options	Automat. register, varnish, anti-copy powder, permanent t°control

i1Profiler is equipped on the X-RITE standard Graphic Arts (XRGA) and its software is developed for the series of steps as a methodology aimed for researching of test-tables and profiles.[2] Principally here there is an options to choose standard table for test or generating special table in order to answer of real terms of test (color, type of papers etc.)

In order to assess printing quality are used ISO 12647-2, compatible media devices as for example IDEAlliance Digital Control, Fogra Media, Color Control Japan. By the help of them can be checked fast and easily such parameters like: optical densities, color spectral characteristics, color

coordinates, color deviation, papers whiteness (Color Checker Proof) and etc.

Figure 2 *Table of i1ProfilerTest*

In this case have been generated standard table file, with proper parameters adequately (compatible) by specific printing technology and papers. Test Chart file is created according software steps: Patch Set, Test Chart, Measurement, Lighting, Profile Settings, ICC Profile. For the test-table (Fig.2) are applied first two steps with editing some changes according printing conditions. After steps Patch set and Test chart then have to be chosen respective adjustments towards:
Comparison between C M Y K, in %;

- Generating of double colors and substrate surface (glossy, matt);
- Ambient lightening; way of black generation;
- Source of light - D50 or D65;
- Device type – monitor, scanner, printer, printing machine;

Figure 3. *Hacamada test for more precise color quality control*

- Color space depending of experimental - RGB or CMYK;

- Number of control color patch; orientation of paper sheet in the machine.

In this study have been include also and Hacamada-test, as an illustrative (Fig.3) test for proper quality control assessment – also visual for more existing colors. This test is a very good because of having specific colors, difficult for reproducing.

III. Materials

Substrates: In our case are used three types of coated papers, *Premium Coated,* WFC, (wood free coated) with different grade. These kind of papers have been compared in the test on the base of the results achieved. [3]

Paper type 1 – WFC, two sided coated, glossy paper: grade m=130 g/m^2; thickness d=122 μm; density = 1,065 g/cm^3, smoothness = 1000 s

Paper type 2 – WFC, two sided coated paper, glossy: grade m=170 g/m^2; thickness d=145 μm; density 1,172 g/cm^3, smoothness - 1100 s

Paper type 3 – WFC, two sided coated glossy paper: grade m=200 g/m^2; thickness d =178 μm; density 1,224 g/cm^3 , smoothness - 1300 s

Inks: This study has processed by using Toyo process printing inks for dry offset. These types of suspensions cover large number of substrates without any requirements. Their characteristics are: high viscosity, adequate for waterless offset, high color intensity, chemical film drying, high rubber resistance, depending on the substrate, compatibility with different varnish systems and finishing processes.

Generally waterless offset inks are specific, completely different of these conventional offset.[4] Dry offset process needs solid high viscosity inks, η = 40-100 Pa.s. In our case this parameter was of around η=85-90 Pa.s. It may be influenced by the temperature during the printing process because there is a lack of dampening solution. When the t° of the machine achieves above 30 °C, then the viscosity can be down by 7-8% and thus may cause plate toning. Besides that, dry offset inks have not to be dried on the inks rollers during their transfer to the offset blankets.

Quickmaster DI is equipped by automatic register system which is big advantage for paper wastages minimizing. Start wastes are at least 40 -50 copies. In the beginning of printing process software fixed such conditions – type of paper, speed of printing, pressure in the nip zone, inking process in different zone and etc. All these can be adjusted

additionally after measurement and visual printouts control for each color. In our case technological factors like – workflow, printing speed, inks and others are kept constant in order to see paper impact on the total print quality.

IV. Results and discussion

The whole results are shown in Table 2 and Fig. 4, 5, 6, 7, 8. Have been measured important for the printing products parameters, as: tonal value increase (*Dot gain), solid inks densities – SID, color coordinates in CIELab, color deviation (Δ E*) *and color gamut as well.*

Achieved results are different according of papers types. For parameter Dot Gain all results can be seen on the Fig. 4, 5, 6 and 7.

The common conclusion is that in the 10-40% tonal interval there are clear differences between paper results, and the next tonal interval up to 100%, all curves are almost interlaced. Nevertheless it is observed that paper type 3 has always lower Dot Gain values.
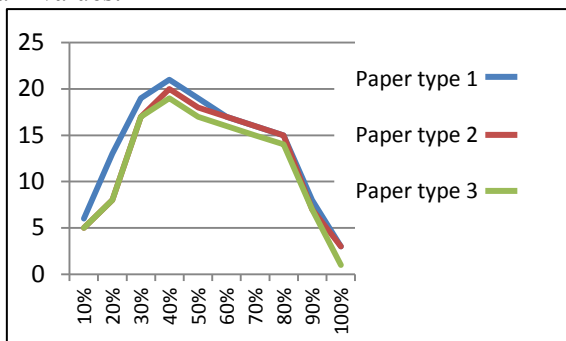
Figure 4. *Tonal values increase in Black*
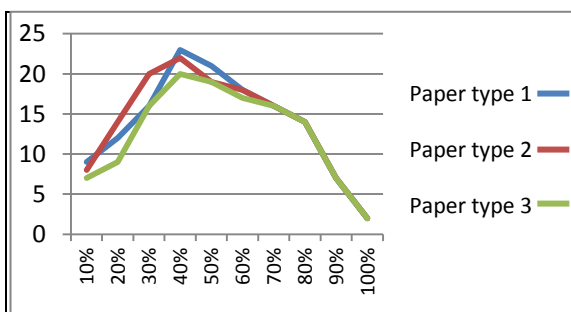
Figure 5. *Tonal values increase in Cyan*

On the Fig.5 can be seen the change of tonal value increase for Cyan. In the middle tones 20 – 50 %, Dot Gain is higher, but in the same time it is different for the separate papers types. In spite of primarily curves interlace for the papers type 1 and type 2 is seen higher Dot Gain values. Then to the end of tonal interval, from 60-100% curves again are interlaced what means that high qualitative coated

wood free papers have in advance lower tonal values increase. This principal here has been kept here.

On the Fig.6 is seen rather important difference of tonal value increase for Magenta, for the paper type 1 compared to other types of papers. It is true for the lightness and for the
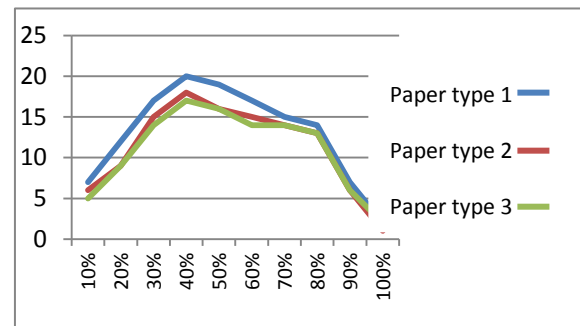
Figure 6. *Tonal values increase in Magenta*

middle tones as well. This difference varies roughly 5% between paper type 1 and paper type 3 what is unacceptable for the whole categories of coated wood free papers.
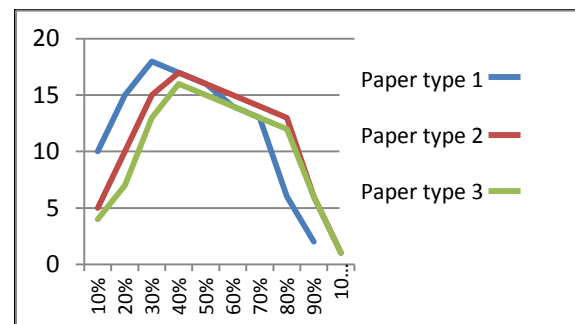
Figure 7. *Tonal values increase in Yellow*

Deviations available for three types of used papers for Yellow ink are shown on the Fig.7. They are clear localized in the intervals 10-40 % and 70-100 %. Bu can be said that almost in the whole tonal interval (lightness, middle tones and deep shadows), all three types of papers are differentiated. It means that the range of papers print quality here is: paper type 3> paper type 2> paper type 1. The lower the measured Dot Gain the higher the paper print quality.

From the whole above said towards this parameter of used papers types became clear that it is very sensitive paper's characteristic. Even in the equal categories of papers types it varies depending on detailed discrepancy which can be important for the print quality. Dot Gain is a considerable factor in the printing of color information for reproducing true colors and fine details. The lower the Dot Gain the closer the print reproduction to the original. Of

course all this is related to so call physical dot gain, what in principle cannot be eliminated, but can be minimized. It is the important reason. Printing process always results on the paper of increasing gradation, tonal values, no matter of many improvements. That is why paper quality with its surface geometry, smoothness and white coatings is one of such factors.

Besides that for achieving optimal inking and optimal transfer of inks are important solid inks densities – SID. (Table 2) During the printing process it is considerable to achieve max value of optical densities with minimal ink quantity. In our study SID are measured for the whole process colors C,M,Y,K, depending on the paper used. Here in advance it is well known that on the wood free coated papers (WFC) must be achieved possibly higher values of SID. Despite of this preliminary prediction our three types of papers have their own values, which correlate with their specifics, like different grade, smoothness, caliper, coating and grade of brightness. But from the result it is not possible to show clear preferable type of paper, because differences are not indicative.

Table 2 *Solid Inks Densities and color deviation ΔE*

CMYK	SID	L^*	a^*	b^*	ΔE
Paper type 1					
C	1,58	60,62	-41,63	-5,02	4,31
M	1,49	52,74	71,83	0,89	5,72
Y	1,42	84,16	2,69	96,82	5,93
K	1,69	21,75	1,65	0,91	2,85
Paper type 2					
C	1,58	59,7	-38,8	-43,9	3,95
M	1,48	52,34	71,95	0,75	5,18
Y	1,39	85,02	-4,36	94,67	5,33
K	1,82	21,55	1,53	0,88	2,60
Paper type 3					
C	1,56	58,2	-37,5	-43,1	3,68
M	1,44	52,11	72,02	0,69	4,86
Y	1,33	85,67	-5,21	91,35	5,02
K	1,56	21,23	1,49	0,83	2,15

Color deviation is a characteristic used for making comparison between two colors by calculating $\Delta E = \sqrt{\Delta a^{*2} + \Delta b^{*2} + \Delta L^{*2}}$, according ISO 12 647-2. [5]

On the base of many measurement can be predicted what kind of color reproduction will have each type of paper and what color gamut would generate each of them. All this is attributive from the total paper quality. [6]

Each paper has generated graph shown color gamut through measuring of color coordinates in the CIEL*a*b* system (L*,a*,b*) and by mathematic calculating. On the Fig. 8 all curves describes color gamut of the corresponding papers types and give possibilities to evaluate them. The larger the color

gamut the better the color reproduction on the paper. Profiles of the color gamut have shown some little preference of paper type 3 compared to other two types. (Fig.8)
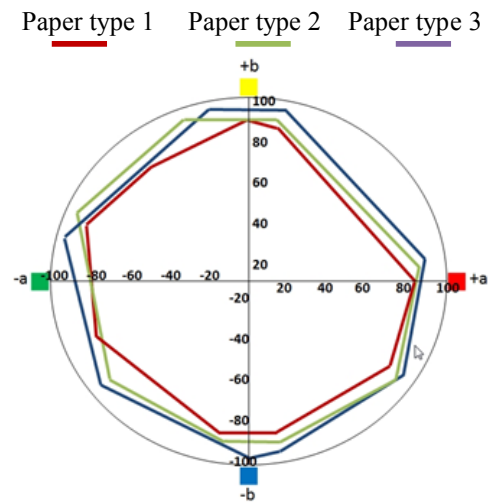
Figure 8. *Color gamut of used types of papers*

The conclusion from gamut in the Fig. 8 is that wood free coated papers (WFC) have high possibilities to reproduce a large color gamut and therefore to achieve higher quality of color printing products. In detailed can be defined parts of this gamut where our papers are

closed and where they are differentiated significantly. For example in red-green field is observed closer gamut even crossing in red-violet, blue-green and yellow. But more visual differences are observed in the fields of violet-blue and blue-green. Also here are detected points of crossing for several color values.

V.Conclusion

Digital dry offset printing technology with direct imaging inside the printing machine (DI) is proper for high quality packaging printing. Possibilities to apply high grade of wood free coated papers named Premium Coated including cardboards, enlarge the source of substrates for packaging industry.

Inks for this technology are modified, in order to achieve chemical and rub resistance, what is very important properties for food packaging. The whole results obtained in this research can be guarantee that this digital printing technology covers basic requirements for color quality reproduction, what is important for packaging printing.

These results confirm that digital DI offset named also as a Smart offset has an important role in the

field of printing industry and its future is not under doubt.

References

[1] Sardjeva R., Printing Technologies, Siela soft and Publishing, ISBN 978-954-28-0606, 424, Sofia, 2009

[2] Instructions for i1Profiler spectrophotometer applying, XRate, 2012

[3] Angelov V. A., Research for printing quality in the field of digital dry offset (DI), diploma work for Master degree, TU Sofia, br. Pd., 01. 2014

[4] Sardjeva R., Inks, Siela Norma, ISBN 978-954-28-1383-5, Sofia, 2013

[5] ISO 12647-2:2004, Graphic Technology – Process control for the production of half-tonecolor separation, proof and production prints –Part 2: Offset lithographic processes

[6] Kipphan, Helmut, Handbook of Print Media, 1.4 Print Quality, 75, 100-105, Springer, 2001, Germany

[7] www.heidelberg.com

APPROACH FOR THE IDENTIFICATION OF HYDRAULIC DRIVE SYSTEMS WITH DIGITAL CONTROL ACTUATOR

I. Angelov[1], A. Mitov[2], J. Kralev[3]

[1]*TU-Sofia, Faculty of Power Engineering and Power Machines, Department: „HAD and HM", e-mail:ilangel@tu-sofia.bg*
[2]*TU-Sofia, Faculty of Power Engineering and Power Machines, Department: „HAD and HM", e-mail:alexander_mitov@mail.bg*
[3]*TU-Sofia, Faculty of Automatics, Department: „Systems and Control", e-mail:jkralev@yahoo.com*

Abstract*: This paper shows an approach for the identification of hydraulic drive system with digital control through numerical approximation of dynamic processes. Dynamic processes in the form of transient characteristics are obtained on the basis of known from previous studies nonlinear mathematical simulation model of the experimental setup consisting mainly of two parallel loop powered, each containing three-way, two-position hydraulic digital control valve and output of pipeline. Two parallel loops driven double acting actuator. Identification is made on the basis of synthesized linear mathematical simulation model allowing to approximate with maximum accuracy the variation of velocity of the actuator at constant values of frequency of the input control signal and different values of actuators stroke.*

Key Words*: Hydraulic System, Digital Control, Actuator, Transient Processes, Identification*

I.   Introduction

The continuous development of digital hydraulics is mainly aimed at two main directions. On the one hand the development and improvement of hydraulic fast switching hydraulic valves and other hand synthesis and analysis of systems built from these devices used for pilot hydraulic control of different size hydraulic capacities. As all contemporary engineering applications and these hydraulic systems require useful mathematical simulation models used for in-depth investigation of the influence not only of the construction parameters, but the parameters of their control. In many cases, however, the synthesis of both the newly designed system and in solving problems related to existing information is necessary to develop a simulation model, based on the obtained experimental or verified simulation data. Then resorting to means and methods of identification systems that solves the issue of the receipt of these models. In its meaning the identification provides the theoretical background and practical means when building mathematical models of systems (processes, objects) based on measured information to convert the signal in these systems. Meanwhile, the development of software products make identification methods and their instruments daily tool to address issues not only practical, but research interest.

As a consequence of a series of simulation studies [1] concerning the hydraulic drive system with digital control actuator in this paper shows an approach for the identification of the system based on already obtained transient processes of an variation of velocity of the actuator. Identification of the experimental system consists primarily in the preparation of linear mathematical simulation model for a given selection of values of time constants and transmission coefficients of its constituent units to achieve maximum approximation of the original set transitional process. Furthermore, the selection of these values itself becomes a visual approximation to (in real time) by developed optimization procedure.

The main objective is that the results of this identification to make it possible to sue for effect of transient processes on the control signal from the viewpoint of moving of the test device, which are already assessed in [2], in terms of quality of regulation. Furthermore, performance of the identification system by transient processes will serve as a basis for further research aimed at determine the transfer function of the system and hence can assess about behavior of the system by means of the frequency characteristics.

Scheme of the experimental setup and system

Fig.1 is a diagram of the simulated experimental system, which is described in detail in [2].
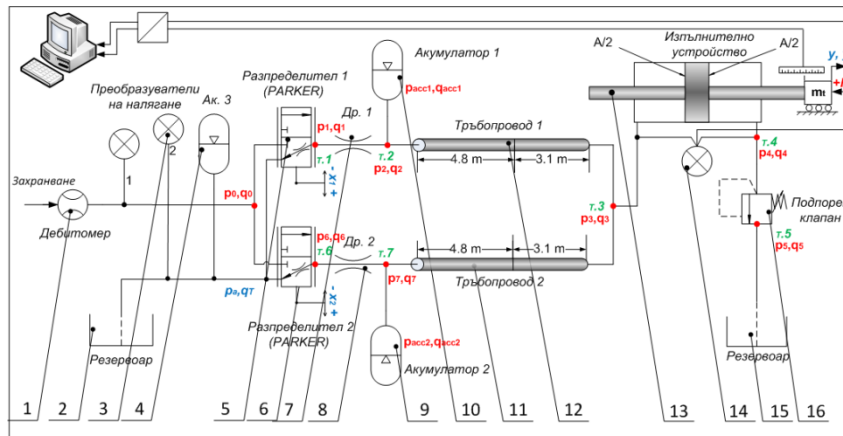
Fig.1 *Scheme of experimental system.*

Mathematical simulation model of transient response

Nonlinear relationships constituting the mathematical model of transient processes velocity and moving the the actuator are described in detail in [1]. The mathematical simulation model is implemented in the environment of the software Matlab / Simulink, through block modeling of building experimental system (Fig. 1) units. Figure 2 and Figure 3 shows a structured model of building blocks having non-linear behavior.
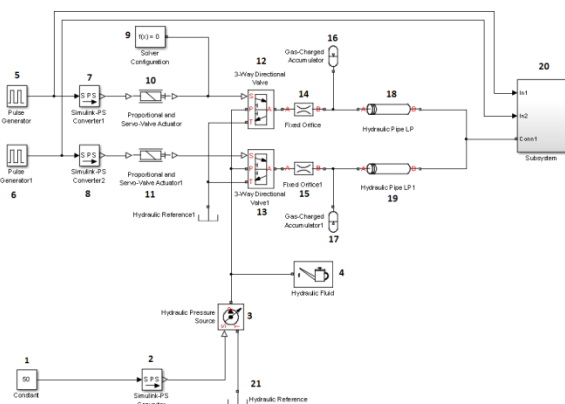
Fig.2 *Simulation model of experimental system Matlab / Simulink [1].*
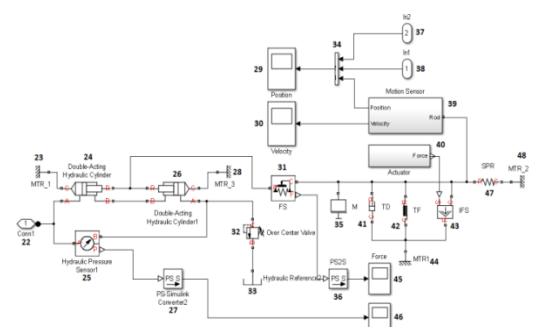
Fig.3 *Subsystem modeling hydraulic actuator device and measuring equipment.*

Identification of the system through the dynamic characteristics

The developed simulation model of study hydraulic drive system with digital control actuator allows to measure dynamic performance simulation in the form of transient response and velocity of movement of the output implementation unit (actuator) in different design and the tuning parameters of the individual components. Previous studies analyzed the response of this type of actuator - double-acting hydraulic cylinder with equal area and relatively small sizes, for various values of the stroke and at the different frequencies of the input digital signal. Figure 4 shows transient response of the actuator at 80Hz frequency and the corresponding values of the stroke in the range 5 ÷ 20mm, taking into account performed in [2] frequency analysis of the input signal.
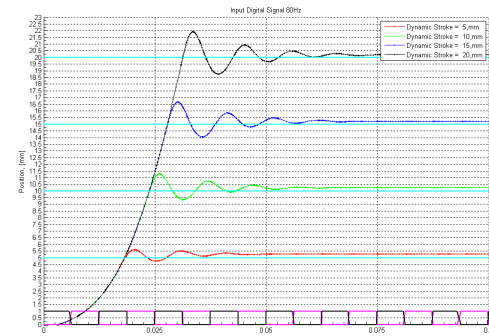
Fig.4 *Transient response of actuator device.*

From the results shown graphically (Fig. 4) clearly seen that the transient response respectively at 5, 10, 15 and 20mm have fluctuating subsiding behavior. This behavior can be described accurately enough by a polynomial of the sixteenth row. This

has been established from the initial approach to identification based on approximation by polinonom by significantly higher (Fig. 5) and inconvenient for further working order, which requires a change of approach for the identification of the test system.
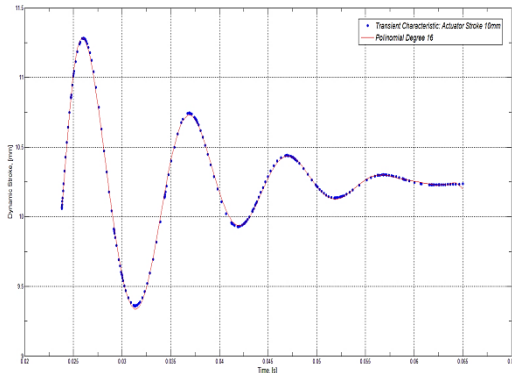
Fig.5. Approximation of fluctuations with high order polynomial.

One of the approaches commonly used for the identification of systems by nonparametric transient characteristics of the object is based on the optimization method. In this sense his approach is to determine the coefficients in a particular parametric model, based on requirements from evaluations transient model (weight function) to be as close to the reference (experimentally or verified simulation) characteristic under the same conditions for forming them . In this particular case the parametric model is a linear model composed enabling optimization procedure by sequentially searching the pattern settings (gain coefficient and time constants) that implement mentioned distance. This approach is very illustrative, since it allows to be monitored in real time the variation optimized parameters with respect to the capabilities of the software used - Matlab / Simulink. For the test a hydraulic system with digital control is more appropriate that the linear model to match the transient response of the velocity of movement of the actuator for the movement according to the power in one direction, until it reaches the preset stroke (indicated in Figure 6) in accordance with transient response of the movement (Fig. 4).
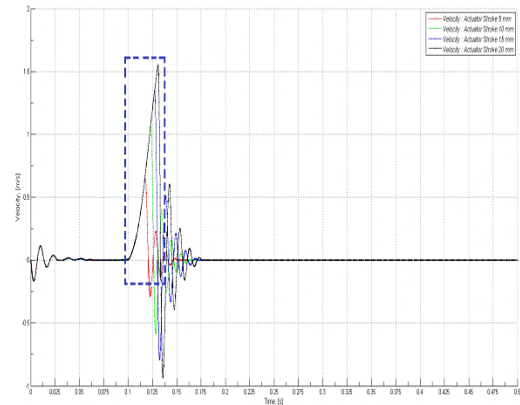
Fig.6 *Transient processes of velocity*.

The structural diagram of a linear model is shown in Fig.7. Another advantage of this approach is that based on the data sample throughout the corresponding iterations of the procedure identification velocity structure can be significantly simplified model by which to obtain data for identification of transition process of movement through integration. This model is shown in Fig. 8.

Optimization procedure is performed based on the method of nonlinear least-squares in the following mathematical description [4]:

$$\min \| f(x) \|_2^2 = \min(f_1(x)^2 + f_2(x)^2 + ... + f_n(x)^2) \ , \qquad (1)$$

where x is a vector of independent variables x_1, x_2, x_n.
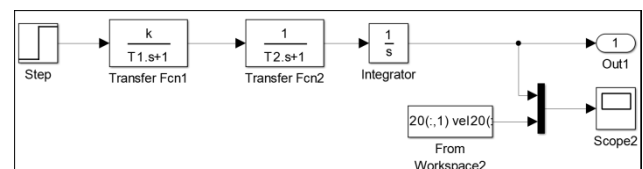
Fig.7 *Linear model*.
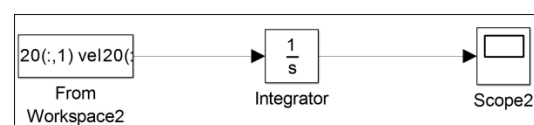
Fig.8 *Model for velocity integrating*.

The results of the identifications of the transition process of velocity and the variation of the parameters T1, T2 and k as a function of iterations of the procedure for different values of S stroke the actuator in the range 5 ÷ 20 mm, are shown in Fig. 9 and Fig. 10.
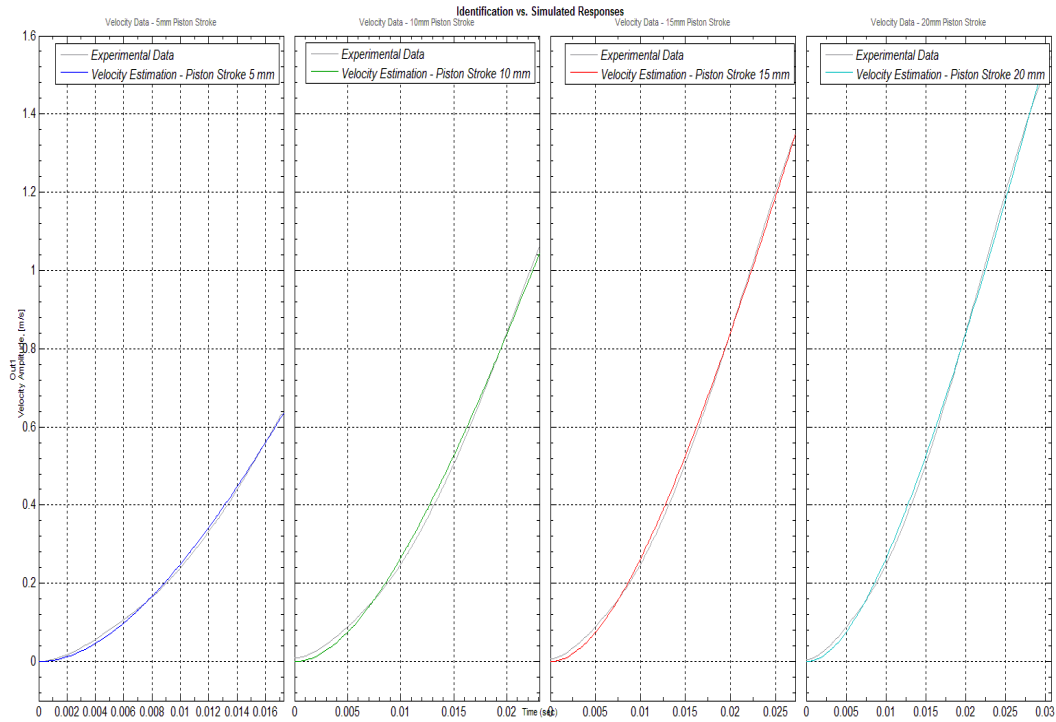
Fig.9 *Results of identification of velocity for different strokes of the actuator.*

Figure 11 shows the results after integrating data from identifications on velocity, which represent the response of the actuator according to the approach adopted for identification.
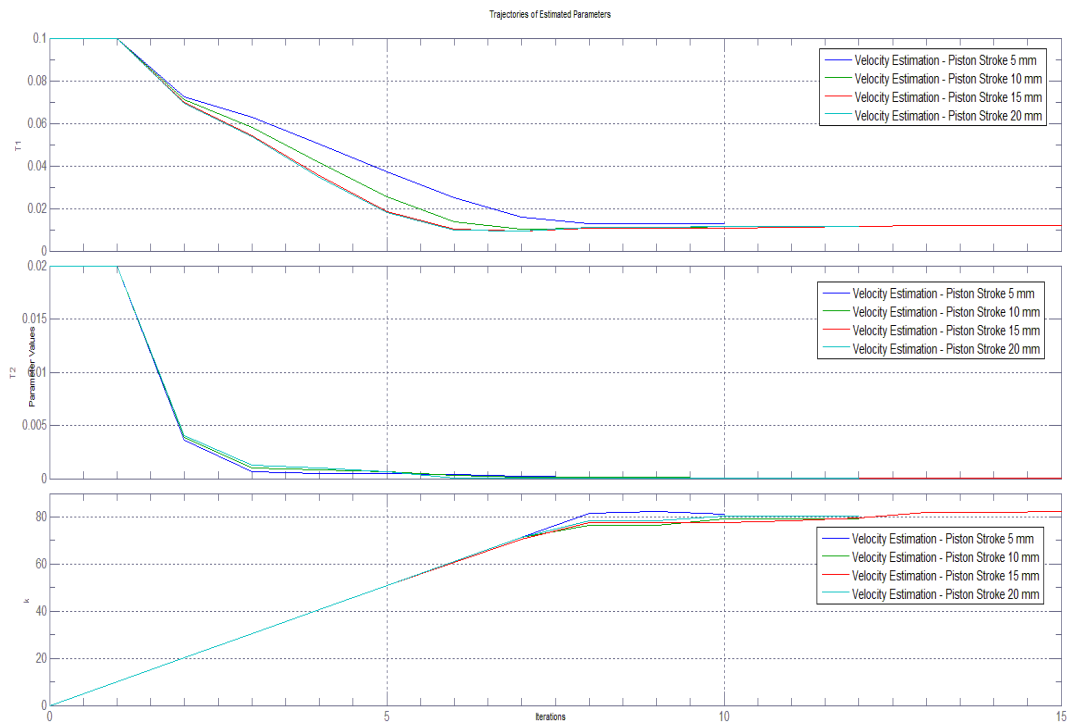
Fig.10 *Variation of parameters throughout on the optimization procedure.*
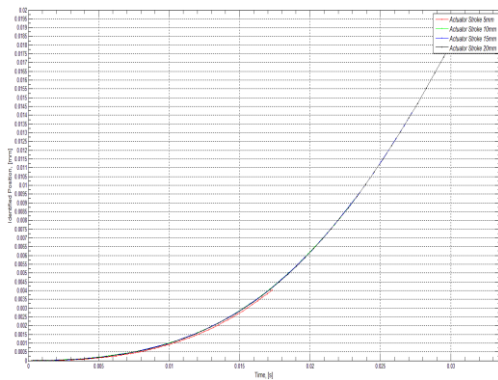
Fig. 11 *Results of the identification of actuator reaction in the range 0 ÷ S_{set}.*

Analysis of the identification results

The analysis of the results of the identification is made on the basis the variation of throughout the cost function of the separate iterations until a local minimum of the used in this case optimization procedure based on the method of nonlinear least-squares. The variation of the cost function in form without dimensions of the different values during the stroke of hydraulic actuator device, generally indicates the deviation of the linear model from the initial time until the limit of the conditions (a local minimum) for a match between both of transient responses. Fig. 12 shows the cost function for the four cases of stroke of the actuator.
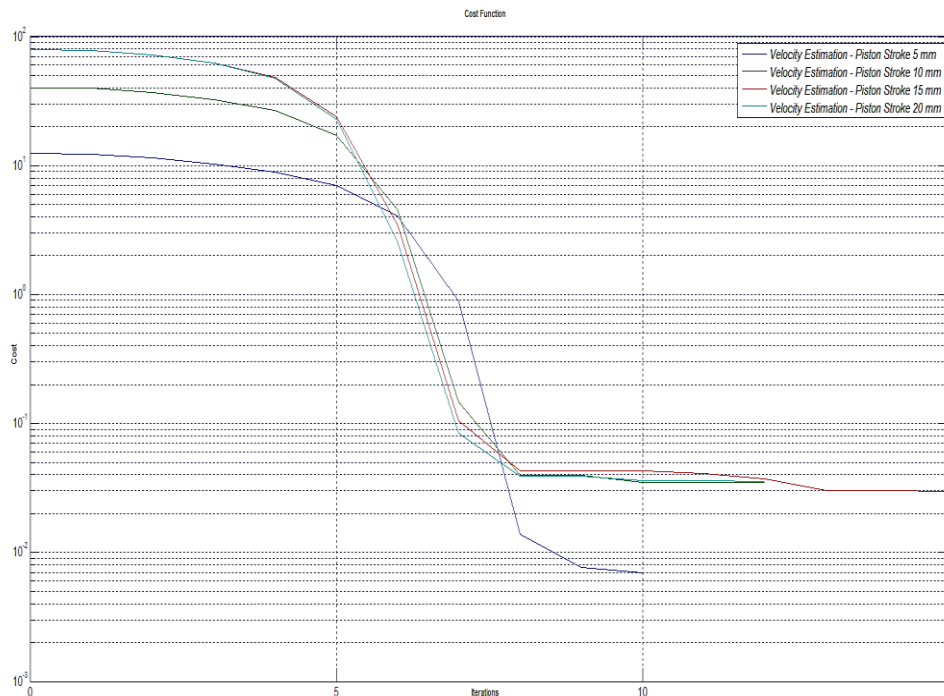
Fig.12 *Variation of the cost function during iterations.*

The graphic result clearly shows that the variation of cost function in logarithmic coordinates, indicating a relatively high accuracy of approximation between the predetermined by the nonlinear model and describe it based on a linear model transient response. At 20 mm stroke actuator cost function varies in the range 80 ÷ 0,03, and at 5 mm stroke actuator function vary in range 12,5 ÷ 0,007 and the number of iterations decreases from 15 to 10.

Quantification of this coincidence is described precisely enough for the purposes of identification with the relative error (proximity) of the cost function change between the beginning and end of the realization procedure. In this regard, we obtain 99% coincidence between both of transient responses, visualized in Fig 9.

Conclusion

Based on this proposed approach for the identification and due to the obtained results it summarized as follows:

1. Composite linear mathematical simulation model by using, on which it is possible identification of the studied hydraulic drive system with digital control actuator by means approximation of the

transitional processes a variation of velocity at different constructive and the tuning parameters. Approximation is made based on an optimization procedure that allows to monitor dynamically the variation of the parameters of the linear model.

2. Based on the results of identification of the system transient response velocity carried out the identification of the reaction of the actuator in accordance with previously obtained transient responses.

3. The implemented approach for identification will serve as a basis for further research aimed to study the dynamic behavior of the system and it is frequency characteristics based on transfer function of a composite in this work linear mathematical simulation model by introducing corrective units to improve the behavior of the system in a wider frequency range.

References

[1] Angelov, Il., Al. Mitov, "Quality Assessment of Regulation at Researching of Transients Processes of Actuator Device in the Hydraulic System with Digital Control", International Scientific Conference EMF`2013, Sozopol 2013.

[2] Angelov, Il., Al. Mitov, "Research of Dynamic Processes in Hydraulic System with Digital Control of Actuator Device", Mechanical Sciencies`2013, FEP-Sliven, 2013.

[3] Angelov, Il., A.Mitov, Research Analysis Of Dynamic Processes Occurring In Pipelines With Digitally Controlled Hydraulic Valve, IFK`2014, Aachen, Germany, 2014.

[4] Гарипов, Е., Идентификация на системи, ТУ-София, 2007.

[5] Wang, P., Kudzma S., Johnston, N., The Influence of Wave Effects on Digital Switching Valve Performance, in The Fourth Workshop on Digital Fluid Power, Linz, Austria, 2011.

[6] Sell, N., N. Johnston, A. Plummer, S. Kudzma, Control Of A Fast Switching Valve For Digital Hydraulics, SICFP2013, Linköping, Sweden, 2013.

COMPARABLE EVALUATION OF AMINO ACID COMPOSITION OF SUNFLOWER PROTEIN ISOLATES

T.T.Nosenko

National University of Food Technology, Kyiv, Ukraine

Abstract. *The microbial protease from Bacillus subtilis (ENZYME, Ukraine) was used for enzyme-assisted extraction of proteins from sunflower meal. Using of protease resulted in an increase of extracted protein amount and protein isolates yield, obtained isolates were less colored. Amino acid composition of sunflower meal, protein isolates (SI) and partly hydrolyzed protein isolates(PHI) were studied too. Three amino acids were limiting in sunflower meal proteins almost in equal extent, notably, valine had amino acid score 71.2 % to FAO/WHO reference protein, isoleucine – 72.5 and lysine – 73.5 %, respectively. Amount of amino acids in SI and PHI had changed comparing with sunflower meal, that is content of sulfur containing amino acids in protein isolates decreased significantly and lysine content decreased too.*

Key word: sunflower meal, protein isolates, partly hydrolyzed proteins, amino acid composition

1. Introduction

Sunflower meal is a by-product of oil extraction process from sunflower seeds. It is known that oil seed meal contains almost all proteins of seeds. Sunflower meal contains about 40 % of protein and could be the important source of food and feed proteins. But still it has been using only for animal feeding.

Nevertheless, the structure, physicochemical and technological properties as well as technology of protein isolates obtaining from sunflower meal are under researching. It was shown that the main storage protein of sunflower seed (heliantinin) consists of two fraction: hexameric 11S and threemeric 7S [2], which have different structure and denaturation temperature. Sunflower albumin presents 2S protein fraction [3]. The dependence of helantinin solubility from pH and ionic strength of solution were studied thoroughly [4, 7, 9].

On the other hand, the amino acid composition of proteins is a main factor for the estimation of its biological value. The biological value of vegetable proteins is suggested to be lower than animal proteins. These values are restricted by the content of limiting amino acids. The sulfur-containing amino acids are generally deficient in most vegetable proteins, for entrance in soy protein. However, it was shown that sunflower seed proteins are depleted in lysine and rich in sulfur-containing amino acids [3, 4,10]. At the same time there data about low content of sulfur-containing amino acids in sunflower seed proteins, notably, amino acid score of them was 69 % [5].

Not all of proteins in sunflower seed are soluble, as well as their solubility depends from technological parameters of pre-treatment of seeds and their processing for oil extraction. Thus the amino acids content of seeds and protein isolates are obviously different and depend from the changes of the protein structure and their solubility. The purpose of this work was to determine and compare the amino acids content of sunflower meal, protein isolates from this meal and partly hydrolyzed proteins from sunflower meal. We have used limited hydrolysis of proteins by protease in order to improve extraction process of proteins.

2. Materials and methods
2.1 Preparation of protein isolates

Protein isolates were obtained from sunflower meal, industrially produced by solvent extraction. Proteins were extracted from meal by sodium chloride solution (70 g/L, pH 7,0) under constant stirring, at 45°C for 40-50 min, meal: solution ratio was 1:10 (w:v).

In order to obtain partly hydrolyzed proteins from sunflower meal the microbial protease from *Bacillus subtilis* (ENZYME, Ukraine) was used with meal: enzyme ratio 100:1. The activity of protease was 0.1 Anson units per gram. The protease activity was stopped by heating of reaction mixture at 80°C for 15 min.

Afterwards, the insoluble residue was precipitated by centrifugation. The supernatant (protein extract) was used for isoelectric protein precipitation at pH 4.0. After protein coagulation, pellet was separated by centrifugation (3,000 x g), washed with water solution (pH adjusted with HCl to 4.0), protein pellet was collected and dried to 6-8% fluidity.

2.2. Determination of protein concentration and the degree of protein hydrolysis

The protein content in protein extracts were determined by the method of Lowry et al. [6]. The

degree of hydrolysis (DH) was determined according to the method of Tsumura et al.[11] as modified by Pericin et al.[8]. To 1 ml of the protein extract an equal volume of 0,5 mol/L TCA was added. The mixture was incubated for 30 min at 4°C and thereafter centrifuged at 3,500 rpm for 10 min. The protein content in supernatants were determined by the method of Lowry et al. [6].

The degree of protein hydrolysis was determined as a percentage of TCA-soluble protein to total proteins contained in protein extracts.

2.3. Determination of amino acid composition of protein isolates

The direct acid hydrolysis of protein isolates was used to obtain hydrolysates suitable for determination of all amino acids except cysteine and tryptophan. Hydrolysis was carried out in test tubes by adding 1 mL of HCl to dry sample, corresponding to 2 mg of protein. The mixture was frozen in a bath at -80°C, the tubes were vacuumized, sealed and incubated at 106°C for 24 h in a thermostat. After

hydrolysis samples were cooled and HCl was removed by evacuating in a dessicator containing NaOH pellet. After drying of samples, 4 mL of deionized water was added and drying procedure was repeated. Dry samples were dissolved in citrate buffers (0,3 mol/L, pH 2.2) and used for amino acid analyses.

Amino acid analyzer T 339 (Czech Republic) was used for amino acid content analysis. Standard amino acid mixture containing 0,5 μmol/L of the 17 commonly occurring amino acids was used to calculate the amount of amino acids in the samples.

2.4. Statistical analysis

Samples were analyzed in triplicate. Statistical analysis was performed using Microsoft Excel 2007 (Microsoft, City of Redmond, USA). The results were reported as mean±SD. Differences were considered to be significant at validity of α=0,95.
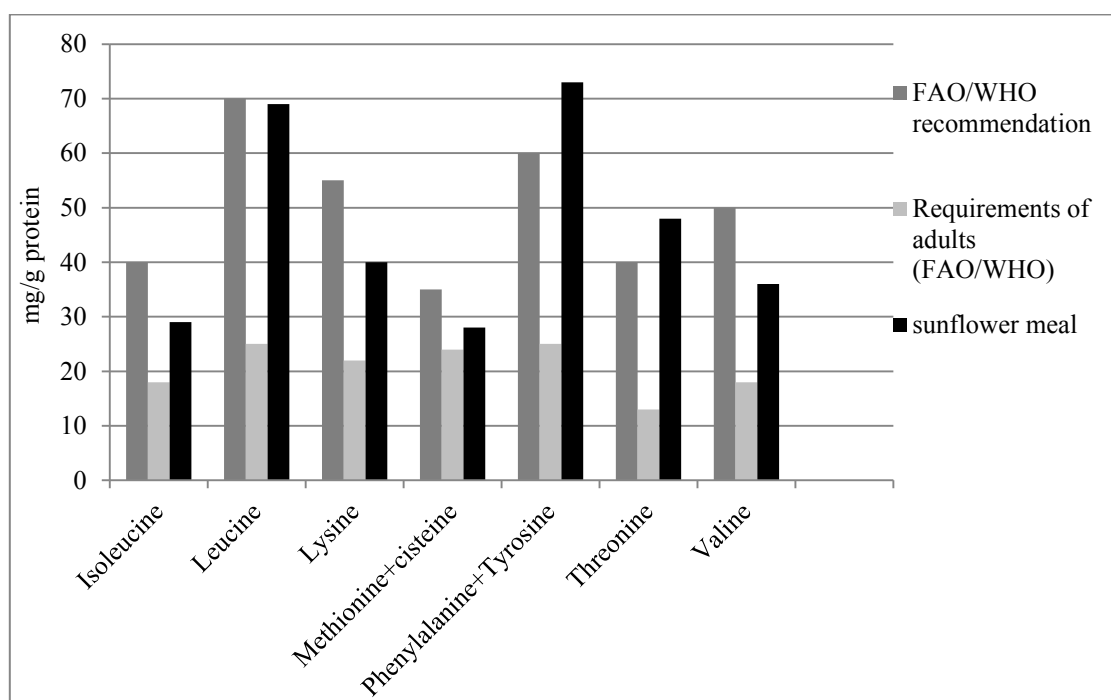
Figure1. *Essential amino acids content in sunflower meal relatively FAO/WHO recommendations.*

Table1. *The influence of protease on the protein extraction*

	Extraction parameters	
	No enzyme (SI)	In the presence of protease (PHI)
Protein extract concentration, mg/ml	32±2	59±3
DH, %	−	12,4±0,6
Protein isolates yield, %	10,5±1,0	17,2±1,5

3. Results and discussion

Amino acid composition of sunflower proteins. The data of essential amino acids content in sunflower meal in comparison with FAO/WHO recommended protein are presented on Fig.1. According to our data, three amino acids are the limiting almost in equal extent, notably, valine had amino acid score 71,2 % to FAO/WHO reference protein [1], isoleucine – 72,5 and lysine – 73,5 %, respectively. The content of sulfur containing amino acids: methionine and cysteine was also limiting for biological value of these proteins and their score was 79,1 %. These data are not agreed with published data concerning high level of these amino acids in sunflower proteins [3,4], but obtained score of lysine was significantly higher than was published for sunflower protein isolates [4].

On the other hand, we have analyzed the essential amino acids content in sunflower meal relatively requirements of adults according to FAO/WHO data [1]. We have found that content of all essential amino acids in sunflower meal exceeds requirements of FAO/WHO for adults.

Enzyme-assisted protein extraction from sunflower meal. The main process during protein isolates obtaining is extraction of proteins from seed meal. The level of extracted proteins first of all depends from their structure and solubility and also from the extraction conditions (pH and ionic strength of solution, temperature, meal:solution ratio etc.) We have suggested that solubility of meal proteins will increase as a result of limited hydrolysis. We have used the protease enzyme for assistance of protein extraction from sunflower meal. We have detected that content of extracted proteins in protein extracts increased in the presence of protease (Table 1). As a result the yield of protein isolates was very high. We suppose that limited protein hydrolysis is undergoing under such conditions and it does not result in loss of isoelectric precipitation property. Indeed, the degree of protein hydrolysis, detected in obtained extracts, was not very high and varied from 8 to 28 % dependently from time and enzyme: meal ratio.

The appearances of protein isolates, obtained in the presence of protease (PHI), differed from that of isolates (SI), which were obtained without enzyme, that is, PHI was cream-colored while SI had more dark color. We had proposed that limited hydrolysis of protein in the presence of protease have prevented chemical interaction of fenolic substances of sunflower meal mainly chlorogenic acid with proteins. Commonly the products of such reaction result in the dark color of sunflower protein isolates.
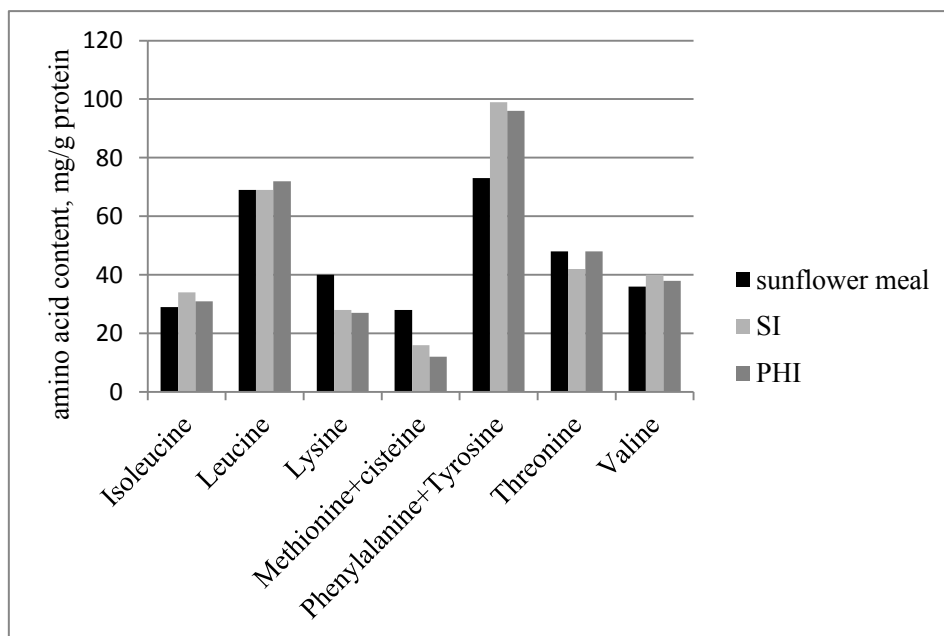
Figure 2. *Essential amino acids content of sunflower isolates (SI) and protein isolates, obtained in the presence of protease (PHI), relatively sunflower meal proteins.*

Amino acid composition of sunflower protein isolates. Results of analysis of amino acids content of SI and PHI are presented on Fig.2. Amount of amino acids in SI and PHI had changed comparing with sunflower meal, that is content of sulfur containing amino acids in protein isolates decreased significantly and lysine content decreased too. At

the same time, aromatic acid content considerably increased. We have proposed that such changes of amino acid composition were resulted by different amino acid composition of soluble and insoluble proteins in sunflower meal.

4. Conclusions

As a result of our study we have concluded that biological value of sunflower proteins according to amino acids score are significantly high. But there are considerable differences between published data on content of limiting amino acids in sunflower proteins.

We have obtained that using of protease at proteins extraction resulted in an increase of extracted protein amount and protein isolates yield. Such isolates were less colored. But content of sulfur containing amino acids in protein isolates, obtained as result of limited hydrolysis, was very low. This problem has to be resolved.

References

[1] FAO/WHO/UNU. Energy and protein requirements. Reports of a joint FAO/WHO/UNU expert consultation. *World Health Organization Technical Report* Series 724. WHO. Geneva, Switzerland, 1985.

[2] González-Pérez S., Vereijken J.M, Merck K. B, van Koningsveld G.A., Gruppen H.,Voragen A.G., 2004, Conformational states of sunflower (Heliantus annuus) Heliantinin: effect of heat and pH, *J Agric Food Chem.* 52(22), pp. 6770-6778.

[3] Gonzalez-Perez S., Vereijken J.M., 2007, Sunflower proteins: overview of their physicochemical, structural and functional properties, *J Sci Food Agric.* 87, pp. 2173–2191.

[4] Ivanova, P., Chalova, V., Koleva, L., Pishtiyski, I., (2013), Amino acid composition and solubility of proteins isolated from sunflower meal produced in Bulgaria, *International Food Research Journal*, 20(6), pp. 2995-3000.

[5] Конарев В.Г., 1981Ресурсы растительного белка и проблемы его качества, *Труды ВИР по прикладной ботанике, генетике и селекции*, 70, 2, pp. 3-12.

[6] Lowry O, Rosenbrough N, Fair A, Randall R., 1951, Protein measurement with the Folin–phenol reagent, *J. Biolog Chem.* 193, pp. 265–275.

[7] Pawar V.D., Patil J.N., Sakhale B.K., Agarkar B.S., 2001, Studies on nitrogen extractability of defatted sunflower meal. *J. Food Sci Technol.* 38, pp. 217–219.

[8] Pericin D., Radulovic-Popovic L.J., Vastag Z., Madarev-Popovic S., Trivic S., 2009, Enzymatic hydrolysis of protein isolate from hull-less pumpkin oil cake: application of response surface methodology, *Food Chem.* 115, pp. 753–757.

[9] Pickardt C., Hager T., Eisner P., Carle R., Dietmar R. Kammerer, 2011, Isoelectric protein precipitation from mild-acidic extracts of de-oiled sunflower (Helianthus annuus L.) press cake, *Eur Food Res Technol.* 233, pp.31–44.

[10] Tkachuk and G. N. Irvine, 1969, Amino Acid Compositions of Cereals and Oilseed Meals, *Cereal Chem.* 46, pp. 206 – 218.

[11] Tsumura K., Kugimya W., Bando N., Hiemori M., Ogawa T., 1999, Preparation of hypoallergic soybean protein with processing functionally by selective enzymatic hydrolysis. *Food Sci Technol.* 5, pp.171–175.

[12] Villanueva A., Vioque J., Sánchez-Vioque R., Clemente A., Pedroche J., Bautista J., Millán F., 1999, Peptide characteristics of sunflower protein hydrolysates, *J. Am. Oil Chem. Soc.* 76, 12, pp. 1455-1460.

COMPARISON OF PRINT CONTRAST AND COLOR GAMUT USING COMPUTER TO FILM AND COMPUTER TO PLATE TECHNOLOGIES (UNDER THE SAME OFFSET PRINTING CONDITIONS)

R. Boeva, I. Spiridonov, T. Bozhkova, Y. Nedelchev

Department of Pulp, Paper and Printing Arts, University of Chemical Technology and Metallurgy, Address: 8, Kl. Ohridski Blvd., 1756 Sofia, Bulgaria, Corresponding author: Iskren Spiridonov, Tel. +359 884 91 92 23, e-mail: i_spiridonov@abv.bg

Abstract. *Since no data have been available in the special literature, a study has been performed about the influence of the process type (conventional CtFilm or CtPlate) on the print contrast value and optimal inking at offset printing. In the industry, especially in packing there are a lot of examples of common use of both technologies – CtPlate and CtFilm. Some printing houses use corrections of tone value curves to compensate the difference between CtFilm and CtPlate, but this method does not always lead to predictable color reproduction quality. The results in this research show that under equal printing conditions, but using different technologies (CtPlate and CtFilm), the optimal inking values are the same, however there is a considerable difference in the print contrast values. This difference indicates that defining of optimal inking for a particular technological situation is obligatory, but not enough condition for obtaining good quality prints. For example, under the same printing conditions- the same paper and printing machine, however applying different imaging technologies, the optimal inking will be the same, but the images in the dark, middle and light tones will be considerably different. For precise determination of influence of plate making technology we have investigated the changes in 2D and 3D color gamuts volume and shape.*

Key Words: Print Quality, Offset Print, Print Contrast, Computer to Plate, Computer to Film, Color gamut

I.   Introduction

A big number of printing houses (using offset printing method) are steel using both technologies – Computer to Plate (CtP) and Computer to Film (CtF). In the perfect case it must be no difference in the quality parameters of printed sheets no matter of used technology – CtP or CtF, but in the practice that is not happened. In many cases at the same print conditions (same printing press, inks, paper, screen frequency), but different printing plates (conventional – produced by CtF, contact copying and CtP) occurs a visual difference between printed images. To minimize this undesired difference, some of the printing houses are making corrections of tone value curves on the RIP of CtP to compensate the difference between two technologies. In many cases this correction method does not lead to predictable results.

That's why there is important to investigate the influence of the method of producing printing plates - conventional (CtFilm, contact copying of film to printing plate) or direct imaging - CtPlate on the accuracy of color reproduction and gradation. There are a number of parameters that can be measured to make that comparison [1, 2]. The print contrast is parameter, which give useful information especially for comparing quality for different printing situations. Printing contrast [3] is used for determination of optimal inking value, relation of ink transfer for printing halftone and solid areas, quality and comparison of different inks and papers, color accuracy and gradation and etc.

II.   Materials and methods

The main goals of this research is to compare (under the same offset printing conditions) the values of Print Contrast - C on printing sheets obtained by two different type of printing plates (conventional printing plates obtained by contact copying of film – CtFilm and printing plates obtained by direct imaging - CtPlate). The second goal of this study is to define and compare optimal inking expressed by Dv for these two cases – CtFilm and CtPlate. The third goal of this research is to investigate the influence of plate making technology on color gamut of printed images.

The type of paper used for this research is 200 g/m2 glossy coated paper, printed on sheet-fed offset printing press.

III. Results and discussion

A test form that have been used contains many different control strips and measuring components: 100% solid patches for cyan, magenta, yellow and black – for control of optical density – Dv and colour characteristics, 80% patches for estimating print contrast, patches for estimating of dot gain and grey balance [4], strip which contains raster lines in different slope for doubling and slur control,

registration marks, test charts containing 1500 patches for ICC color profiles with different GCR and TAC values and etc. All measuring components are with screen value 60 cm^{-1} (150 lpi).

For this experiment were used two sets of positive printing plates:

1. Conventional printing plates Kodak PP3 obtained by contact copying of film.

2. CtP Plates obtained on Luescher XPose 130 device.

All two devices – CtP and CtF have been calibrated and linearized and experiment [5] was carried out under standard conditions.

For conventional positive plates the control of the plate exposure is done in accordance of FOGRA method with a microline patch on a control wedge. The Ugra Plate Control Wedge 1982 and Fogra PMS-1 scales have been used to define optimal exposure time to copying film on printing plate in contact copier [6,7,8]. The time ratio without/with dispersion sheet/film is 60%/40% from exposure time.

All two sets of printing plates have been measured and checked by ICPlate II device for tone value transfer accuracy. The deviation between measured values on CtPlate plates and defined on file (control patches 5%, 10%, 15%,…, 100%) were less than plus/minus 1%. The tonal change from the film copy to the printing plate should lie within narrow tolerances. In this case for these conditions and screen frequency, the decrease in tone value from film to printing form was approximately 3-5% in the middle tone.

The paper, which has been used, is 200 g/m^2 glossy coated paper. Colour characteristics of used papers (print substrate colour) are in accordance with ISO 12647-2 [9] tolerances (L±3, a±2, b±2). The printing inks, which have been used, are manufactured by "Huber gruppe".

A spectrophotometer/densitometer of type SpectroEye of GretagMacbeth has been used for measuring of optical density and the colour characteristics in the CIE Lab colour system. All measurements are in accordance with ISO 12647-1[10]: D50 illuminant, 2° observer, 0/45 or 45/0 geometry, black backing and in accordance with [11,12,13]. The test chart ECI 2002 is measured with i1Profiler software and X-rite i1i0 spectrophotometer and automatic scanning device.

The offset printing machine, which has been used, is five colour sheet-fed HEIDELBERG SM 74.

In the above-mentioned conditions and according [9, 10, 14, 15], were printed two series of samples characterized by gradual smooth changes in ink quantity - from underinking to overinking. This two series of test samples were printed at the same print conditions (same inks, paper, sheet-fed press), with two different type of positive printing plates (CtPlate and conventional, described above in the text). From the already printed paper fortuitously are taken printed sheets, which have not a slur, doubling or other defects.

In order to achieve the goals of the experiment, series of measurements of Dv and Print Contrast have been performed (from underinking to overinking) for defining the optimal inking by the method of maximum print contrast for Cyan, Magenta, Yellow and Black for two different types of offset printing fofrms. A statistical analysis of the results was performed.

The experimental data, representing the changes in the print contrast – C (the ordinate axis on the figures) for the CtPlate and CtFilm, depending on the Dv for the process colors, are given in Figures 1, 2, 3 and 4.
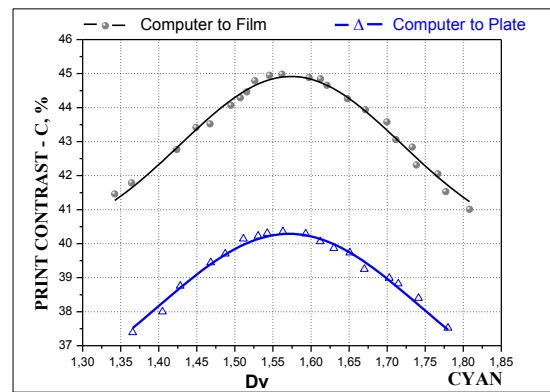
Figure 1. *Comparison of Print Contrast for Cyan*
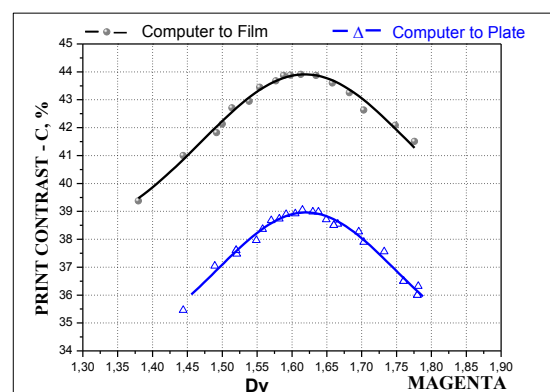
Figure 2. *Comparison of Print Contrast for Magenta*

The graphs show clearly visible peaks, visualizing the maximal value of the print contrast and its corresponding D$_v$. By the method of maximal print contrast the values of optimal quantity of printing inks defined through D$_v$ have been

experimentally defined for the glossy coated paper. The results are shown in Table 1.
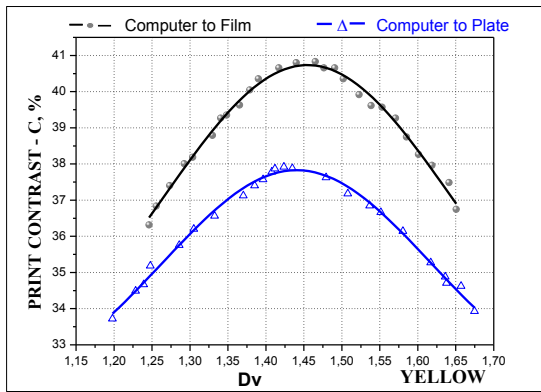
Figure 3. *Comparison of Print Contrast for Yellow*
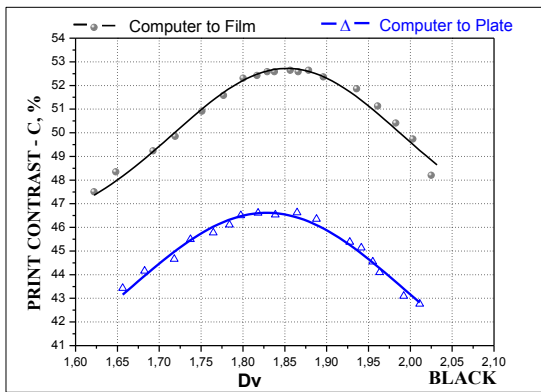
Figure 4. *Comparison of Print Contrast for Black*

The graphs from figures 1-4 shows, that for all two types of printing plates the experimental defined values for optimal inking – Dv are equal, but occurs a essential difference in contrast values.

Table 1. *Experimental defined values for optimal quantity of printing inks for glossy coated paper.*

Type of paper	Dv, (optical density of 100% solids)			
	Cyan	**Magenta**	**Yellow**	**Black**
Glossy coated	1.57	1.63	1.45	1.85

Experimental defined values for maximal value of print contrast – C, and difference in C measured on printing sheets obtained with two different types of printing plates are shown in table 2.

Analyses of the experimental data and graphs shows:

1. There are relatively big differences in print contrast - C for the each of process colours between

printed sheets with two used types of plates. The differences are between 3 and 6.5% of Contrast. The biggest difference is for Black - 6.5%, for Cyan and Magenta – 4.5% and 5% and for Yellow – 3%. These differences in Contrast for all process colours will result in different tonal and colour reproduction on printed sheets with two sets of printing plates. That is clearly visible from the images used for visual evaluation of the sheets.

Table 2. *Experimental defined maximal values of print contrast – C, and difference in C measured on printing sheets obtained with two different type of printing plates (conventional printing plates obtained by contact copying of film – CtFilm and printing plates obtained by direct imaging - CtPlate)*

Type of imaging technology	Maximal value of Print Contrast – C,%			
	Cyan	**Magenta**	**Yellow**	**Black**
1. Computer to Film (CtF)	45	44	41	53
2. Computer to Plate (CtP)	40.5	39	38	46.5
3. Difference in Print Contrast (1-2)	4.5	5	3	6.5

That means, that in same printing conditions the implementation of these two different plate making methods results in different colour reproduction of images, different colour accuracy, different dot gain, etc.

2. The print contrast – C have a maximal values (peaks) at the same value of Dv for conventional and digitally imaged plates – CtPlate. The results show that the value of optimal inking quantity expressed by Dv for two technologies is equal.

Investigation and comparison of color gamuts in dependence of plate making technology.

The graphically presentation of color gamut – 3D and 2D, gives valuable and comprehensive information for the colors, that can be reproduced in specific printing and plate making conditions. In this study for precise determination of influence of plate making technology we have investigated the changes in 2D and 3D color gamuts volume and shape.

The comparison of 3D graphs of color gamuts shows (fig. 5), that CtPlate and Ctfilm are relatively equal each to the others. CtPlate color body has generally biggest color gamut than CtFilm in all tones areas by L = 0 to 100. The main reason is that the CtPlate technology gives 4-5% higher tone values on printing plates of tones of C, M, Y, K.
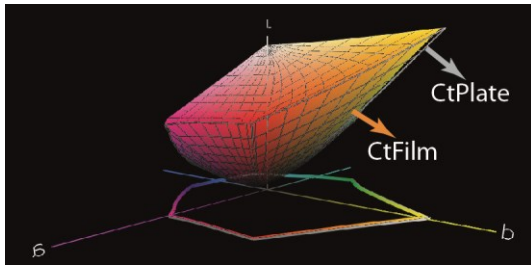
Figure 5. *3D presentation of color gamuts in dependence of plate making technology in CIE Lab, 320% TAC, GCR3 (graph is generated by Chromix Color ThinkPro)*
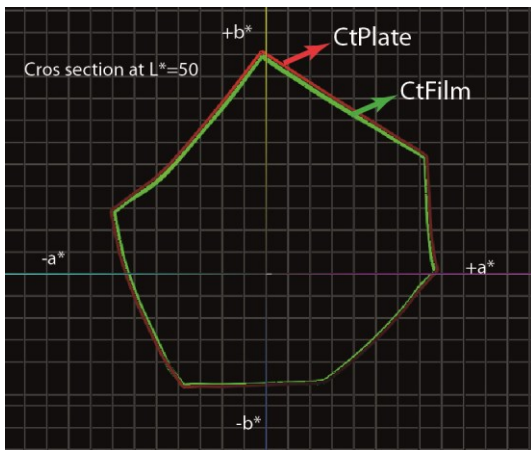
(a - midtones) graph is generated by Chromix Color ThinkPro
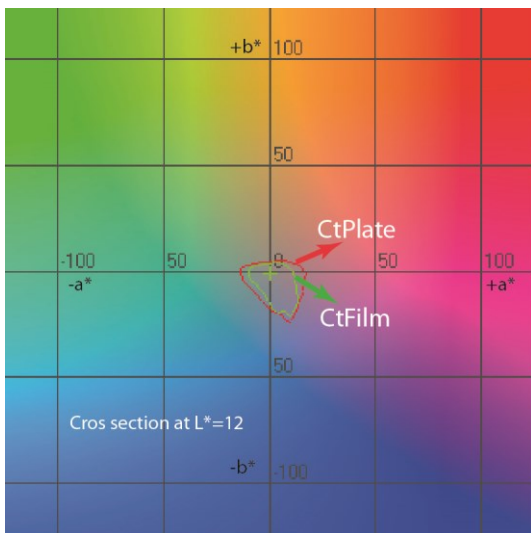
(b – dark tones) graph is generated by GM ProfileMaker

2D graphical presentation of gamuts at different cross-section of CIE L* coordinate are used to collect more detailed information for analyses and comparison of reproduction accuracy and characteristics of any combination of specific combination of printing and plate technology / printing substrate / printing inks / separation settings like GCR, TAC etc.
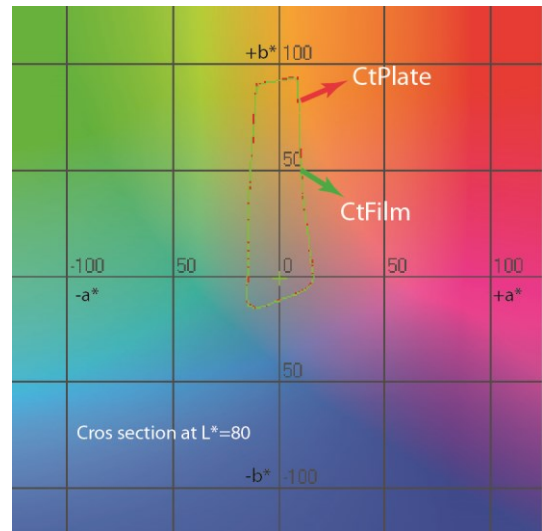
(c - highlights) graph is generated by GM ProfileMaker

Figure 6. *2D presentation of color gamuts in dependence of plate making technology in CIE Lab: (a) mid-tones by L = 50, 320% TAC, GCR3; (b) by L = 12, dark tones, 320% TAC, GCR3; (c) by L = 80, highlight tones, 320% TAC, GCR3*

A 2D color gamuts in dark, middle and highlight tones are presented at figure 6 (a, b, c) for more comprehensive characterization the effect of CtPlate and CtFilm technology on colors. The comparison of 2D color gamuts shows that plate technology affects mostly dark and middle tones. There is about 4-8% difference in surface areas between CtPlate and CtFilm area. Meanwhile, the difference in highlights is only about 0,5%.

IV. Conclusions

The results achieved are important from practical point of view. They lead to the conclusion that it is necessarily taking into strict consideration the concrete plate making method, because relatively big differences in print contrast from 3% to 6.5 % are occurred.

In an experimental way a well-grounded proof has been achieved for a substantial difference in color reproduction for two plate making methods with comparison of print contrast.

The difference in print contrast between two technologies comes from the tonal change from the film copy to the printing plate. In this case the decrease in tone value from film to printing form was approximately 3-5% in the middle tone. In CtPlate the accuracy in tone transfer is less than 1%.

This difference reflects on print contrast value and leads to difference in colour reproduction on printing sheets between CtPlate and CtFilm plate making.

According to the results of investigation of color reproduction accuracy, switching the plate making technology leads to changes in color gamut volumes and shapes (2D and 3D). The changes affect mostly dark and middle tones. There is about 4-8% difference in surface areas and volumes between CtPlate and CtFilm area.

Some printing houses use corrections of tone value curves to compensate the difference between CtFilm and CtPlate, but in many cases this method does not lead to predictable results.

For accurate human perception of printed images, it is very important to achieve maximal predictable and precise colour reproduction no matter of plate technology. The best performance from the viewpoint of accuracy of colour reproduction is the generation of ICC colour profiles for concrete technological conditions. The experience has shown that during the ICC profile application, both concrete plate making conditions are taken into consideration and there is not a visual difference in colour reproduction and printed images.

Acknowledgements

References

[1] Bugnon, T., Brichon, M., Hersch, R., "Model-based deduction of CMYK surface coverages from visible and Infrared spectral measurements of halftone prints", Proc. SPIE Vol. 6493, 649310-1 - 649310-10 (2007).

[2] Neumann, E., Bohan, M., "Ink Optimization: An Evaluation of the Different Strategies", GATFWorld, Vol. 20 (2), 46-48 (2008).

[3] Kachin N., Spiridonov I., Printing Processes, Part I. Theoretical Bases, Pleiada, Sofia, 2000

[4] Spiridonov, I., Determination of the deviations and variations tolerances of the process-colour solids from the OK Print in offset printing method, IC Journal (Germany), (Journal of International Circular of Graphic Education and Research), vol. 6, 2013

[5] Spiridonov, I., „Comparison of Optimal Inking of Process Colors Obtained by Two Different Methods for LWC Paper Printed on Heatset Offset Press", 2013, vol. 6, 53-60, TAGA's J. of Graphic Technology – USA

[6] fogra praxis report Nr.28, Die FOGRA-PMS, Druckkontrolleiste

[7] fogra praxis report Nr.34, FOGRA PMS I und UGRA-Offsettestkeil 1982

[8] Standardisierung des Offsetdruckverfahren (Das Wichtigste in Kuerze), Technik+Forschung Flachdruck, 1992

[9] ISO 12647-2, Graphic technology - Process control for the production of half-tone colour separations, proof and production prints - Part 2: Offset lithographic processes

[10] ISO 12647-1, Graphic technology - Process control for the production of half-tone colour separations, proof and production prints - Part 1: Parameters and measurement methods

[11] ISO 5-3, Photography and graphic technology - Density measurements - Part 3: Spectral conditions

[12] ISO 5-1, Photography and graphic technology - Density measurements - Part 1: Geometry and functional notation

[13] ISO 5-4, Photography and graphic technology - Density measurements - Part 4: Geometric conditions for reflection density

[14] ISO 13656, Graphic technology - Application of reflection densitometry and colorimetry to process control or evaluation of prints and proofs

[15] ISO 2846-1, Graphic technology — Colour and transparency of ink sets for four-colour-printing

DRYING OF DANDELION ROOTS

A.Lupaşco, M. Bernic, E. Rotari, M. Guţu

Technical University of Moldova, bd. Stefan cel Mare 168, MD-2004, Chisinau, Republic of Moldova, tel/fax (+373)22 50 99 56, bragalena@rambler.ru

Abstract: *The paper presents the study of the drying process of vegetable matter, especially dandelion roots, with the use of energy intake by convection and combined (convection + microwave). Dehydration kinetics on the first and the second period of drying is analyzed, analysis of the characteristics drying is presented and the influence of thermal agent on the drying speed and drying speed coefficients in the two periods is investigated.*

Keywords: drying, dandelion roots, convection, microwave convection, drying speed, drying constant

I. INTRODUCTION

Vegetable materials are complex not only by their chemical structure, but also by the functions they perform. It is known that in nature, plants are the perfect laboratory for transfer of organic matter from the inorganic, without which human life would be impossible [2].

Keeping quality of vegetable products is an essential condition for ensuring human health.

In the carried study particular attention is given to the use of plants from the family *Compositae* especially roots of the dandelion.

One of the main stages of processing of vegetable raw materials consists of organizing of their proper harvest and post-harvest works. In particular, the collection of medicinal plants is necessary to establish the exact harvesting period, to respect optimal harvest hours, quick decision making on keeping material fresh vegetable products and their harvest until the drying process starting [3].

Currently drying of roots of the dandelion is performed by classical methods: sun drying, drying in the shade, drying in the ovens, drying in the drying rooms with convective heat input [2, 3, 4, 5, 6, 7]. These methods have a lot of disadvantages such as: long duration of drying, large work surfaces, etc.

Therefore, for the correct performance of the drying process is necessary a clear record of the complex phenomena arising in vegetal systems.

II. DESCRIPTION OF EXPERIMENTAL EQUIPMENT AND RESEARCH METHOD OF DRYING PROCESS KINETICS

For research were selected dandelion roots harvested in August-September, due to the high content of chemical substances [5].

Drying of dandelion was carried out on an experimental installation for the study of the drying kinetics of vegetal material with different energy input: convection and combined (microwave convection under oscillating regime). The installation operates in the following manner (fig. 1): vegetable material sample is placed in the chamber (6), on the support (5) fixed on the electric scale (3). Mass decrease recorded by electric scale (3) is registered on the computer (9). The hot air is circulated at the bottom of the working chamber through the air duct (2), so that the product subjected to drying to be in direct contact with the air flow. The air aspirated by the fan (11) is blown through the heater (12) where is heated up to drying temperature (60 – 100 ºC).

The thermal agent is removed from the working chamber thru air duct (4). Temperature of thermal agent is adjusted with the electronic system of control „thermostat CIMU-UMU-1". To record thermal agent temperature in the air duct is installed thermocouple (13). For combined drying with use of SHF currents the installation is equipped with a magnetron (7). Electric energy consumption is recorded using electric meter (10).

During the experiments were recorded: air parameters at the entrance of calorifier (t_0 the initial temperature and φ_0 relative humidity) and at the exit of calorifier t_1 [1]. Drying of Dandelion roots with the use of microwaves has been performed in three modes of oscillation 5 s, 10 s and 15 s with a 10 s pause between pulses. Initial mass of the sample was $150 \pm 0,1$ g.

Thermal agent temperature varies from 60 to 100 ºC, with step of 10 ºC.

According to the initial moisture of the investigated product, the humidity reported on dry matter at any moment of time was determined [2, 4]:
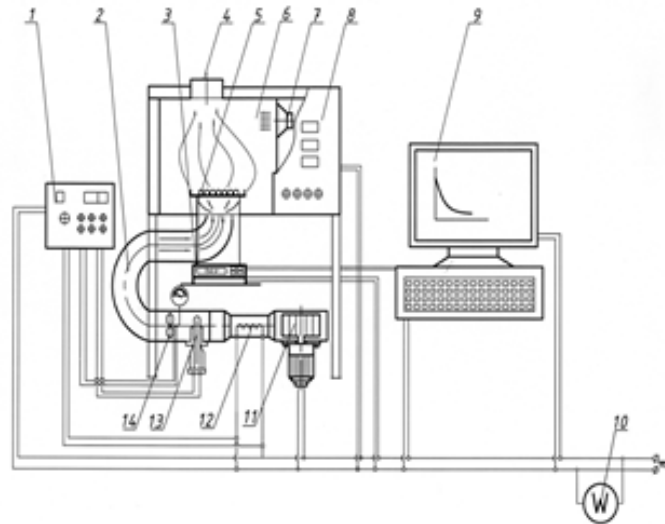
Figure 1. *Scheme of drying experimental installation:*
1 - command and control system; 2, 4 - air duct; 3 - electric scales; 5 - product support; 6 - drying room; 7 - magnetron, 8 - control panel; 9 - computer, 10 - electric meter, 11 - Fan, 12 - electric heater, 13 - thermocouple, 14 - anemometer.

$$u^c = \frac{G_{apă}}{G_{usc}} \cdot 100 = \left(\frac{G_i}{G_{usc}} - 1\right) \cdot 100 \ . \qquad (1)$$

The final weight of the analyzed sample, until is necessary to perform the drying process was calculated using the formula:

$$G_{fin} = \frac{u^c_{fin} \cdot G_{usc}}{100} + G_{usc} = G_{usc}\left(\frac{u^c_{fin}}{100} + 1\right), \qquad (2)$$

where: u^c_{fin} - is the final moisture content in the product reported on dry matter.

Based on obtained results

Drying curves and drying speed curves were plotted which were determined by the discrete differentiation of the functions tabulated in accordance with the relationship [6]:

$$\frac{du}{d\tau}\left(\overline{u_2}\right) = \frac{-11\overline{u_4} + 3\overline{u}_3 + 7\overline{u_2} - \overline{u_1}}{20 \cdot n}, \qquad (5)$$

- for the penultimate point:

$$\frac{du}{d\tau}\left(\overline{u_{n-1}}\right) = \frac{-\overline{u_n} + 7\overline{u}_{n-1} - 3\overline{u_{n-2}} + 11\overline{u_{n-3}}}{20 \cdot n} \qquad (6)$$

- for the last point:

$$\frac{du}{d\tau}\left(\overline{u_n}\right) = \frac{-9\overline{u_n} - 17\overline{u}_{n-1} - 13\overline{u_{n-2}} + 21\overline{u_{n-3}}}{20 \cdot n} \qquad (7)$$

Kinetic characteristics of the drying process namely, the drying speed coefficient in the first period of drying K1 and the drying coefficient in the

$$\frac{du}{d\tau}\left(\overline{u_0}\right) = \frac{\displaystyle\sum_{m=-p}^{p} m \cdot \overline{u_m}}{\displaystyle\sum_{m=-p}^{p} m^2} , \qquad (3)$$

where: $\frac{du}{d\tau}\left(\overline{u_0}\right)$ - is the value of drying speed for the moisture content average u_o, %/ time (min);

$\overline{u_o}$ - the average value of moisture content moisture in the mass of material before and after the moment of time at which the humidity was u_o, %;

m = -2; -1; 0; 1; 2.

Value of the drying speed for the first and last two points was determined with the formulas:
- for the first point:

$$\frac{du}{d\tau}\left(\overline{u_1}\right) = \frac{-21\overline{u_4} + 13\overline{u}_3 + 17\overline{u_2} - 9\overline{u_1}}{20 \cdot n}, \qquad 4)$$

- for the second point:

second drying period K2 have been calculated according to the formulas 8 and 9 [4]:

$$K_1 = \frac{du/d\tau}{S \cdot (x_s - x_0)}, \frac{\%}{s \cdot m^2 \cdot kg/kg\,air}, \qquad (8)$$

where: $du/d\tau$ – constant speed of drying (speed in the first period), % /min;

S – area of contact of drying roots with drying agent, m^2;

x_0 – The moisture content of the air at the inlet in the drying installation, kg / kg dry air;

x_s – the moisture content of the saturated air at drying temperature, kg / kg dry air (on the material surface).

x_0 şi x_s is determined from Ramzin's diagram, knowing air parameters: temperature and relative humidity.

$$K_2 = \frac{du/d\tau}{u'_{cr.} - u_{ech.}},\qquad(9)$$

where: $du/d\tau$ − drying constant speed (speed in the first period), %/s;

$u'_{cr.}$ − reduced critical humidity of dandelion root determined by the drying speed curve, %;

$u_{ech.}$ − equilibrium humidity of dandelion root relative to dried substance, %.

Based on the obtained data were presented correlation between the drying speed coefficients for the first and second period and thermal agent temperature.

III. RESULTS AND DISCUSSION

According drying curves of dandelion roots (fig. 2.a) by convection, is observed that with increasing temperature of the drying agent, drying time is reduced. Thus, at heat agent temperature of 60 °C, from 230.3% initial moisture up to 7,2% final moisture, duration is 130 min, however, starting with temperatures of 70, 80, 90 and 100 °C the drying process arising respectively in 115, 100, 90 and 75 min. Hence, raising the temperature of the drying from 60 to 100 °C decreases the duration of the drying process 1,73 times.

Figure 2. *Drying curve (a) and drying speed curve (b) of dandelion root by convective method*

Drying speed curves of dandelion roots were obtained by derivation of tabulated function of drying curve (Fig. 2a and 3.a.). The curve form corresponds to the form described in the literature, for capillary-porous colloidal bodies [2, 4].

The analysis of drying speed curves of dandelion roots (Fig. 2 b and 3 b), demonstrates that the use of convective heat input confirm known theoretical concepts on the mechanism of mass transfer in the drying process. Are highlights three periods: heating, constant speed drying and decreasing drying speed.

Maximum drying speed increases with increasing drying agent temperature as can be seen on the diagram (Fig. 2. b). Therefore, at 60 °C it is 3.50 %/min and at 100 °C - 4.60 %/min. The maximum speed of moisture removal increases with the drying agent temperature from 60 °C to 100 °C for approx. 1.57 times.

As shown in Figure 3.a is observed that with increasing temperature of drying agent from 60 °C to 100 °C the drying time is reduced. For example, at

60 °C heat agent temperature the drying process is 55 min. And at 100 ° C heat agent temperature - 35 min. It results, that drying process of dandelion roots is reduced 1,57 times by increasing heat agent temperature.

Maximum drying speed increases with increasing drying agent temperature (fig. 3 b). Thus, at 60 °C it is 7,66 %/min and at a temperature of 100 °C, corresponding to 11,01 %/min. So the maximum speed of moisture removing increases 1.43 times with temperature increasing from 60 to 100 °C.

Based on drying curves and drying speed curves drying speed constants were calculated in the first and second period [3, 5]. The influence of drying agent temperature on constants in the two periods is shown graphically in Fig. 4 *a* and *b*.

As shown in Fig. 4. *a* with drying agent temperature increasing, drying coefficient K1 is decreasing according to a linear law. However, it is noted that the values of K1 are higher compared to convection drying regime of approx. 1.62 times for combined drying in mentioned regime.
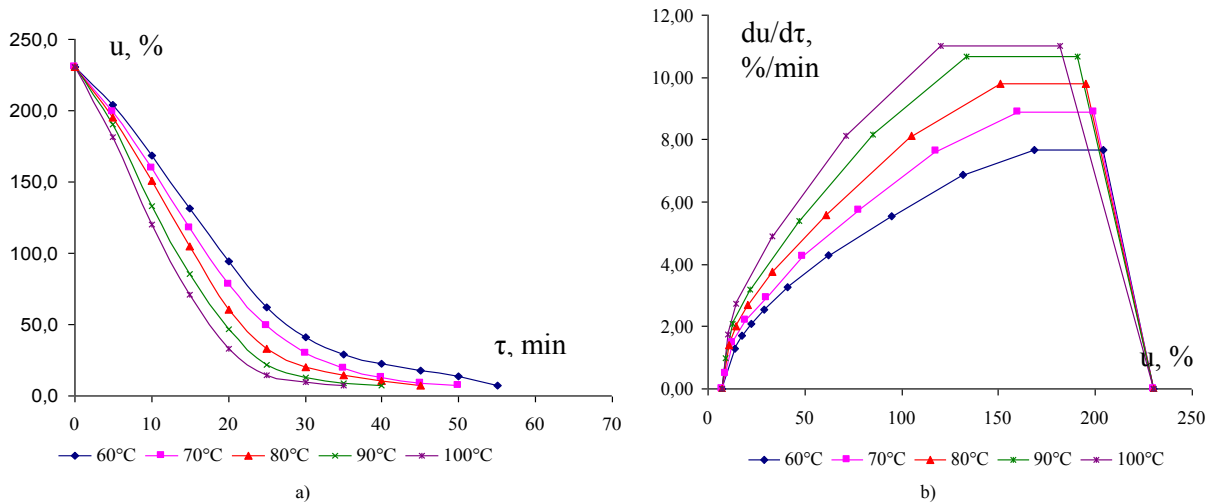
Figure 3. *Drying curve (a) and drying speed curve (b) of dandelion root by combined method in oscillation regime of 15s /10s*

Decreasing K1 values for combined drying influenced by temperature increase thermal agent is faster than convection drying.

If drying constant K1 for the first period decreases with drying agent temperature for both methods, then drying constant K2 increases according to the same linear regularities (Fig. 4. b). Increasing the temperature of the drying agent within the limits of 60-100 °C has caused an increase of K2 drying constant 2.2 times for drying by convection and 4 times for combined drying.
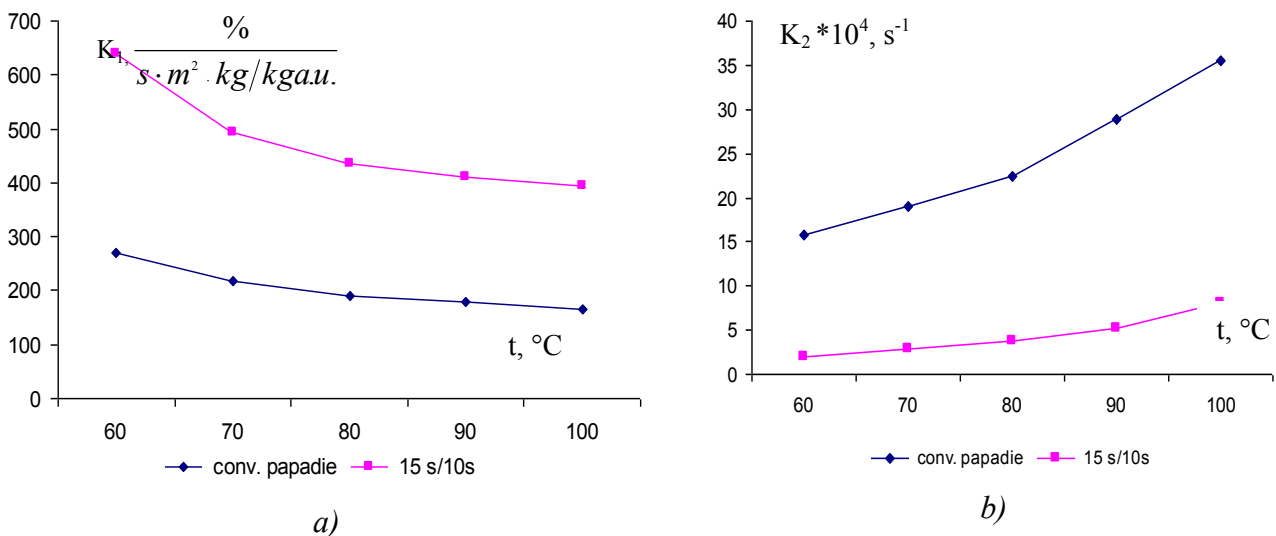
Figure 4. *The influence of drying agent temperature on drying speed constants during the first period (a) and the second period (b) for combined and convective drying.*

Decreasing K1 values for combined drying influenced by temperature increase thermal agent is faster than convection drying.

If drying constant K1 for the first period decreases with drying agent temperature for both methods, then drying constant K2 increases according to the same linear regularities (Fig. 4. b). Increasing the temperature of the drying agent within the limits of 60-100 °C has caused an increase of K2 drying constant 2.2 times for drying by convection and 4 times for combined drying.

IV. CONCLUSIONS

Analyzing the above data it was found that application of microwave energy to dry dandelion roots cause intensification of this process. This was demonstrated by the increase of the drying speeds constants in the first and second period, due to increasing the drying speeds. So combined drying: convection and microwave can be considered an optimal drying method of the dandelion roots.

REFERENCES

1. *Lupaşco A., Bantea-Zagareanu V., Rotari E. Drying method of the burdock roots by applying S.H.F fields. In: Physics and technique. Processes, models, experiments. 2010.*

2. *Ginzburg A. S. Osnový teorii i texniki sushki pishhevýx produktov.* – M.: Pishhevaya promýshlennost`, 1973. – 528 s.

3. *Ghinzburg A., Savina I. Massovlagoobmennýe xaraktepistiki pishhevaya produktov.* – M.: Lyogkaya i pishhevaya promýshlennost`, 1982, p. 280.

4. *Lýkov A. V. Teoriya sushki.* – *M.:* Ènerg*iya.*, 1968, p. 47.

5. **Vorob`ev M. P.** *Lekarstvennýe rasteniya.* Yaga Rossii, ZAO Kniga 2010, p. 544.

6. *Verzhbiczkij V. M. Osnový chislennýx metodov uchbnik dlya vuzov*. – M. Výsshaya shkola, 2005, p. 480.

7. **Ginzburg A. S.** *Sushka pishchevykh produktov*. M.: Pishchevaya promyshlennost', 1973, p. 528.

EFFECT OF EXTRUSION VARIABLES ON THE DYNAMIC VISCOSITY OF EXTRUDED LENTIL FLOURS

A. Simitchiev[1], T. Petrova[2], M. Ruskova[2], N. Penov[1]

[1]*University of Food Technology - Plovdiv, Bulgaria*
[2]*Food Research and Development Institute - Plovdiv, Bulgaria*

Abstract :*Lentil semolina was extruded in a laboratory single screw extruder (Brabender 20 DN, Germany). Effects of moisture content, barrel temperature, metering zone temperature, screw speed, and screw compression ratio on dynamic viscosity of the extruded lentil flours were studied. Response surface methodology with combinations of moisture content (18, 22, 25, 28, 32%), metering zone temperature (136, 150, 160, 170, 184°C), barrel temperature (136, 150, 160, 170, 184°C), screw speed (132, 160, 180, 200, 228 rpm), and screw compression ratio (1:1, 2:1, 3:1, 4:1, 5:1) was applied.*

The dynamic viscosity of the extruded lentil flours was measured with a viscometer "Brookfield RV-DV II + Pro", USA. The dynamic viscosity values varied from 25 to 95 mPa.s. The linear effect due to the moisture content had mostly influence on the dynamic viscosity.

Keywords: Dynamic viscosity, Extrusion, Lentil, Rheology.

I. Introduction

Extrusion cooking technology plays a central role in the modern cereal-based food industry especially for the production of snack and breakfast cereal products from maize, wheat, rice, and oats. Maize flour is widely used to elaborate extruded products, while application of extrusion to legume flours is a relatively new area of investigation with the exception of soy bean [10, 14]. This processing method is not being commercially used for legumes seeds owing to the perception that legumes do not expand well in extrusion. Limited information is available on changes in physicochemical and functional properties during extrusion of beans [5].

Development of new products and optimization of existing processes requires understanding the interactions between ingredients, process parameters and equipment design. The physical and chemical complexity of many foodstuffs, however, means that such relationships can rarely be predicted in advance [7].

Rheology is used in food science to define the consistency of different products. Rheologically the consistency is described by two components, the viscosity and the elasticity. In practice, therefore, rheology stands for viscosity measurements, characterization of flow behaviour and determination of material structure. Basic knowledge of these subjects is essential in process design and product quality evaluation.

Food products are usually non-Newtonian liquids. These are materials, which cannot be defined by a single viscosity value at a specified temperature. Their viscosity must always be stated together with a corresponding temperature, shear stress and shear rate [1, 2, 3, 4].

The rheological properties of extruded blend dispersions, which influence the breakfast porridge-making process, are essential for producing high-quality products. Recent studies concentrated on extrusion cooking processing effects for creating new products and evaluation of physical and chemical properties [6, 15]. Only a few studies are conducted on the steady-state-flow properties of extruded blend dispersions [9, 13].

The object of this work was to study the effect of extrusion conditions on the dynamic viscosity of extruded lentil flours.

II. Materials and methods

Material and feed preparation for extrusion

Representative sample of commercial lentil cultivar, namely Ilina, was obtained from Dobroudja Agricultural Institute, General Toshevo, Bulgaria.

Lentil seeds were ground using a hammer mill and passed through standard sieves. Prepared particle size of lentil semolina was about 0.5 mm. Lentil semolina was mixed with distilled water to be obtained various moisture contents (Table 1). The wet materials were placed and kept in sealed plastic bags for 12 h in a refrigerator at 5°C. The samples were tempered for 2 h at room temperature prior to extrusion.

Extrusion process

Lentil semolina was extruded in a laboratory single screw extruder (Brabender 20 DN, Germany). The compression ratio of the screw was 1:1, 2:1, 3:1, 4:1, 5:1 according to the experimental design (Table 1). The extruder barrel (476.5 mm in length and 20 mm in diameter) contained three sections and

independently controlled die assembly electric heaters. The screw speed was 132, 160, 180, 200, 228 rpm. The temperature of the feed zone was 150ºC, that of the metering zone was 136, 150, 160, 170, 184ºC, and that of the extruder die was 136, 150, 160, 170, 184ºC. The feed screw speed was fixed at 70 rpm and the die diameter was 5 mm.

Table 1. *Independent Variable Values and Corresponding Levels*

Independent Variables	Levels				
	- 2.378	- 1	0	+ 1	+ 2.378
X1, Moisture (W), %	18	22	25	28	32
X_2, Barrel Temperature (Tm), °C	136	150	160	170	184
X_3, II^{-nd} Zone Temperature (T_2), °C	136	150	160	170	184
X_4, Screw Speed (n), rpm	132	160	180	200	228
X_5, Screw Compression Ratio (K)	1:1	2:1	3:1	4:1	5:1

Extruded lentil flours and preparation of model systems (pastes)

The extrudates were crushed into powder in a laboratory hammer mill with a size range of 0.10 - 0.25 mm to be obtained the extruded lentil flours.

Each one of the model systems was prepared by mixing extruded lentil flour and water in the ratio 1:10.

Dynamic viscosity measurement

The extruded lentil model system was tempered for 30 minutes at 70°C in a thermostat.

Preliminary experiments were conducted to establish the range of shear rates in which to measure the dynamic viscosity of the pastes. The experiments shown that the changes in the shear rate doesn't affect the dynamic viscosity – therefore all the products exhibit non-newtonian behaviour.

The dynamic viscosity of each paste was measured in threefold with a "Brookfield RV-DV II + Pro" viscometer (Spindle №2; Speed 100 rpm) and after that was calculated the average value.

Experimental design and data analysis

A central composite rotatable design (Table 1) was used to show interactions of moisture content, metering zone temperature, barrel temperature, screw speed, and screw compression ratio on the extrudate in 52 runs of which 32 were for the factorial points, 10 were for axial points, and 10 were for centre points [12].

A second order polynomial model for the dependent variable was established to fit the experimental data:

$$y = b_0 + \sum_{i=1}^{n} b_i x_i + \sum_{i=1}^{n} b_{ii} x_i^2 + \sum_{i=1}^{n} \sum_{j=1}^{n} b_{ij} x_i x_j \qquad (1)$$

where b_0, b_i, b_{ii}, and b_{ij} are constant coefficients.

SYSTAT statistical software (SPSS Inc., Chicago, USA, version 7.1) and Excel were used to analyze the data results.

III. Results and discussion

The average dynamic viscosity values of the extruded lentil flours are given in Table 2.

The results of the statistical analysis of variance (ANOVA) for the dynamic viscosity show that 10 effects have p-values less than 0.05, indicating that they are significantly different from zero at the 95.0% confidence level. The R-squared statistic is 0.81; the standard error of the estimate - 8.78, the mean absolute error - 4.70. The R-squared is defined as the ratio of the explained variation to the total variation and is a measure of the degree of fit [8]. As the R-squared value for the model is more than 80% it can be considered for further analysis.

The regression equation describing the effect of extrusion variables on the dynamic viscosity of the extruded lentil flours is given in Table 3. The coefficients in the regression equation can be used to examine the significance of each term relative to each other when used with coded values. Statistical analysis shows that feed moisture content, barrel temperature, metering zone temperature, and screw compression ratio have an effect on the dynamic viscosity (p < 0.05), whereas screw speed has no effect on the viscosity.

Each of the estimated effects and interactions are shown in the standardized diagram (Fig. 1). It consists of horizontal blocks with lengths proportional to the absolute values of the estimated effects, divided by their standard errors. A vertical line that represents the value of the Student criterion at 95 % confidence level has been added to facilitate the chart. The linear effect due to the moisture content of lentil semolina mostly influences on the dynamic viscosity followed by squared and linear effects due to the screw compression ratio.

The residual quantity distribution for the regression model of the dynamic viscosity is

uniformly distributed around zero and no values exceed two times the standard error (Fig. 2).

Based on the results from ANOVA after removing the insignificant effects the following regression equation is obtained:

Table 2. *Dynamic viscosity of extruded lentil flours*

№	η, mPa.s	№	η, mPa.s	№	η, mPa.s	№	η, mPa.s
1.	53.8	14.	94.3	27.	51.5	40.	65.7
2.	95.1	15.	55.8	28.	59.4	41.	25.4
3.	51.8	16.	80.3	29.	87.1	42.	57.7
4.	78.1	17.	48.2	30.	83.1	43.	75.6
5.	44.0	18.	85.9	31.	88.1	44.	82.5
6.	76.9	19.	44.6	32.	77.6	45.	64.7
7.	73.1	20.	73.2	33.	52.9	46.	76.8
8.	76.2	21.	73.5	34.	89.6	47.	79.3
9.	45.5	22.	86.8	35.	69.6	48.	84.3
10.	80.2	23.	71.6	36.	46.0	49.	78.1
11.	43.2	24.	83.1	37.	87.8	50.	77.3
12.	66.3	25.	60.7	38.	67.2	51.	76.5
13.	50.9	26.	79.6	39.	71.0	52.	78.5
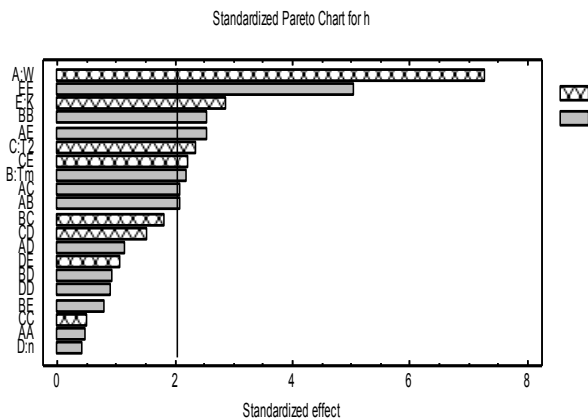
Fig.1. *Estimated effects of regression model coefficients on the dynamic viscosity*
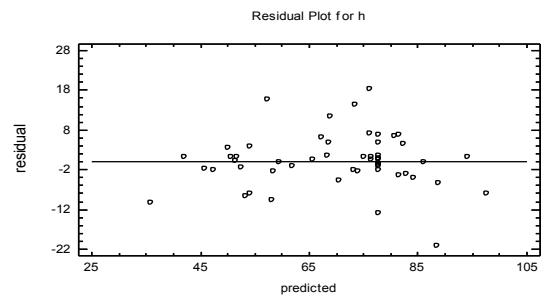
Fig.2. *Residual distribution diagram*

$$\eta = -881.003 + 50.13W + 8.91Tm - 6.47T_2 + 21.30K - 0.11WTm - 0.11WT_2 - 1.31WK - 0.03Tm^2 + 0.34T_2K - 5.79K^2, \text{ mPa.s} \quad (2)$$

The viscosity of a paste depends on a large extent on the degree of gelatinization of the starch granules and the extent of their molecular breakdown. The maximum viscosity value of 95.1 mPa.s is observed for sample 2 (moisture content 28%, barrel temperature 150°C, metering zone temperature 150°C, screw speed 160 rpm, and screw compression ratio 2:1) while the least value of 25.4 mPa.s is recorded for design point 41 (moisture content 25%, barrel temperature 160°C, metering zone temperature 160°C, screw speed 180 rpm, and screw compression ratio 1:1).

As can be seen from Fig. 1, the extrusion parameter of moisture content has the most effective influence on the dynamic viscosity of the extruded flour paste. The viscosity value increases from 52.9 to 89.6 mPa.s (about 40%) with raising the moisture content from 18 to 32% at barrel temperature 160°C, metering zone temperature 160°C, screw speed 180 rpm, and screw compression ratio 3:1 due to the fact that the moisture, acting as a plasticizer during extrusion cooking, reduced the degradation of starch and protein granules which resulted in an increased capacity for water absorption. The similar observations are reported by Pérez et al. [14] for maize/soybean pastes.

When the extrusion temperature increases from 136 to 184°C, the reduction in the viscosity value is observed probably due to the increase in starch and protein degradation.

Table 3.

Regression equation coefficients and analysis of variance for dynamic viscosity of extruded lentil flours

Variables	Coefficients	DF	MS	p values
Constant	-881.003			
A:W	50.129	1	4072.38	0.0000*
B:Tm	8.913	1	377.26	0.0344*
C:T$_2$	-6,473	1	428.94	0.0248*
D:n	0.667	1	14.32	0.6693
E:K	21.301	1	631.01	0.0075*
AA	-0.060	1	16.84	0.6434
AB	-0.108	1	336.05	0.0450*
AC	-0.109	1	339.95	0.0439*
AD	-0.030	1	100.47	0.2622
AE	-1.311	1	495.34	0.0165*
BB	-0.029	1	496.98	0.0163*
BC	0.028	1	253.69	0.0792
BD	-0.007	1	68.15	0.3542
BE	-0.125	1	49.75	0.4277
CC	0.006	1	18.91	0.6237
CD	0.012	1	181.93	0.1345
CE	0.345	1	380.19	0.0337*
DD	-0.003	1	64.41	0.3675
DE	0.082	1	86.79	0.2967
EE	-5.787	1	1959.78	0.0000*

DF – degree of freedom, MS – mean square.

*Significant at 95% CI.
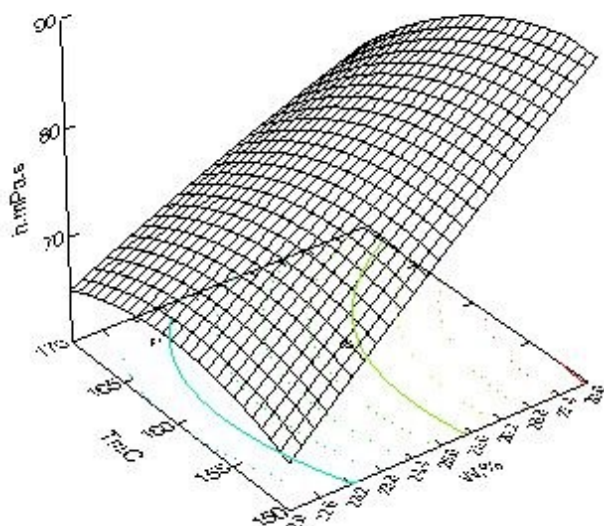
Fig.3. *Dynamic viscosity (η, mPa.s) depending on moisture content (W, %) and barrel temperature (Tm, ℃) at metering zone temperature 160℃, screw speed 180 rpm, and screw compression ratio 3:1*
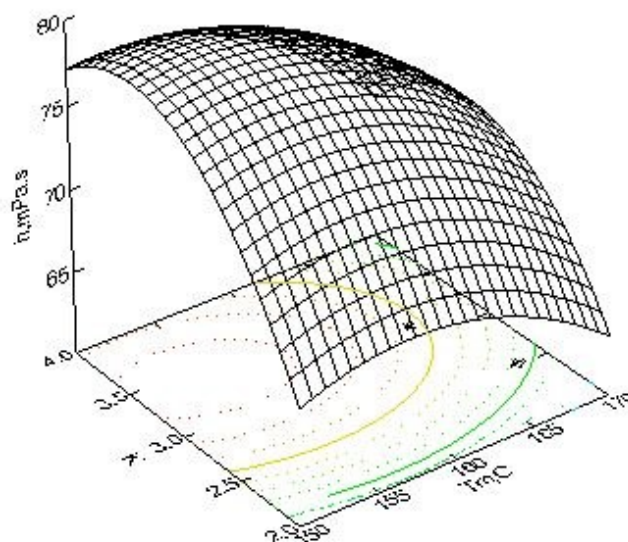
Fig.4. *Dynamic viscosity (η, mPa.s) depending on barrel temperature (Tm, ℃) and screw compression ratio (K) at moisture content 25%, metering zone temperature 160℃, and screw speed 180 rpm*

Increased screw speed (from 132 to 228 rpm) results in an increase in input energy which cause stretching and sometimes fracture of protein-protein matrix, thus, making product less viscous when reconstituted. Likimani et al. [11] report that extrusion induced starch dextrinization which results in reduction of viscosity in gruel.

The effects of some extrusion conditions on the dynamic viscosity of extruded lentil flour pastes are shown in Fig. 3 and 4. As can be seen from the figures, higher values of the viscosity are obtained by the combination of high moisture content and low barrel temperature as well as the combination of high screw compression ratio and low temperature.

IV. Conclusions

The effect of extrusion variables on the dynamic viscosity of extruded lentil flours was studied. All of the studied pastes exhibit non-newtonian behaviour. The linear effect due to the moisture content of lentil semolina had mostly influence on the dynamic viscosity followed by squared and linear effects due to the screw compression ratio. The dynamic viscosity values varied from 25 to 95 mPa.s.

References

[1] Ivanova P., 2012. Izsledvane i razrabotvane na tehnologia i komponentni systavi na produkti ot pypeshi. Disertation, Plovdiv.

[2] Ivanova P., T. Petrova, 2010. Reologicheskaya characteristika fruktoviyh purre na osnove diyni. VII Mejdunarodnoj nauchno-prakticheskoy konferencii "Pishta. Ekologia. Kacehstvo", 23-24 september, 2010. Novosibirsk, 93-95.

[3] Penov, N. 2000. Izsledvane na ekstruziata na smessi ot spsnachno brashno i pshenichen gris, prednaznacheni za instantni hrani. Dissertation, Plovdiv.

[4] Petrova, Iv. 2012. Vyzmojnosti za izpolzvaneto na eldata v hranitelnite produkti. Dissertation, Plovdiv.

[5] Berrios, J., M. Camara, M. Torija, M. Alonso. 2002. Effect of extrusion cooking and sodium bicarbonate addition on the carbohydrate composition of black bean flours. Journal of Food Processing Preservation. 26: 113–128.

[6] Chaiyakul, S., K. Jangchud, A. Jangchud, P. Wuttijumnong, R. Winger. 2009. Effect of extrusion conditions on physical and chemical properties of high protein glutinous rice-based snack. LWT – Food Science and Technology. 42 (3): 781–787.

[7] Cheyne, A., J. Barnes, S. Gedney, D. Wilson. 2005. Extrusion behaviour of cohesive potato starch pastes: II. Microstructure – process interactions. Journal of Food Engineering. 66: 13–24.

[8] Haber, A., R. Runyon. 1977. General Statistics. 3rd ed., Addison-Wesley Publishing Company, Reading, MA. 343 p.

[9] Hagenimana, A., X. Ding, T. Fang. 2006. Evaluation of rice modified by extrusion cooking. Journal of Cereal Science. 43 (1): 38–46.

[10] Lazou, A., P. Michailidis, S. Thymi, M. Krokida, G. Bisharat. 2007. Structural properties of corn-legume based extrudates as a function of processing conditions and raw material characteristics. International Journal of Food Properties. 10: 721–738.

[11] Likimani T., J. Sofos, J. Maga, J. Harper. 1991. Extrusion cooking of corn/soy bean mix is presence of thermostable α-amylase. Journal of Food Science. 56 (1): 99–105.

[12] Montgomery, D. 2011. Design and Analysis of Experiments. 7th ed. Hoboken: John Wiley & Sons, Inc. ISBN 978-0-470-16990-2, 114 p.

[13] Pérez, A., S. Drago, C. Carrara, D. De Greef, R. Torres, R. González. 2008. Extrusion cooking of a maize / soybean mixture: factors affecting expanded product characteristics and flour dispersion viscosity. Journal of Food Engineering. 87 (3): 333–340.

[14] Rocha-Guzman, N., J. Gallegos-Infante, R. Gonzalez-Laredo, P. Castillo-Antonio, E. Delgado-Licon, F. Ibarra-Perez. 2006. Functional properties of three common bean (*Phaseolus vulgaris*) cultivars stored under accelerated conditions followed by extrusion. LWT - Food Science and Technology. 39: 6–10.

[15] Ruiz-Ruiz, J., A. Martinez-Ayala, S. Drago, R. González, D. Betancur-Ancona, L. Chel-Guerrero. 2008. Extrusion of a hard-to-cook bean (*Phaseolus vulgaris* L.) and quality protein maize (*Zea mays* L.) flour blend. LWT – Food Science and Technology. 41 (10): 1799–1807.

EXPERIMENTAL DETERMINATION OF THE RATIONAL PARAMETERS IN THE PROCESS OF FOAMING AND DRYING OF RAW FISH

A. Yashonkov[1], V. Sukmnov[2]

1 - Kerch State Maritime Technological University. Kerch, Crimea; 2- Donetsk National M. Tugan - Baranovsky University of Economics and Trade. Donetsk, Ukraine

Abstract. *The article provides the results of development and conduct of the multi-factor experiment. The recommendations are given concerning rational parameters of the foaming and raw fish drying processes in the output of snacks produced from round goby (Neogobius melanostomus) minced flesh.*

Key words: raw fish processing, snacks produced from round goby minced flesh, multi-factor experiment, process rational parameters

I. Introduction

Reduction in amount of fish yields in the World Ocean [1] required from fish processing plants to process and implement new waste-free ways of aquatic organisms processing. The authors proposed a new method [2] of producing foamed mixtures made of raw fish up to the temperature 55^0C. It makes possible to preserve thermolabile vitamins in the finished product. In order to implement the above mentioned method into the production it is necessary to develop recommendations concerning the rational parameters of the process.

The objective of the paper is to estimate rational parameters for the process of foaming and drying of raw fish.

II. Materials and methods

The research was carried out on the basis of producing the food stuff – snacks made of minced fish meat of a round goby.

In order to determine the impact of regimes on the process of foaming and drying the statistical method of the experiment planning [3, 4] was applied and the multifactorial experiment was undertaken. As input parameters the following ones were taken: temperature (t, ^{0}C) and pressure (P, kPa) in the process chamber and the density of stuffing of granules (ρ, kg/m^3). The output parameter was taken as duration of the process (τ, min.), affecting the productivity and expenses of energy.

III. Results and discussion

In order to preserve thermolabile vitamins and provide the required foaming and hardness of the product, basing on the preliminary experiments the intervals of varying the input parameters were determined [5].

The affecting parameters and interval of varying are given in Table 1.

Table 1. *Input factors and intervals of varying*

Factors	Basic level	Unit of varying	High level	Low level	Code identification of the factor
P, kPa	12, 5	2, 5	15, 0	10, 0	x_1
t, ^{0}C	50, 0	5, 0	55, 0	45, 0	x_2
ρ, kg/m^3	1 160, 0	60, 0	1 220, 0	1 100, 0	x_3

In order to simplify the record of the experiment conditions as well as data processing the encoded values of factors were taken. Along with this the high level of the factor corresponds to +1, the low one -1, and the basic one – zero.

The encoded values of the factors were calculated according to the following formula:

$$X = \frac{\overline{X}_j - \overline{X_{jo}}}{I_j},\tag{1}$$

where X_j – encoded value of the factors;
$\overline{X}_j$ – natural value of a factor;
$\overline{x_{j0}}$ – natural value of the basic level;
I_j – the interval of variation;
j – a number of the factor.

That is $X_1 = \frac{P - 12{,}5}{2{,}5}$;

$X_2 = \frac{t - 50,0}{5,0}$;

$X_3 = \frac{\rho - 1\,160,0}{60,0}$.

Matrix for planning of the comprehensive factor experiment of 2^3 type (Table 2) consists of three vector-columns created under the rule of alteration of symbols and divided into two blocks. Furthermore, the intra-block effect is mixed with the triple effect of interaction $P_6 = x_1x_2x_3$, which should be neglected. In order to compensate the affect of systematic errors, the experiments are randomized in time. Full factorial experiment of 2^3 type possesses the properties of symmetry, standardization and orthogonality.

Every experiment contains elements of uncertainty. It is necessary to establish the error of the parallel experiments, i.e. the error of

reproducibility. Dispersion serves to measure this error:

$$S^2 = \frac{\sum_{1}^{n}(y_q - \overline{y})^2}{\psi}, ,$$

(2)

where y_q – the result of each experiment;

$\overline{y}$ - arithmetic average value;

ψ – a number of degrees of freedom, $\psi = (N-1)$;

N – a number of experiments

The results of the experimental research undertaken are given in Table 3.

Table 2. *Matrix for planning the experiment of 2^3 type*

No. of the experiment	X₁	X₂	X₃
1	+	+	-
2	-	+	+
3	+	-	+
4	-	-	-
5	-	-	+
6	-	+	-
7	+	+	+
8	+	-	-

Table 3. *The results of three-factor experiment*

No. of the experiment	y₁	y₂	y₃	y₄	y₅	y₆	y₇	y₈	y₉	Y₁₀	$\overline{y}$	S_i^2
1	128, 1	127, 5	125, 8	135, 1	132, 7	135, 3	136, 2	137, 5	137, 8	133, 1	132, 9	18, 82
2	155, 2	154, 3	148, 1	145, 8	145. 1	143, 1	143, 2	149, 5	152, 2	152, 2	148, 9	20, 20
3	175, 8	174, 2	178, 8	180, 9	182, 2	182, 1	182, 9	185, 3	186, 2	176, 2	180, 5	16, 67
4	141, 3	143, 2	146, 8	148, 2	151, 1	151, 8	140, 8	140, 3	143, 2	141, 2	144, 8	18, 98
5	179, 2	174, 1	167, 9	165, 1	168, 8	171, 8	172, 2	169, 3	168, 5	167, 5	170, 4	16, 27
6	121, 2	126, 5	127, 9	120, 3	122, 3	127, 2	127, 9	129, 2	124, 5	127, 2	125, 4	9, 86
7	156, 2	159, 2	152, 3	157, 6	152, 1	151, 1	160, 5	159, 5	158, 5	159, 1	156, 6	12, 27
8	145, 5	147, 6	155, 2	151, 8	157, 5	153, 2	154, 1	145, 9	148, 1	149, 3	150, 8	17, 09

The verification of the results of the experimental data for rough errors was carried out applying Student's statistical criterion which made up t=2.2622 [4] with the confidential probability of 95%.

The homogeneity of dispersions was checked by calculated Fisher's criterion (F_P), which was compared with the tabular value ($F_{табл}$):

$$F_P < F_{табл.}$$

(3)

$$F_P = \frac{S_{max}^2}{S_{min}^2},$$

The calculated Fisher's criterion, $F_{p=2}$, 05. The tabular Fisher's criterion for the degrees of freedom $\psi_1 = \psi_2 = 9$ is equal $F_{табл} = 3$, 18 [3]. As $F_p < F_{табл}$, so dispersions are homogenous.

In order to evaluate reproducibility of the results of the experiments the calculated statistical Cohren's criterion (G_P) was determined which was compared with the tabular value ($G_{табл.}$):

$$G_P < G_{табл.}$$

$$G_P = \frac{S^2_{max}}{\sum\limits_1^N S_i^2}, , \qquad (4)$$

Calculated value of Cohren's criterion is equal to $G_p=0, 155$. The tabular value of Cohren's criterion is $G_{табл.}=0, 266$ [3]. As $G_p < G_{табл}$, so dispersions are homogenous.

The response function regarding dual effects of the interaction was represented as a polynomial of the second degree:

$$y = b_0 + b_1 x_1 + b_2 x_2 + b_3 x_3 + b_{12} x_1 x_2 + \\ + b_{23} x_2 x_3 + b_{13} x_1 x_3 \qquad (5)$$

where b_0, b_1, b_2, b_3, b_{12}, b_{23}, b_{13} are rates which were calculated by formulas:

$$b_0 = \frac{\sum\limits_1^N \overline{y_i}}{N} \quad b_1 = \frac{\sum\limits_1^N x_1 \overline{y_i}}{N} \quad b_2 = \frac{\sum\limits_1^N x_2 \overline{y_i}}{N}$$

$$b_3 = \frac{\sum\limits_1^N x_3 \overline{y_i}}{N} \quad b_{12} = \frac{\sum\limits_1^N x_1 x_2 \overline{y_i}}{N} \qquad (6)$$

$$b_{23} = \frac{\sum\limits_1^N x_2 x_3 \overline{y_i}}{N} \quad b_{13} = \frac{\sum\limits_1^N x_1 x_3 \overline{y_i}}{N},$$

In order to calculate the rates in the equation (5) the auxiliary calculation table 4 was drawn up.

Table 4. *Auxiliary table for calculation of equation rates*

No. of the experiment	X_1	X_2	X_3	$\overline{y}$	$X_1\overline{Y}$	$X_2\overline{Y}$	$X_3\overline{Y}$	$X_1X_2\overline{Y}$	$X_1X_3\overline{Y}$	$X_2X_3\overline{Y}$
1	+	+	−	132, 9	132, 9	132, 9	-132, 9	132, 9	-132, 9	-132, 9
2	−	+	+	148, 9	-148, 9	148, 9	148, 9	-148, 9	-148, 9	148, 9
3	+	−	+	180, 5	180, 5	-180, 5	180, 5	-180, 5	180, 5	-180, 5
4	−	−	−	144, 8	-144, 8	-144, 8	-144, 8	144, 8	144, 8	144, 8
5	−	−	+	170, 4	-170, 4	-170, 4	170, 4	170, 4	-170, 4	-170, 4
6	−	+	−	125, 4	-125, 4	125, 4	-125, 4	-125, 4	125, 4	-125, 4
7	+	+	+	156, 6	156, 6	156, 6	156, 6	156, 6	156, 6	156, 6
8	+	−	−	150, 8	150, 8	-150, 8	-150, 8	-150, 8	-150, 8	150, 8
$\sum$				1 210, 3	31, 3	-82, 7	102, 4	-0, 8	4, 2	-8, 1
b_i				151, 29	3, 91	-10, 34	12, 81	-0, 10	0, 53	-1, 02

The response function was produced as:

$$y=151, 29+3, 91X_1-10, 34X_2+12, 81X_3- \\ -0, 10X_1X_2-0, 53X_1X_3-1, 02X_2X_3 \qquad (7)$$

The values of the equation rates were calculated by the confidence interval Δb_i:

$$\Delta b_i = \pm t \cdot S\{bi\}, \qquad (8)$$

where t is a tabular value of Student's coefficient with the number of degrees of freedom, with which $S\{bi\}$ was calculated in the chosen level of significance, $t=1, 9944$ [5];
$S^2\{bi\}$ is dispersion of the regression coefficient, $S\{b_i\} = \sqrt{S^2\{b_i\}}$.

$$S^2\{b_i\} = \frac{S^2\{y\}}{N}, \qquad (9)$$

where $S^2\{y\}$ is a dispersion of the reproducibility of the experiment,

$$S^2\{y\} = \frac{\sum\limits_1^N \psi_i S_i^2}{\sum\limits_1^N \psi_i},$$

According to the results of the calculations the following values were determined: dispersion of the experiment reproducibility $S^2\{y\} = 16, 42$; dispersion of the regression coefficient $S\{b_i\}=2, 05$; confidence interval $\Delta b_i=2, 8575$. Thus, in the equation (7) there are four significant coefficients $b_0=151, 29$; $b_1=3, 91$; $b_2=-10, 34$; $b_3=12, 81$, so this equation (7) may be represented as follows:

$$y=151, 29+3, 91X_1-10, 34X_2+12, 81X_3 \qquad (10)$$

The analysis of the equation (10) demonstrated that the duration of the process increased with the increased pressure in the process chamber and density of stuffing of granules as well as with reduced temperature in the process chamber.

The model is called adequate if the following requirement is met: forecast by means of the model the response value in some similarity, where coordinates of the realized experiments are included, should not differ from factorial more than for the preliminarily given value. The verification of the model adequacy was made by Fisher's F-criterion:

$$F_P < F_{табл.}$$

$$F = \frac{S_{ад}^2}{S^2\{y\}} \qquad (11)$$

where $S^2_{ад}$ is dispersion of adequacy,

$$S_{ад}^2 = \frac{\sum_1^T \Delta y_i^2}{\psi}$$

Δy_i^2 – the residual sum of squares of difference between estimated and average value of y;

ψ – a number of degrees of freedom equal to the difference between a number of experiments and a number of coefficients (constants) being calculated by the results of the experiments independently of each other.

To verify the adequacy of the model the auxiliary calculation table 5 was drawn up.

Table 5. *Auxiliary table to calculate dispersion of adequacy*

No. of the experiment	$\overline{y}$	Y_p	ΔY	ΔY^2
1	132, 9	132, 1	0, 85	0, 7
2	148, 9	149, 9	0, 98	1, 0
3	180, 5	178, 3	2, 12	4, 5
4	144, 8	144, 9	0, 12	0, 0
5	170, 4	170, 5	0, 08	0, 0
6	125, 4	124, 2	1, 18	1, 4
7	156, 6	157, 7	1, 06	1, 1
8	150, 8	152, 7	1, 91	3, 7

According to Table 5 the dispersion of adequacy $S^2_{ад}$=3, 1 was calculated. Fisher's predictive criterion made up F_P=0, 19. Fisher's tabular criterion for the degrees of freedom 4-9 is equal to $F_{табл}$=3, 63 [3]. Thus, $F<F_{табл.}$, i.e. with the confidence likelihood ratio 0, 95 the model may be treated as adequate.

With true variables the equation 11 may be represented as:

$$\tau = 1, 564 \cdot P - 2, 068 \cdot t + 0, 2135 \cdot \rho - 12, 52 \qquad (12)$$

In order to estimate the minimal value of the equation (12) with the given limits of the variable factors (Table 1) methods of convex optimization (simplex methods) applying the function of "Finding solutions" in the table editor Excel. The outcomes for the variable parameters made up: P=10 кПа, t=55°C, ρ=1100 kg/m³.

IV. Conclusions

Thus, with the reference to three-factorial experiment to minimize the duration of foaming and drying while producing snacks made of minced meat of round goby the rational parameters for the process were estimated, these being as follows P=10 kPa, t=55⁰C, ρ=1 100 kg/m³.

The obtained parameters made possible to develop specifications, technical instruction and procedures to implement the proposed method of raw fish processing into foamed mixtures in the production.

References

[1] Sukmanov V.A., Yashonkov A.A. Substantiation of the necessity to process fish resources adding thermally labial biologically active supplements and their utilization as floating feeds for fish farming. *Equipment and technologies of food production* 2011; 26, pp. 474-479 (Сукманов В.А., Яшонков А.А. Обгрунтування необхідності переробки рибної сировини з додаванням термолабільних біологічно активних добавок та її використання як плаваючих кормів для рибництва. *Обладнання та технології харчових виробництв : темат. зб. наук. пр.* 2011; 26, С. 474-479).

[2] Pat. 65473 Ukraine, MPK A01K61/00 A method of producing foamed mixtures / V.A. Sukmanov, A.A. Yashonkov (Пат. 65473 Україна, МПК А01К61/00. Спосіб отримання спінених сумішей / В.О. Сукманов, О.А. Яшонков (Україна) ; заявник та патентовласник Керченський державний морський технологічний університет. – № u 2011 05429 ; заявл. 28.04.11 ; опубл. 12.12.11, Бюл. №23)

[3] Adler U.P., Markova E.V. *Planning an experiment in finding the optimal conditions,* Moscow Nauka, 1976 (Адлер, Ю.П., Маркова Е.П. *Планирование эксперимента при поиске оптимальных условий,* Москва, Наука, 1976)

[4] Shenk H. *Theories of engineering experimentation,* Moscow, Mir, 1972 (Шенк, Х. *Теория инженерного эксперимента,* Москва, Мир, 1972)

[5] Sukmanov V.A., Yashonkov A.A. To the problem of experimental research of fish raw material foaming. *Fishing industry of Ukraine* 2011; 6(77), pp. 40-43 (Сукманов, В.А., Яшонков А.А. К вопросу экспериментальных исследований вспениваемости рыбного сырья. *Рибне господарство України* 2011; 6(77), С. 40-43.)

EXPERIMENTAL TEST STAND
FOR THE STUDY OF COATINGS RESISTANCE

V. S. Rupetsov

University of Plovdiv "P. Hilendarski"
Technical College Smolyan

Summary: *The quality of the surfaces of the joint working details depends both on their geometric accuracy and precision, and on the ability to counteract to the factors causing different types of wear. The wear resistance of the working surfaces is evaluated by means of various types of tests, some of which are laboratory tests carried out with the aid of various test stands and simulators having the joint name tribometers. In this work constructively - technological characteristics of the stand realized on the scheme "ball-on-plate" are discussed. The purpose of the test stand is to make an abrasive testing of the samples in mode adapted to the actual operating conditions and evaluating the results by comparing the wear of different coatings laid on their working surfaces.*

Keywords: tribometer, wear, hard coatings, ball-on-plate, wear resistance.

I   Introduction.

To study the tribological properties of hard coatings, there is still no one accepted methodology. Depending on the goals and tasks, the authors of various studies set the particular matter and the variety in many cases makes the research results difficult to compare.

The test stands for tribological studies reflect (to a lesser or greater extent) the actual operating conditions. In recent years, devices with high accuracy for complex evaluation of the tribological properties of nanostructured surfaces and micro and nanoleveled coatings were designed by leading manufacturers. Testing machines for friction and wear are not produced in the Republic of Bulgaria, so it is a practice that researchers and research laboratories design and produce special systems for their own purposes, working on common patterns of friction [2,3,4] .

This paper presents the design of a test stand for experimental testing of wear resistance by determining the differential characteristic of wear intensity I_w.

II   Purpose of the test stand

The test stand is designed to test wear resistance of test samples of a certain size. It is used mainly for evaluation of the wear resistance of hard thin coatings with a thickness greater than $1\mu m$ put on planar surfaces of the samples. It is realized a method of friction "Ball on Flat Sliding Wear Test" [1,7] with

horizontal orientation of the test surface. The test ball is fixed in a holder on which is assigned a specific load, with friction on linear reciprocation drive sample *(Reciprocation drive)* without any lubricant and it works in air at room temperature.

III Description of the construction of the test stand СИИП-1 for carrying out the experimental tests of the wear resistance.

In constructing the test stand were reported the following specific requirements:

- The axes of the holder of the counter body shall be perpendicular to the surface of movement;
- The device is to be stable, so that during use at maximum load and speed of slide, the axis of the holder to retain perpendicular to the tested surface;
- Linear accuracy and stability of reciprocation movement;
- Stable and accurate fastening of the counter body and the sample (which shall not deform during the fixation);
- The center of the spherical counter body shall lie on the axis of the holder;
- The load shall have a constant nominal value throughout the duration of the test and others.

The three-dimensional model of the test stand СИИП-1 for carrying out experimental tests of the wear resistance is shown in Fig. 1.
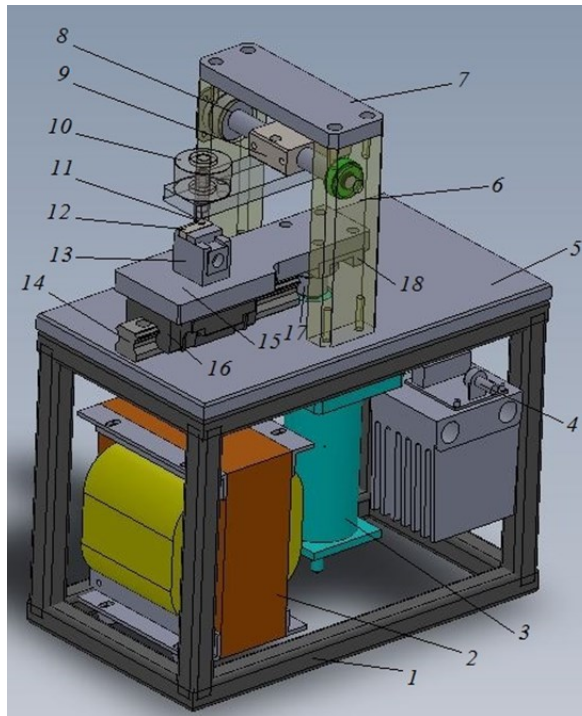
Fig. 1. *Constructive model of the test stand СИИП-1 for wear resistance.*
1.Frame 2.Transformer 3.Motor-reducer 4.PWM DC controller 5.Main plate 6.Side Beam 7.Connecting beam
8.Axis 9.Loading lever. 10.Load 11.Ball holder 12.Test sample 13.Sample holder 14.Linear guideway
*15.Reciprocatingly moving base 16.Ball slider 17.Eccentric 18. Bearing slide*r

In the inner space of frame *1* there is a power transformer *2*, the motor-reducer *3* (DC 24 V) and the control unit *4* for adjusting the spinning speed mounted to a radiator. On the base plate *5*, attached to the top of frame *1* are fitted the other elements. The two side beams *6* are connected by beam *7*. In the bearing holes of beams *6* are set the bearing of axle *8*. Loading lever *9* is designed with shifted center of gravity in order to put it into its original balance before placing load *10* and it is also possible to readjust the equilibrium. The load lever can be moved longitudinally along the axis *8*. This enables the establishment of a sample *12* in the sample holder *13* to get a variety of marks on the sample in case of change in the experimental conditions: - loading, time or way of friction, the linear speed of the reciprocating motion and others.

Ball holder *11* is fitted at the front end of the lever. The center of gravity coincides with the axis *10* of the holder.

The driving is via a DC motor-reducer *3*, with eccentric *17*, fitted on the output shaft of the reducer. The conversion of the rotary motion into reciprocating is made through the pair of eccentric

slider. Linear reciprocating motion is realized by linear guideways *14* and ball slider *16*. The base *15* is fixed immovably on ball slider *16* and at its rear edge is fitted slider *18*. On base *15* is fixed firmly sample holder *13*, where the tested sample *12* is placed. Counting the number of double movements are performed by counter (Register), receiving a signal from a sensor (Magnetic Sensor) in one revolution of the eccentric *17* (Fig. 2).

Speeds of rotation of the DC engine are controlled, keeping the rotating moment and using PVM DC Motor Controler (Fig. 2). A potentiometer is used to determine the coefficient of filling of PWM signal. Each pushing of S_1 for more than half second changes the frequency of the PWM signal. There are programmed three different frequencies: 980Hz, 3.8KHz, 15,6 *KHz*. They are indicated by two light diodes: *LED1* (red) – when it is lit the frequency is 15,6 *KHz*, when it twinkles fast 3.8K*Hz*, when it twinkles slowly 980*Hz*; light diodes *LED2* (green) indicates that the power is on.

General view of the test stand СИИП-1 is shown in Figure 3, and the specifications are listed in Table 1.
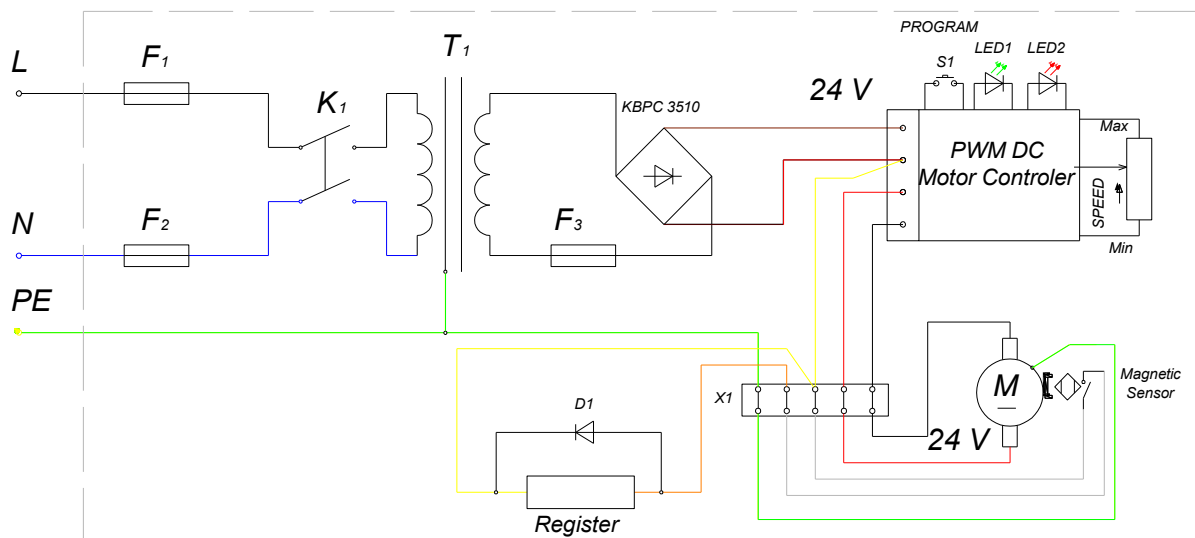
Fig.2. *Electric diagram of the test stand СИИП-1 for wear resistance.*

Fig.3. *General view of test stand СИИП-1 for wear resistance.*

Table 1

TECHNICAL SPECIFICATION OF STAND СИИП-1	
Dimensions LxBxH, mm	320x180x430
Supply voltage, V	220/24
Linear speed (average), mm/s	0,01÷31.5
Stroke length, mm	11
Load, N	0,5÷10
Counter body	Ball with diameter 3 mm
Material of the counter body	Steel, Al_2O_3, Si_3N_4, WC-Co and others.
Orientation of the tested surface	horizontal
Tested environment	air
Mass, kg	24.25
Work conditions:	
- Temperature,°C	23±2
- Humidity, %	50±10

IV   Methodology of the study.

4.1. Necessary materials and tools.

For the test there are needed:

- Test Stand;
- stopwatch;
- tared weights;
- sample;
- counter body - ball;
- cleaning liquids (heptane or isopropyl alcohol);
- measuring microscope with magnification x 100-500.

4.2. Preparation and setup for testing.

- Pre-prepared and coated test sample is cleaned and dried and it is put in sample holder *13* so that the test area falls within the scope of the course of the slider.
- The ball is put in the holder 11 and the holder is attached to loading lever *9*.
- Balance the loading lever *9*.
- Adjust the average linear speed of the reciprocating motion to obtain the desired value. It is performed by measuring with a stopwatch of the number of double movements, recorded by the counter for a minute. Regulation is through controller *4*.

For test stand $l_{mot move.}$ = 22 mm = const.

At known speed *V*, mm/s, and time *t* = 1 min, the number of double movements per minute:

$$n_{mot \cdot move} = \frac{V.t.60}{l_{mot \cdot move}} = \frac{V.t.60}{22} \qquad (1)$$

The past by the slider distance *L*, is determined by:

$$L = n_{mot.move}.l_{mot.move}.10^{-3}, \ m \qquad (2)$$

- Place a burden with determined values on loading lever *9*.
- Make a test with a predetermined number of cycles corresponding to a path *L*.
- Recalculation of the real speed V_m, mm/s:

$$V_m = \frac{n_{mot.move} \, l_{mot.move}}{t.60}, \ mm/s \qquad (3)$$

where, *t* is the time of friction, *min.*

- Wear scratches hall shall be observed with a microscope with a minimum magnification of 10X for: breakthrough or wrenching, uneven or even wear, transfer of material, construction debris from wear and others.
- Determining the sizes of the wear scratches is done by using a measuring microscope.

4.3. Methodology for determining the intensity of wear using the volumetric method.

The intensity of wear I_w shall be determined by the dependency:

$$I_w = \frac{V}{N.L}, \ mm^3/N.m , \qquad (4)$$

where:
V - volume of the amount of material removed (trace), mm^3;
N – normal load, *N;*
L – travel time or distance of the sample compared to counter body distance, *m.*

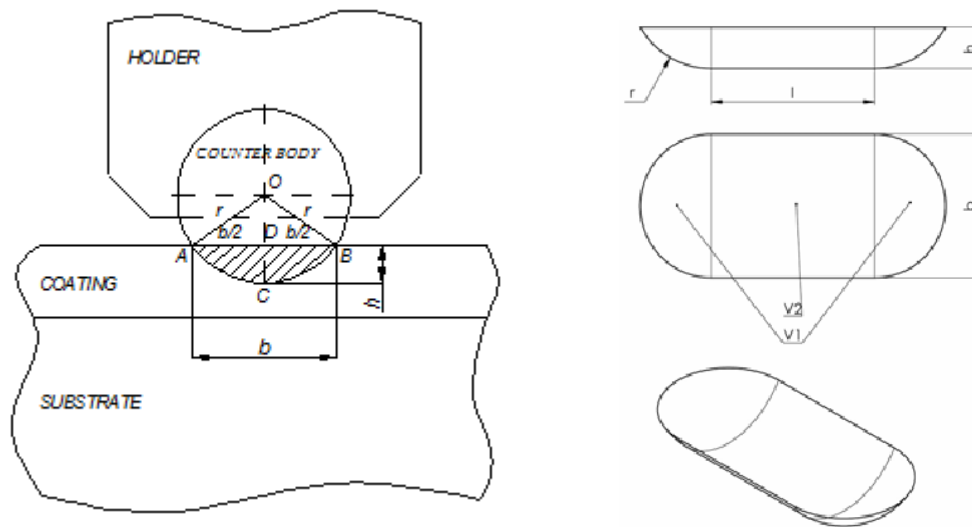The wear canal on the surface has the form shown in FIG.4. [5, 6]

Fig. 4. *Chanel on the surface of the test sample in tribological test "ball-on-plate".*

Its volume V can be considered as consisting of two parts. Gathered together, both ends of the chanel represent a segment of a sphere having a volume V_1. Among them is the segment of a cylinder with a volume V_2. In this case, the volume of the trace is defined as:

$$V = V_1 + V_2, \; mm^3 \quad (5)$$

For finding these two volumes, it is first necessary to calculate the depth h, where the counter body has reached. It is known that:

$$h = r - \sqrt{r^2 - \frac{b^2}{4}}, mm^3 \quad (6)$$

where:
r – is the radius of the ball, *mm*;
b – width of the trace, *mm*.
The volume of the spherical segment V_1 is:

$$V_1 = \frac{\pi}{3}.h^2(3r - h), \; mm^3 \quad (7)$$

The volume of the rectilinear part of the trace (segment of a cylinder) is determined by the formula:

$$V_2 = S.l_1, \; mm^3$$

where:
l_1 - length of the straight part of the trace, *mm*;
S - the face of the cross-section of the trace, mm^2.

After transformation we obtain:

$$V_2 = l.\frac{r^2}{2}\left[2\arccos\left(\frac{r-h}{2}\right) - \sin\left(2\arccos\left(\frac{r-h}{2}\right)\right) \right]$$
$$, mm^3 \quad (8)$$

V. Conclusion.

It is proposed arrangement of a test stand for experimental research of wear resistance of test samples by calculating the characteristic intensity of wear using the volumetric method. The design of the test stand provides smooth and free of gaps rectilinear reciprocating movement of the tankety ball which is bearing the test sample. The test stand can be used to test a wide range of the samples with small shape and dimensions with the necessary holders for them. The driving and loading systems enable the realization of different conditions of friction by adjusting the parameters of speed V and load N.

References:

[1] BDS EN 1071-12:2010 Metodi za izpitvane na keramichni pokritia. Izpitvane na iztrivane pri vazvratno-postapatelno dvijenie.

[2] Bojkov S., Stanev L. Konstruktivno-tehnologichni osobenosti na stend za izpitvane na triene i iznosvane v sleda ot abraziv I dobavki. NTK "Plovdiv – 2003", Sb. Dokladi, ISSN 1310-8271, str.69-73, Plovdiv, 2003.

[3] Dishliev St. Test stand for an experimental investigation of the wear resistance. Journal of the Technical University Sofia, branch Plovdiv "Fundamental Sciences and Applications", ISSN

1310-271 , Vol. 14, 2009 International Conference Engineering, Technologies and Systems TechSys '2009 BULGARIA.

[4] Komitov G., Stanev L., Staneva G. Konstruktivno-tehnologichni osobenosti na stend za izpitvane na triene I iznosvane pri vazvratno-postapatelno dvijenie. NTK s mejdunarodno uchastie, Sliven, sp. "Mechanika na mashinite", ISSN 0861-9727, kn. 48, Varna, 2003, s. 113…115.

[5] Mishev G., Dishliev S., Rupetsov V. Povishavane na iznosoustoichivostta na shpricformi s pomostta na PVD–

pokritia. Sofia, Tribological Journal BULTRIB Vol. 4, 2013, ISSN 1313-9878.

[6] Mishev G., Dishliev S., Rupetsov V. Increase the wear resistance of injection molds using PVD coatings. The19th International Colloquium Tribology, 21-32 January 2014, Stutgard/Ostfildern, Germany, ISBN-№ 978-3-943563-10-8

[7] http://www.astm.org/Standards/G133.htm, ASTM G133 – 05 (2010) Standard Test Method for Linearly Reciprocating Ball-on-Flat Sliding Wear.

HIGHLY ACTIVE PROBIOTIC CONCENTRATES WITH LONG SHELF LIFE OBTAINED USING CRYOPROTECTANTS OF PLANT ORIGIN

R. S. Denkova[1], L. V. Georgieva, Z. R. Denkova[2]

[1] *Department of "Biotechnology", Sofia University "St. Kliment Ohridski", Sofia, Bulgaria;*
[2]*Department of "Microbiology", University of food technologies, Plovdiv, Bulgaria*

Abstract: *Freeze-drying of probiotics also facilitates their preservation for a long period of storage and low cost transportation. Selected probiotic strains L.acidophilus A2, L.delbrueckii ssp. bulgaricus GB and Bifidobacterium sp. Bif. 4 are immobilized and freeze-dried using combined hydrocolloid matrix - high-ester pectin and sodium alginate. Biotechnology with the following main stages: selection, immobilization of the selected strains in the hydrocolloid matrix, cryoprotection, freezing and freeze-drying is established. The survival of the three lyophilized microorganisms after freeze-drying and during storage for 12 months is monitored - the three strains retain high concentrations of active cells - 10^{10}CFU/g. The hydrocolloids used are suitable agents for the mechanical immobilization of cell cultures and as cryoprotectants during the lyophilization of the probiotic strains. The applied combined biotechnology makes it possible to prepare probiotic biological products with long shelf life and intact probiotic potential for application in the prophylaxis of disbioses and as supplements for foods with dietary purpose.*

Keywords: Probiotic, immobilization, cryoprotection, freezing, freeze-drying (lyophilization)

I.   Introduction.

When incorporating a probiotic strain into a food matrix there are two main problems to be addressed, the resistance of the probiotic to the technological conditions of the food production [19] and the maintenance of viability up to the expiring date of the food, since the manufacturer has to ensure an optimal administration of the probiotics throughout the life of the product. That could limit the use of probiotics in long-life products specially if they are not refrigerated during storage. One of the most common methods used to preserve probiotics is freeze-drying. However, this method is not considered optimal, at least as the only strategy, since it just protects probiotics from the humidity but does not confer protection from certain environmental and technological conditions such as varying temperatures, oxygen toxicity or passage through the intestinal tract [15]. It is also frequent that probiotics experience decreased viability during or after freeze-drying.

In this sense, microencapsulation, which is defined as a process in which the cells are retained within an encapsulating matrix or membrane, may provide an approach for protecting probiotics. This technique would allow the isolation of a probiotic from the environment thus increasing its resistance to the conditions of production and would also improve its viability throughout the storage. The protective effect of microencapsulation is generally explained by limited diffusion of inhibitory substances such as metabolic products from starter cultures, H_2O_2, lactic acid, and bacteriocin into the capsules [11, 17].

The new generation of bioproducts contains probiotic components (probiotic lactic acid cultures), prebiotics and synbiotics (a combination of probiotic and prebiotic). Separately, both probiotics and prebiotics have determinative physiological effects on the body, but the cumulative physiological effect of their combination is significantly higher. There is also a poly-functionality of the components used with regard to their technological properties. For example oligo- and polysaccharides enrich new bioproducts with alimentary fibers, on one hand, and act as cryoprotectants and matrices for immobilization of the probiotic cultures, on the other.

Various materials have been used for microencapsulation of probiotics, such as alginate [18], κ-carrageenan [1], cellulose acetate phthalate [8], gelatin [2] and pectin [10].

Freeze-drying of lactic acid bacteria (LAB) facilitates their preservation for a long period of storage and low cost transportation and thus, results in ready-to-use cultures for dairy and other food-related industries, particularly in the emerging and continuously growing field of probiotics. The most commonly used cryoprotectants for the freeze-drying of probiotics are as various sugars (e.g. glucose, fructose, lactose, mannose), sugar alcohols (e.g.

sorbitol and inositol) and non-reducing sugars (e.g. sucrose, trehalose) [24].

The hydrocolloids used are sodium alginate and high-ester pectin and they act as matrices for the immobilization of the cell material and as cryoprotectants. They are natural, vegetable raw materials, with well known content of biologically active substances and proven beneficial physiological effects on the body [9, 12].

Entrapment of probiotic bacteria in alginate matrices is among the most widely used immobisation techniques [14]. This approach has been shown to enhance bacterial cell tolerance to alcohols, phenols, antibiotics or quaternary ammonium sanitizers [16] and resistance to adverse processing techniques such as freezing [20] and freeze-drying [13] and hostile environments such as simulated gastric environment [3].

The main objective of the present study is to obtain highly active probiotic lyophilisates of selected strains of lactic acid bacteria and bifidobacteria of human origin by applying combined modern biotechnology.

II. Materials and Methods

Microorganisms:

Probiotic microorganisms: *Lactobacillus acidophilus* A2, *Lactobacillus delbrueckii* ssp. *bulgarisus* GB and *Bifidobacterium* sp. Bif. 4 of human origin

Media:

MRS-broth. (Scharlau).

MRS-agar. Composition (g/dm^3): MRS-broth (Scharlau) + 2% agar (Scharlau).

Sterile skimmed milk with titratable acidity 16-18ºT. (Scharlau).

Saline solution.

Solid medium for *Bifidobacterium* sp. Composition (g/dm^3): peptone - 10, yeast extract - 10 lactose - 10, $MnSO_4$ - 1 casein hydrolyzate - 8, $NaCl$ – 3,2, CH_3COONa – 1, agar - 20. pH is adjusted to 6,6 – 6,8.

Hydrocolloid matrices: pectin + sodium alginate / 1:1 / - 1,2% solution of sodium alginate, and 4% solution of pectin. The concentrations of the hydrocolloid solutions were determined on the basis of the physicochemical parameters of the hydrocolloids used. The application of hydrocolloids of plant origin was in compliance with the requirements for physiological activity, safety and microbial stability [21].

Methods:

Cultivation. The cultivation of the probiotic strains was carried out in a laboratory bioreactor with a

working volume of 1.5 dm^3 with constant stirring at 150 rpm at 37±1°C. The bioreactor was equipped with a control unit "Sartorius A2" that included control devices for the stirring rate, the temperature, the pH and other parameters.

The freeze-dried probiotic concentrates were obtained by a three-stage technology:

1. Primary processing the cellular suspensions - the cellular suspensions of the selected strains of lactic acid bacteria and bifidobacteria were diluted, equilibrated, dosed and immobilized by inclusion in the polymer matrix that acts as a cryoprotectant.

2. Freezing – it was performed in chambers with forced convection of the air environment at a temperature of -30°C to -35°C for 12-15 hours.

3. Freeze-drying – it was performed in a vacuum sublimation installation "Hochvakuum-TG -16.50" with contact heating of the plates at the ICFT - Institute of Cryobiology and Food Technologies, Sofia, Bulgaria.

After lyophilization, the freeze-dried concentrates were digested in the granulator "Erveka". The digested lyophilized bioproducts are packed in three layer aluminum foil, sealed under vacuum.

Microbiology

1. The microbiological status of the native and the freeze-dried samples - acc. BS 1670-82 and Ordinance № 5 of the MH - SG 39/84, BS EN ISO 4833.

Indicators:

• lactic acid bacteria and bifidobacteria - CFU/g;

• total number of mesophilic aerobic and facultative anaerobic microorganisms - CFU/g;

• coliforms in 0,1 g of product;

• pathogens including *Salmonella* sp. in 25,0 g of product;

• pathogenic staphylococci in 1,0 g of product;

• sulfite reducing clostridia in 0,1 g of product;

• spores of microscopic molds, CFU/g;

• yeasts, CFU/g;

III. Results and Discussion

The strains *Lactobacillus acidophilus* A2, *Lactobacillus delbrueckii* ssp. *bulgaricus* GB and *Bifidobacterium* sp. Bif. 4 possess proven probiotic properties. They are of human origin; they are resistant to the simulated gastric juice and different concentrations of bile salts; they exhibit antimicrobial activity against pathogenic microorganisms; they are resistant to most of the antibiotics, commmonly applied in medical practice; they adhere to a model monolayer

epithelial non-cancer cell line [4, 5, 6, 7, 23]. The three strains were cultured in a laboratory bioreactor. Immobilization in the presence of a hydrocolloid matrix consisting of high-ester apple pectin and sodium alginate, followed by freeze-drying of the three strains was carried out. The resulting lyophilized bioproducts were stored at 20°C - 22°C and the dynamics of cellular survival of lactobacilli and bifidobacteria for 12 months of storage was monitored (Fig. 1, Fig. 2 and Fig. 3).

The examinations of the lyophilized bioproducts according to the standard methods showed absence of insemination with pathogenic microflora (Table 1):

**Table 1.** *Microbiological status of the probiotic lyophilisates*

Type of pathogens	Norm according to BS	Number of tested microorganisms, CFU/g
1. General number of mesophilic aerobic microorganisms, CFU/g	No more than 800	220
2. Coliform bacteria in 0.1 g of the product	Not to be found	Not found
3. Sulfite reducing clostridia in 0.1 g of the product	Not to be found	Not found
4. *Salmonella* sp. in 25.0 g of the product	Not to be found	Not found
5. *Staphylococcus aureus* in 1.0 g of the product	Not to be found	Not found
6. Spores of microscopic molds, 100 CFU/g	No more than 100	30 -35
7. Yeasts, CFU/g	No more than 100	28 – 40

The probiotic lyophilisates did not contain pathogenic microorganisms and meet the standard requirements for microbial purity of food.

In the process of freeze-drying the number of viable cells decreased slightly - by about 1.2 to 1.5 logN, due to the optimally conducted process, including using a combined cryoprotectant hydrocolloid matrix.

The survival of the lyophilizates, i.e. the resistance of the organism during long-term storage, was monitored. The probiotic lyophilized concentrates of viable cells of *Lactobacillus acidophilus* A2, *Lactobacillus delbrueckii* ssp. *bulgaricus* GB and *Bifidobacterium* sp. Bif. 4 of human origin were stored

at 20°C - 22°C for 12 months, taking samples every three months and determining the number of viable cells. The results of this examination are shown on Fig. 1 for *Lactobacillus acidophilus* A2, Fig. 2 for *Lactobacillus delbrueckii* ssp. *bulgaricus* GB and Fig. 3 for *Bifidobacterium* sp. Bif. 4.
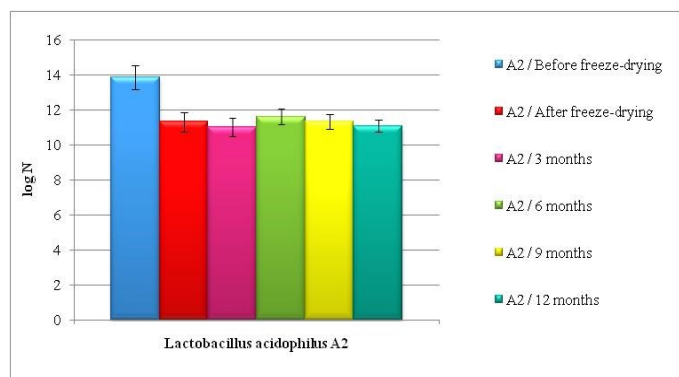
Figure 1. *Survival of the cells of Lactobacillus acidophilus A2 after lyophilization and during storage of the freeze-dried bioproduct for 12 months at 20°C - 22°C.*
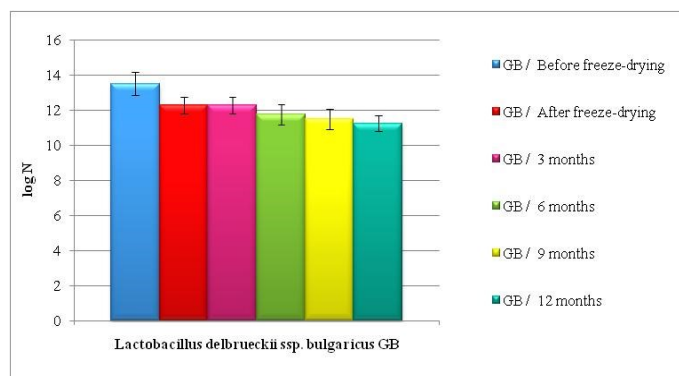
Figure 2. *Survival of the cells of Lactobacillus delbrueckii ssp. bulgaricus GB after lyophilization and during storage of the freeze-dried bioproduct for 12 months at 20°C - 22°C.*
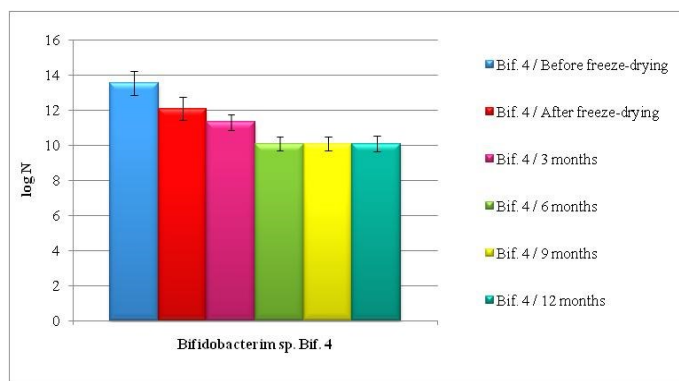
Figure 3. *Survival of the cells of Bifidobacterium sp. Bif. 4 after lyophilization and during storage of the freeze-dried bioproduct for 12 months at 20°C - 22°C.*

Moreover, the higher the degree of dehydration is, as in our bioproducts (residual moisture content - below 5,0%), the lower the survival of the pathogenic microflora is.

Experimental data demonstrate that in the course of storage for 12 months the three probiotic concentrates' content of viable cells was above $10^9 CFU/g$ (Fig. 1, Fig. 2, Fig. 3). According to Wolfson [22], 1999 $10^9 CFU/g$ is the required minimum concentration of cells of probiotic bacteria in order for a concentrate to be classified as highly effective probiotic preparation. Moreover, the storage of the freeze-dried concentrates continues as well as the monitoring of the change in the number of living probiotic cells suggesting that the obtained bioconcentrates could be applied as highly effective probiotic preparations for even longer period of time than 12 months.

The number of living cells before the lyophilization was over $10^{13} CFU/cm^3$ and after freeze-drying it was over $10^{12} CFU/cm^3$. This effect is due to the effectiveness of the hydrocolloids used - a combined hydrocolloid matrix, consisting of sodium alginate and high-ester apple pectin, as a cryoprotectant medium. The hydrocolloids used for the mechanical immobilisation of the probiotic strains of microorganisms, as well as as a cryoprotectant medium, sodium alginate and high-ester apple pectin, are highly efficient, as evidenced by the high survival rate of the freeze-dried microorganisms.

Probably, as a hydrocolloid matrix for the immobilization of the probiotic cultures alginate and pectin enable a number of effects: the significant stabilization of the enzymatic activity of the immobilized cells; the stabilization and the increase of the overall activity of the immobilized probiotic system, which is beneficial for their survival after lyophilization and during storage.

The obtained positive results associated with the high survival rate of the tested lactobacilli and bifidobacteria in the lyophilized biological products are due to the optimal development of the whole process - freezing conditions, applying appropriate cryoprotectant medium and regime parameters of freeze-drying, proper determination of the duration of the cycle, which provides low residual moisture content in the final lyophilizates, resistance to the thermal processes and extension of their storage.

IV. Conclusions

The obtained probiotic lactobacilli and bifidobacteria bioconcentrates retained high concentrations of viable cells up to the 12th month of storage at room temperature. The used combined hydrocolloid matrix of sodium alginate and high-ester apple pectin can be determined as a highly effective cryoprotectant of endocellular type which increases the survival of lactobacilli and bifidobacteria during lyophilization. The absence of pathogenic microflora and the low residual moisture content of the new freeze-dried organic bioproducts are factors determining the prolonged storage. During the examined 12-month period no adverse changes in the microbiological purity and activity of the lyophilizates were established.

References

[1] Adhikari K., Mustapha A., Grün I. U. Survival and metabolic activity of microencapsulated *Bifidobacterium longum* in stirred yoghurt. *Journal of Food Science* 2006; 68, pp. 275–280.

[2] Annan N.T., Borza A.D., Hansen L.T. Encapsulation in alginate-coated gelatin microspheres improves survival of the probiotic Bifidobacterium adolescentis 15703 T during exposure to simulated gastro-intestinal conditions. *Food Research International* 2008; 41, pp. 184–193.

[3] Brachkova M.I., Duarte M.A., Pinto J.F.. Preservation of viability and antibacterial activity of *Lactobacillus* spp. in calcium alginate beads. *European Journal of Pharmaceutical Sciences* 2010; 41, pp. 589–596.

[4] Denkova R., Dimbareva D., Denkova Z. Probiotic properties of *Lactobacillus acidophilus* A2 of human origin. International Conference „Modern Technologies an the Food Industry - 2012", MFTI – 2012 Chişinău, 1-3 November 2012, Volume 1, pp. 334 - 339.

[5] Denkova, R., Ilieva S., Denkova Z., Yanakieva V. Probiotic properties of strains of *Lactobacillus delbrueckii* ssp. *bulgaricus*, isolated from different

sources. International scientific conference "Technologies, food, health" 50 years CANRI – Plovdiv, 8.11.2012, 2012b; pp. 67 - 72.

[6] Denkova R., Yanakieva V., Denkova Z., Mancheva P. Antimicrobial activity of a probiotic strain *Lactobacillus acidophilus* A2 of human origin against pathogens. *Journal of Food and Packaging Science Technique and Technologies*, Issue II, №2, 2013a; pp. 26 - 30.

[7] Denkova, R., Yanakieva V., Denkova Z., Hristozova P. Inhibitory activity of the probiotic strain *Bifidobacterium bifidum* Bif. 4 of human origin against pathogens. *Journal of Food and Packaging Science Technique and Technologies*, Issue II, №2, 2013b, pp. 21 - 25.

[8] Fávaro-Trindade C.S., Grosso C.R.F.. Microencapsulation of *L. acidophilus* (La-05) and *B. lactis* (Bb-12) and evaluation of their survival at the pH values of the stomach and in bile. *Journal of Microencapsulation* 2002; 19, pp. 485–494.

[9] Georgieva L. „Development of new cryobiotechnologies as a scientific basis for obtaining effective lyophilized foods for health", DSc Thesis, Institute of Cryobiology and Food Technologies 2009, Sofia, Bulgaria.

[10] Gerez C.L., Font De Valdez G., Gigante M. L., Grosso C.R.F. Whey protein coating bead improves the survival of the probiotic *Lactobacillus rhammnous* CRL 1505 to low pH. *Letters in Applied Microbiology* 2012, 54, pp. 552–556.

[11] Heidebach T., Först P., Kulozik U. Microencapsulation of probiotic cells for food applications. *Critical Reviews in Food Science and Nutrition* 2012; 52, pp. 291 - 311.

[12] Idris A., Wahidin S. Effect of sodium alginate concentration, bead diameter, initial pH and temperature on lactic acid production from pineapple waste using immobilized *Lactobacillus delbrueckii*. *Process Biochemistry* 2006; 41(5), pp. 1117-1123.

[13] Kearney L., Upton M., Loughlin A.M.C. Enhancing the viability of *Lactobacillus plantarum* inoculum by immobilizing the cells in calcium-alginate beads incorporating cryoprotectants. *Appl. Environ. Microbiol.* 1990; 56, pp. 3112–3116.

[14] Klinkenberg G., Lystad K.Q., Levine D.W., Dyrset, N. Cell release from alginate-immobilized *Lactococcus lactis* ssp. *lactis* in chitosan and alginate coated beads. *J. Dairy Sci.* 2001; 84, pp. 1118–1127.

[15] Krasaekoopt W., Bhandari B., Deeth H. Evaluation of encapsulation techniques of probiotics for yoghurt. *International Dairy Journal* 2003; 13, pp. 3 - 13.

[16] Lacroix C, Grattepanche F, Doleyres Y, Bergmaier D *Immobilised cell technologies for the dairy industry*. Nedovic, V, Willaert, R (Eds.), *Applications of Cell Immobilisation Biotechnology*. Springer, The Netherlands, pp. 295–321.

[17] Martin M.J., Lara-Villoslada F., Ruiz M.A., Morales M.E. Effect of unmodified starch on viability of alginate-encapsulated *Lactobacillus fermentum* CECT5716. *LWT - Food Science and Technology* 2013; 53, pp. 480 – 486.

[18] Mandal S., Puniya A.K., Singh K. Effect of alginate concentrations on survival of microencapsulated *Lactobacillus casei* NCDC-298. *International Dairy Journal* 2006; 16, pp. 1190–1195.

[19] Saarela M., Mogensen G., Fondén R., Mätö J., Mattila-Sandholm T. Probiotic bacteria: safety, functional and technological properties. *Journal of Biotechnology* 2000; 84, pp. 197 - 215.

[20] Sheu T.Y., Marshall R.T., Heymann H. Improving survival of culture bacteria in frozen desserts by microentrapment. *J. Dairy Sci.* 1993; 76, 1902–1907.

[21] Willemer H. Quality control during freeze-drying of biological products. 16th International Congress of refrigeration. Paris, International Institute of refrigeration 1983; pp. 78-83.

[22] Wolfson N.P. A probiotics primer. *Nutrition Science News* 1999, 4(6), pp. 276-280.

[23] Zavaglia A.G., Kociubinski G., Perez P., Antoni G. Isolation an characterization of *Bifidobacterium* strans for probiotic formulation. *Journal of food protection* 1998 (USA), V. 61(7), pp. 865-873.

[24] Zayed G., Roos Y.H. Influence of trehalose and moisture content on survival of *Lactobacillus salivarius* subjected to freeze-drying and storage. *Process Biochemistry* 2004; 39(9), pp. 1081–1086.

INFLUENCES OF MESH DENSITY ON THE RESULT QUALITY OF NUMERICAL CALCULATION IN 3D MODEL OF CORRUGATED TUBE

M. S. Angelov, P. R. Raynov

University of Food Technologies, Plovdiv

Abstract: *The aim of the work is to perform studies to determine the independence of the solution by the density of the mesh. The influence to the density of the mesh on the accuracy of the decision in a 3D model of a tube with a complex geometric shape was studied. For the purpose to the work 3D geometric model of corrugated tube with a diameter d = 14 mm and a length l = 1 200 mm was created. Because using mesh is structured for the purpose to the work three different densities was created. A solution to the Navier Stokes equations was made and k-ε realizable turbulence model included Enhanced Wall Treatment function was used. Three cross-sections in the typical area were created. First (L1) is in the early area (smooth tube). The second cross-section (L2) was chosen so that tracks the evolution to the parameters in the beginning on the corrugated tube. The cross-section (L3) is in the ribbed area.*

Keywords: CFD, modeling, intensification, hydrodynamics, meshing.

I. Introduction:

One of the key moments in the numerical studies is choice of appropriate mesh. Due to the fact that the decisions are extremely dependent on its shape and density, have to verify the independence of the decision by mesh. No universal shape or density.

Often physical time which is spent on the creation of an adequate mesh may be much greater than the very numerical modeling. Each model has its specifics and each one must be created corresponding computing mesh.

For examplex, in a study on hydrodynamic and heat transfer in the tubes because the transfer processes are carried out in the zone near the wall is necessary to create a corresponding mesh with the appropriate density near the wall which discretized the zone on the boundary layer.

II. Materials and methods.

The aim of the work is to perform studies to determine the independence of the solution by the density of the mesh. The influence to the density of the mesh on the accuracy of the decision in a 3D model of a tube with a complex geometric shape which, at a later stage will be tested to determine the main and turbulent characteristics of the flow was studied.

For the purpose to the work, 3D geometric model of corrugated tube with a diameter d = 14 mm and a length l = 1 200 mm was created [6], [7]. The early straight area with a length l = 50d was created and model is shown in Figure 1. In this way it is guaranteed that the flow is fully developed turbulent on entering the area of the corrugated tube.

Because using mesh is structured for the purpose to the work three different densities with parameters shown in Table. 1.1 was created:

Table 1.1. *Parameters of the studied mesh.*

№	Absolute maximum cell size	Total number of cells
M1	1 mm	4 918 716
M2	1,1 mm	4 426 189
M3	1,2 mm	3 875 344

Feature in the creation of mesh is the presence of two pronounced areas:
- near the streamlined wall (the area of the boundary layer).
- area of a developed turbulent flow.

In order to accurately calculate the characteristics of the flow in the zone of the boundary layer are provided 15 layers adjacent to the wall, as shown in Figure 2 and Figure 3.

A solution to the Navier Stokes equations was made and k-ε realizable turbulence model included Enhanced Wall Treatment function was used. The purpose of this model was to incorporate the influence of the changing shape of the streamlined wall which follows the shape of a corrugated surface. The numerical solution is carried out in ANSYS FLUENT at Re = 40.10^3.

Three cross-sections in the typical area were created. First (L1) is in the early area (smooth tube). The second cross-section (L2) was chosen so that tracks the evolution to the parameters in the beginning on the corrugated tube. The cross-section (L3) is in the ribbed area (corrugated tube). These three cross-sections are shown in Figure 4.

III. Analysis of results and discussion.

The analysis of the change in velocity has two purposes, namely proving that turbulent flow is developed, and that the values of the velocities in

different points do not change with a change in the density of the mesh. From Figure 5 a. it is seen that the velocity profile in the zone to be establishing turbulent flow (after the early area) for flow in a smooth pipe (L1 = 15d) and there was no difference in the velocity profiles at the three studied densities of the computing mesh. For cross-sections L2 = 53d and L3 = 114d is observed asymmetry of the velocity profiles, which is due to the helical rib. It could be argued that the density of the mesh does not affect by the accuracy of the result.

Assessment for turbulizing flow in corrugated tube can be made based on change of the basic turbulence characteristics: turbulent kinetic energy, turbulent intensity and turbulent viscosity. Figure 6 shows the change of the turbulent kinetic energy for the three sections at three densities of computing mesh. The profile of the turbulent kinetic energy is typically with a maximum of near the ribbed surface. The small difference (<0,5%) in profile amendment in the third section was observed.

Presented in Figure 7 results on the amendment to dissipation of the turbulent kinetic energy confirmed the independence of the solution by the density of the mesh. Figure 8 and Figure 9 presented amendment to turbulent intensity and turbulent viscosity. From the analysis by the amendment of quantity can be argued that the density of the computing mesh does not affect the accuracy by the solution and can provide model and simulation studies.

IV. Conclusion:

The analysis of the results from the model tests with three different densities of the computing mesh shows that it can be assumed to reach solution independent from the density of the mesh. Can make the following conclusions:

1. Basic parameters for turbulent flow in a corrugated tubes are not affected by the density of the mesh with the parameters described above.

2. Established density of the mesh that will continue the design and simulation studies.

References.

[1] Anderson J. D. *Computational Fluid Dynamics: The basics with applications*. Library of Congress Cataloging in Publication Data. 1995.

[2] ANSYS. *ANSYS Meshing User's Guide*. Southpointe 275 Technology Drive Canonsburg. 2010.

[3] Chung T. J. *Computational Fluid Dynamics*. University Press, Cambridge. 2002.

[4] Peyret R. *Handbook of Computational Fluid Mechanics*. Elsevier Science & Technology Books**.** 1996**.**

[5] Versteeg H. K., Malalasekera W. *An introduction to Computional Fluid Dynamics*. British Library Cataloguing in Publication Data. 1995.

[6] Zimparov V. D.. et al. *Heat Transfer and Friction Characteristiques of Spirally Corrugated Tubes for Power Plant Condensers. Part1–Experimental Investigation and Performance Evaluation*. Int. J. Heat Mass Transfer. 4. No.9. pp. 2187-2197. 1991.

[7] Райнов П. *Методика за построяване на спирално оребрена тръба чрез автоматизирана система*. Национална конференция с международно участие. Сливен 28-30 Юни. 2013 г.. Сп. Топлотехника. ISSN 1314-2550. бр. 5. стр. 32-35. 2013 г.

[8] Стоева Д. *Анализ и съпоставка на изчислителната мрежа във вертикален въздушен канал*. Хранителна наука, техника и технологии УХТ-Пловдив, периодично научно издание, Volume III. 2011.
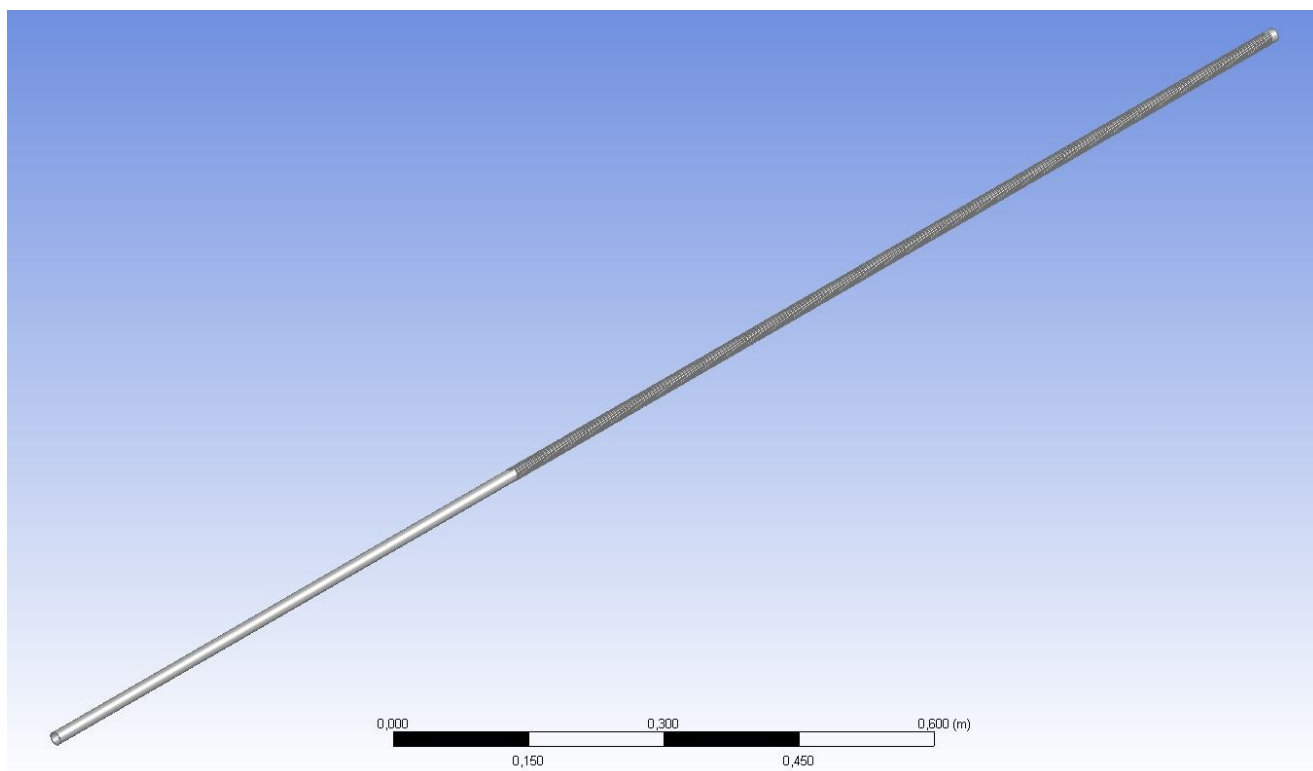
Fig.1. *General view of the 3D model.*
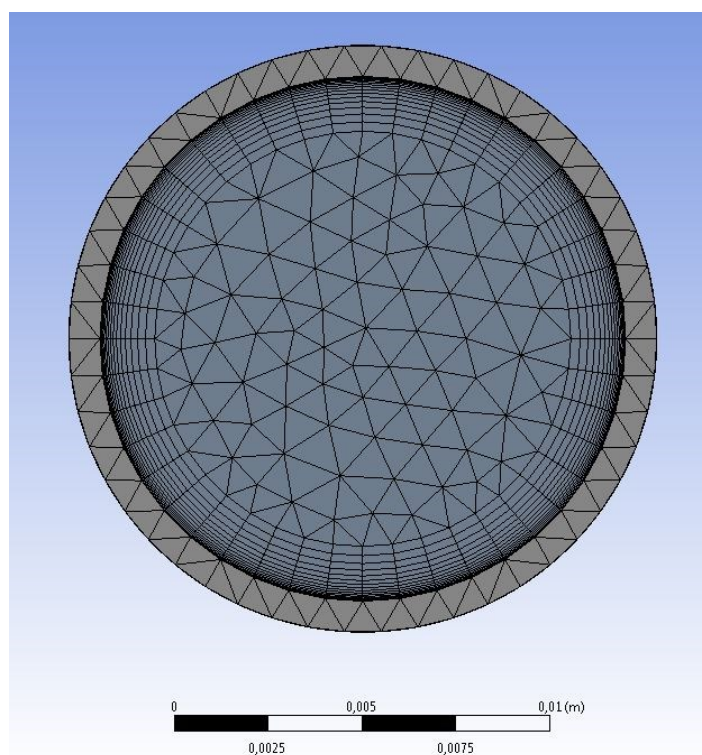
Fig.2. *Distribution of the mesh in the cross section.*
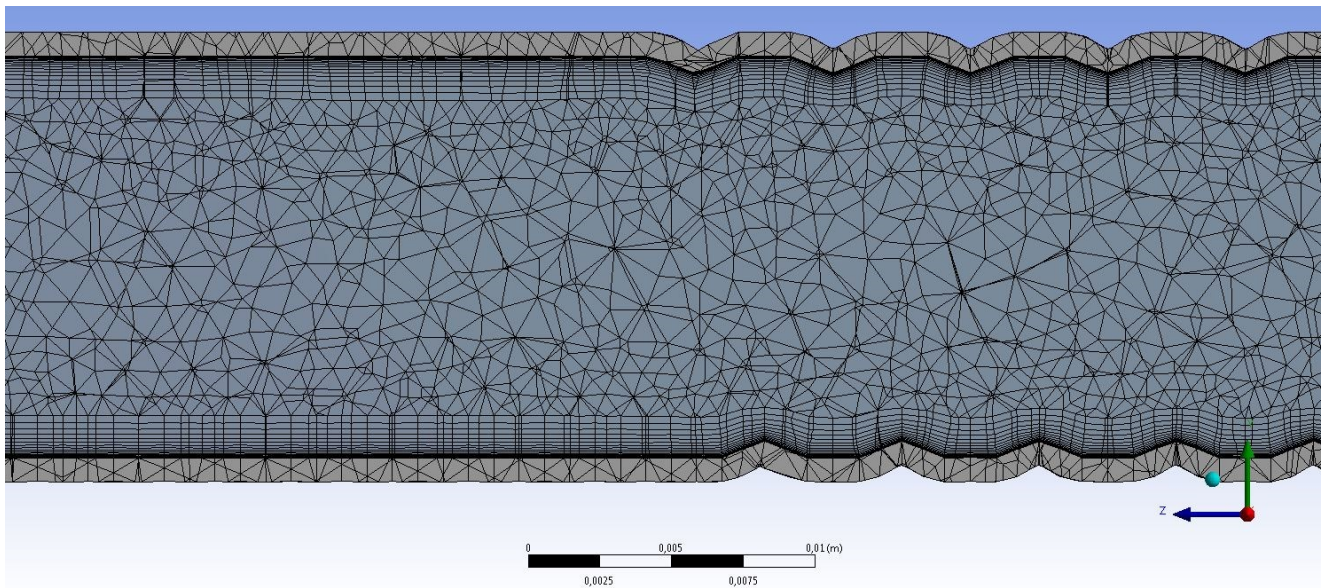
Fig.3. *Distribution of the mesh along the pipeline.*
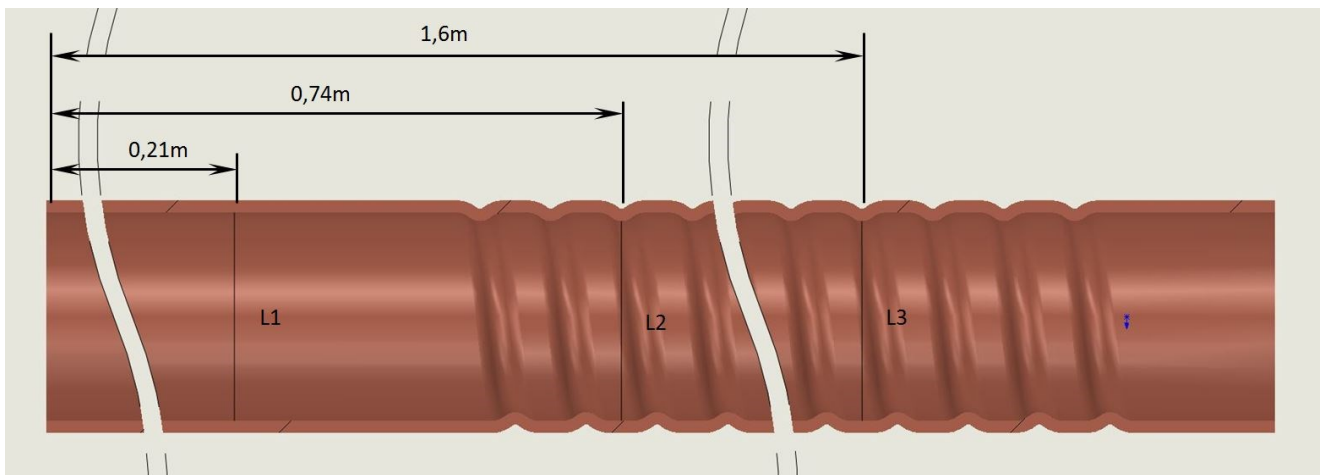
Fig.4. *Locations of the created cross sections along the pipeline.*
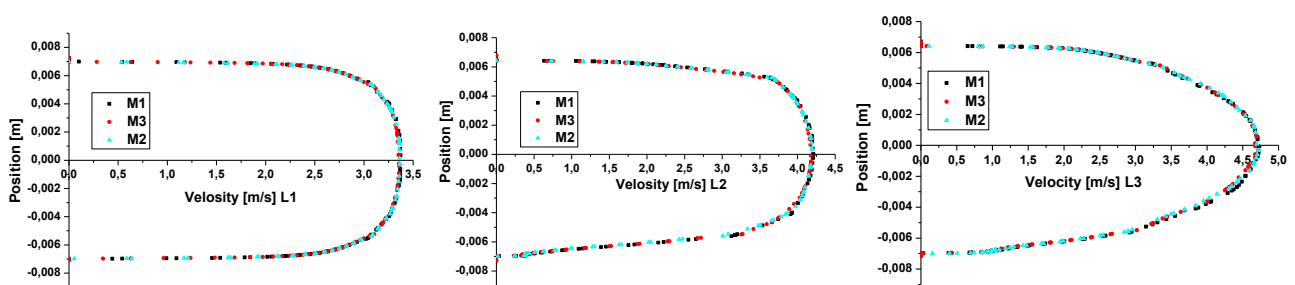
a.) *L₁=15d*

b.) *L₂=53d*

c.) *L₃=114d*

Fig.5. *Velocity profiles in the three typical sections for three different densities of the mesh.*

a.) *L₁=15d* **b.)** *L₂=53d* **c.)** *L₃=114d*

Fig.6. *Variation of the turbulent kinetic energy for three different densities of the mesh.*

a.) *L₁=15d* **b.)** *L₂=53d* **c.)** *L₃=114d*

Fig.7. *Variation of dissipation on turbulent kinetic energy for three different densities of the mesh.*

a.) *L₁=15d* **b.)** *L₂=53d* **c.)** *L₃=114d*

Fig.8. *Variation of turbulence intensity for three different densities of the mesh.*

a.) *L₁=15d* **b.)** *L₂=53d* **c.)** *L₃=114d*

Fig.9. *Variation of turbulent viscosity for three different densities of the mesh.*

INTENSIFYING PROCESSES STEP-BY-STEP SEPARATION OF PIECE GOODS IN THE SYSTEM TRAYS-FEEDERS MACHINES-VENDING MACHINES

A.N. Gavva, L.A. Krivoplyas-Volodina, E.A. Kohan

[1] *Chair of technical mechanics and packing technique,* [2] *Chair of bakery and confectionary goods technology, Faculty of engineering mechanics and packing technique, National University of Food Technologies, 68 Volodimirs`ka St., Kiev, Ukraine, e-mail: kaf_upak_tmm@bk.ru*

Abstract. *Formation of steady transport packets provides, near binding of tare loads in a packet, their layout according to the appropriate scheme. [2,5]. Schemes in which loads are located to, joint providing bandaging compliance beforehand the loads concluded in a layer, are created of variously oriented tare loads. For change of orientation of a tare load in the horizontal plane, concerning its situation on the giving conveyor, in a packet creating machines apply various constructions of mechanisms of orientation. These mechanisms can tear a load on 90 ° or change situation concerning its original layout. Devices of orientation can be executed with passive, active and combined working organs.*

Key words: carton box, washing machine, gift shop packs, conveyor.

I. Introduction

Also orientations of a load can be executed both on one, and on several bearing planes of transport systems of packet creating machines

From the point of view of nature of action of loads of loading that moves in orientation mechanisms, we can select frictional and inertial, kinematic and combined orientations

Frictional and inertial orientation is reached by support of simultaneous contact of a mobile load with the mobile and fixed bearing planes therefore load under the action of power of inertia and friction. Kinematic orientation is executed by special mechanisms with working items like capture or clamp.

A combined method of orientation of loads are used In the modern samples a packet of creating machines. This method is as follow during orientation the load contacts with two planes one of which is bearing, and another - a guide. Guide can be fixed (it`s used more often) or mobile. The combination of force influence of a directing surface, the frictional forces operating on a reference surface of a load from the bearing plane and inertial forces provide necessary load orientations in case of high performance of mechanisms of orientation and the machine as a whole. The orienting surface can be rectilinear (a coordinating oar) or the curvilinear (an orienting emphasis of the whip type or the curvilinear performances of side walls of construction). Preferential use of mechanisms of orientation of this kind is caused by simplicity of their construction, high performance, sufficient

reliability in case of a correct choice of geometrical, kinematic and other design data of the mechanism of orientation.

Process of orientation of tare loads is carried out under the influence of inertial forces, friction, responses of communication and is difficult plane movement of load orientation.

Key parameters with which it is possible to characterize operation of orientation of loads is productivity, that is the orientation duration, quality of orientation (a load turn on the given angle and relocation in the standard position) and costs of energy of operation execution. These parameters can be provided only in case of the correct assessment of all factors influencing orientation of a load.

II. Materials and methods

The technique of determination of parameters of movement of tare loads in devices of orientation of packet creating machines is given in scientific works [1,5,6]. Ways of intensification of operation of orientation aren't justified an aren`t formulated in the received results of researches

Considering that in any mechanisms of orientation of a load the load makes difficult plane movement in the packet creating machines, we will analyze the equations describing movement of a load in these mechanisms and we will define ways of influence on parameters of quality of orientation. On Fig. 1 the diagram of force impact on a tare load is given during its turn in the bearing plane by the whip emphasis. Movement of a load is characterized as difficult plane of a turn on the bearing plane and
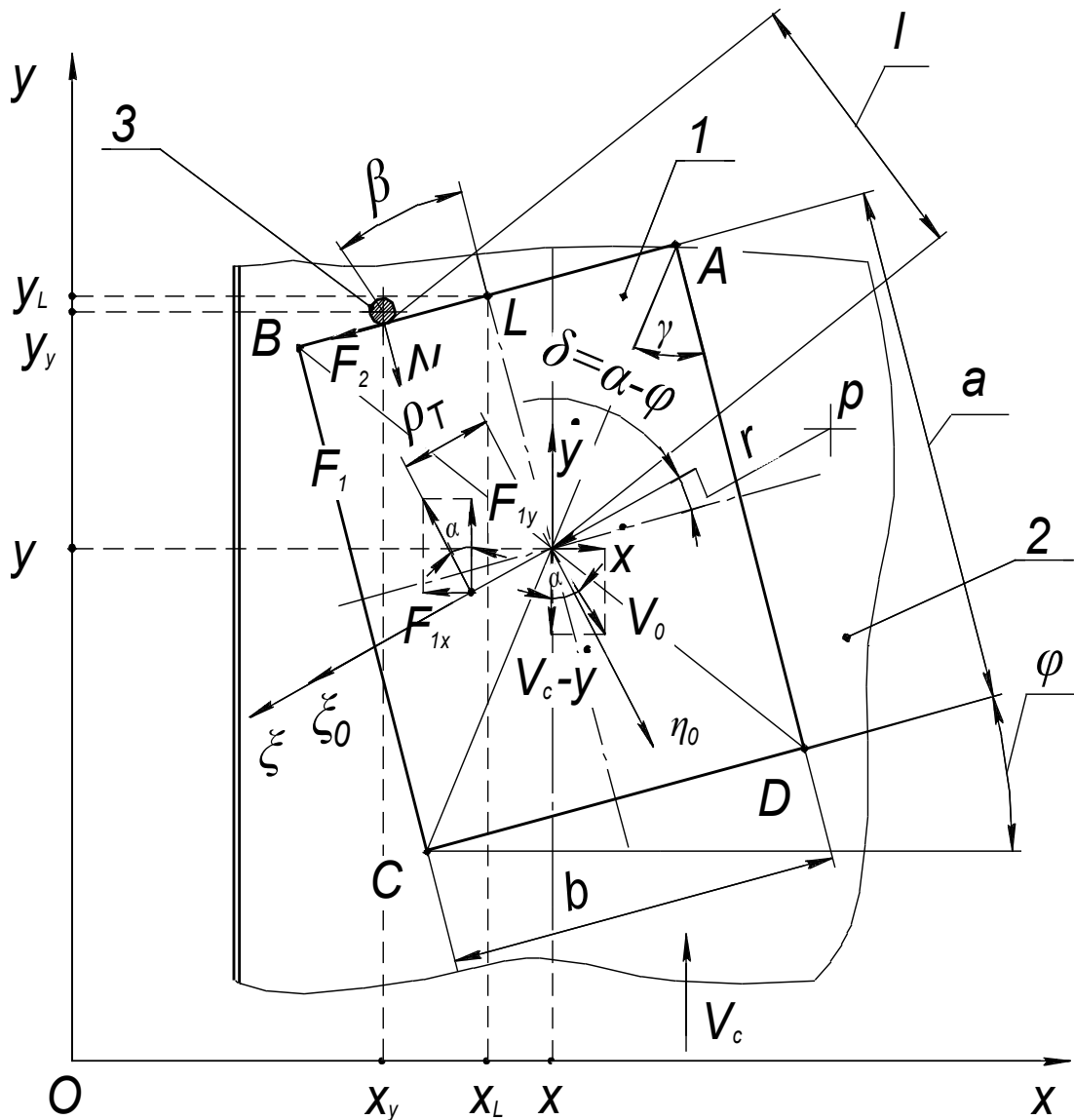
Figure 1. *The diagram of interaction of forces in case of a turn of a tare load
an immovable emphasis on the bearing plane of a packet creating machines :
1- tare load; 2- the bearing plane of the conveyor; 3- fixed bearing*

simultaneous sliding of its lateral face on an emphasis surface. For the mathematical description of movement of a load we will accept the assumption: the center of masses of a load is located in the geometrical center of a load; the load is a solid body; load friction coefficients on bearing and orienting to the planes within change of the relative speeds of movement of a load are values constant; emphasis radius insignificant in comparison with the load sizes.

On accepted conditions the load is affected by a normal component *N and tangent F_2* full reaction *R* from a support, principal vector of sliding frictional forces F_1 reference surface of a load on the bearing plane of the conveyor. Principal vector of frictional forces F_1 is sent to the opposite side of a vector of

the relative speed V_0 reference surface of a load of rather bearing plane also it is enclosed in the point located at distance ρ_T from geometrical center of a reference surface of a load.

Distance ρ_T is characterized as the radius of friction and is defined:

$$\rho_T = L \,/\, F_1 - r, \tag{1}$$

where *L* – moment of frictional forces of a reference surface of a load relatively the instantaneous center of motion speeds of a load; *r* – the radius defining distance from the instantaneous center *p* of speeds to geometrical center of a reference surface of a load, is defined as:

$$r = \frac{1}{\dot{\varphi}}\sqrt{\left(V_c - \dot{y}\right)^2 + \dot{x}^2}\ , \tag{2}$$

where: V_c – traverse speed of the bearing plane of the pipeline;

$\dot{x}$, $\dot{y}$ – projections to axes Ox, Oy traverse speeds of geometrical center of a reference surface of a load;

$\dot{\varphi}$ – angular speed of rotation of a load of rather geometrical center of a reference surface of a load.

In a general view the moment of frictional forces and the principal vector of frictional forces can be determined by formulas:

$$
\begin{cases}
L = \int_{\eta_1}^{\eta_2} \int_{\psi_1(\eta)}^{\psi_2(\eta)} f_1 \cdot q(\eta,\xi) \cdot \sqrt{\eta^2 + \xi^2}\, d\xi\ d\eta + ... \\[2mm]
..+ \int_{\eta_2}^{\eta_3} \int_{\psi_4(\eta)}^{\psi_2(\eta)} f_1 \cdot q(\eta,\xi) \cdot \sqrt{\eta^2 + \xi^2}\, d\xi\ d\eta + ... \\[2mm]
...+ \int_{\eta_3}^{\eta_4} \int_{\psi_4(\eta)}^{\psi_3(\eta)} f_1 \cdot q(\eta,\xi) \cdot \sqrt{\eta^2 + \xi^2}\, d\xi\ d\eta; \\[2mm]
F_1 = \sqrt{F_{1x}^2 + F_{1y}^2},
\end{cases}
\tag{3}
$$

$$
where \quad
\begin{aligned}
&\eta_1 = -0,5 \cdot \sqrt{a^2 + b^2} \cdot \cos(\delta - \gamma); \\
&\eta_2 = -0,5 \cdot \sqrt{a^2 + b^2} \cdot \cos(\delta + \gamma);
\end{aligned}
$$

$$\eta_3 = 0,5 \cdot \sqrt{a^2 + b^2} \cdot \cos(\delta + \gamma);$$

$$\eta_4 = 0,5 \cdot \sqrt{a^2 + b^2} \cdot \cos(\delta - \gamma)$$

$$\delta = \alpha - \varphi; \alpha = arctg(\dot{x}/(V_c - \dot{y}));$$

$$\gamma = arctg(b/a);$$

$$\psi_1(\eta) = -\eta \cdot ctg\,\delta + r - (0,5a/\sin\delta);$$

$$\psi_2(\eta) = \eta \cdot tg\,\delta + r + (0,5b/\cos\delta);$$

$$\psi_3(\eta) = -\eta \cdot ctg\,\delta + r + (0,5a/\sin\delta);$$

$$\psi_4(\eta) = \eta \cdot tg\,\delta + r - (0,5b/\cos\delta);$$

f_1 - sliding friction coefficient of a reference surface of a load on the bearing plane of the conveyor;

$q(\eta,\xi)$ - pressure upon a reference surface of a load determine:

$$
q(\eta,\xi) = q_0 + \eta\left(\frac{M_{\xi 0}}{I_{\xi 0}} \cdot \cos\delta\right) - \frac{M_{\eta 0}}{I_{\eta 0}} \cdot \sin\delta\right) + ...
$$

$$
...+ (\xi - r)\left(\frac{M_{\xi 0}}{I_{\xi 0}} \cdot \sin\delta + \frac{M_{\eta 0}}{I_{\eta 0}} \cdot \cos\delta\right)
\tag{4}
$$

where q_0 – pressure upon a reference surface of a load in case of uniform distribution of load of it,

generally determine as $q_0 = \dfrac{m \cdot g}{a \cdot b}$; a, b – overall dimensions of a load; $M_{\xi 0}$, $M_{\eta 0}$ – the principal moments of external forces concerning axes ξ_0, η_0, carried out through geometrical center of a reference surface; $I_{\xi 0}$, $I_{\eta 0}$ – inertia moments of a reference surface of a load concerning axes ξ_0, η_0.

Difficult plane movement of a load on the bearing plane of the conveyor can be described the equations:

$$
\begin{cases}
\dfrac{d^2 x}{dt^2} = \dfrac{1}{m} \cdot (N \cdot \sin\varphi - F_2 \cdot \cos\varphi - F_{1x}); \\[2mm]
\dfrac{d^2 y}{dt^2} = \dfrac{1}{m} \cdot (F_{1y} - N \cdot \cos\varphi - F_2 \cdot \sin\varphi); \\[2mm]
\dfrac{d^2 \varphi}{dt^2} = \dfrac{12}{m \cdot c^2} (N \cdot l_\varphi + F_2 \cdot 0,5 \cdot c \cdot \sin\varphi - M_0),
\end{cases}
\tag{5}
$$

where $c = \sqrt{a^2 + b^2}$; $F_2 = f_2 \cdot N$; f_2 – sliding friction coefficient of a lateral surface of a load on a surface of a fixed emphasis; l_φ - distance from the line of action of normal response N to center of masses of a load; M_0 – the moment of frictional forces concerning center of masses of a load.

The moment of frictional forces M_0 can be defined from expression:

$$M_0 = F_1 \cdot \rho_T = L - F_1 \cdot r. \tag{6}$$

III. Results and discussion

On the basis of the analysis of expressions (5) and (6) it is possible to draw an output that it is necessary for increase in angular acceleration of rotation of a load, in case of the given constructional parameters of the mechanism of the orientation, the bearing plane of the conveyor and load parameters, to reduce the moment of frictional forces M_0. And it is possible on condition of reduction of radius of friction ρ_T. of reduce radius ρ_T is possible due to pressure redistribution on a reference surface and due to change of a field of the relative speeds of movement of a reference surface. On Fig. 2 diagrams of change of angular coordinate of a load are given during its turn by an immovable emphasis in case of uniform distribution of pressure and non-uniform, but a load responding to static stability in the bearing plane [3]. Diagrams are constructed on the basis of numerical calculations of the non-linear differential equations describing multi-stage process of orientation [5] provided on Figure 2.
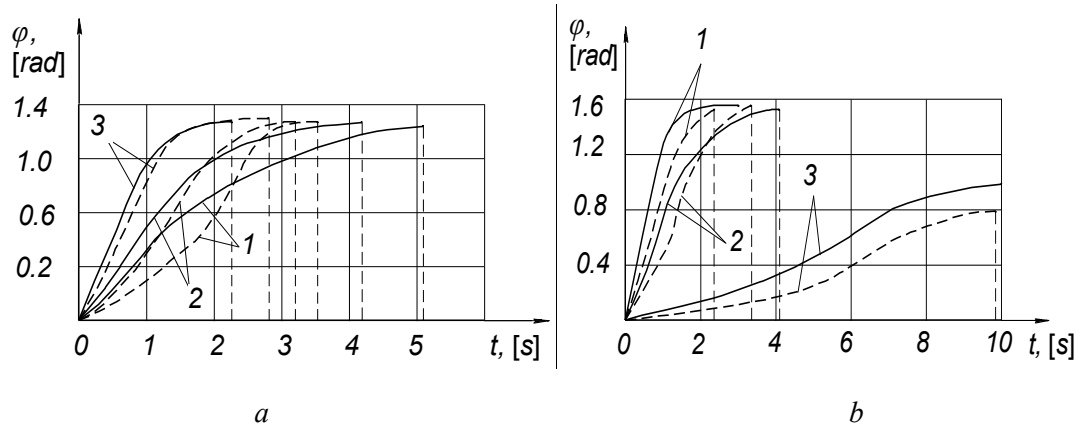
Figure 2. *Diagrams of change of angular coordinate of a load in the course of its turn an immovable emphasis:*

a) $V_c = 0,5$ m/s: 1- β = 0,139 rad; 2- β = 0,241 rad; 3- β = 0,337 rad;

б) β = 0,139 rad: 1- $V_\varPi$ = 1,0 m/s; 2- $V_\varPi$ = 0,5 m/s; 3 - $V_\varPi$ = 0,1 m/s

(solid lines correspond to uniform distribution of pressure $q = q_0$, the shaped – non-uniform pressure distribution $q(\eta,\xi) = q_0 + \eta \cdot \dfrac{M_{\xi 0}}{I_{\xi 0}}$).

From Fig.2 it is possible to draw an output that in case of the appropriate ratios of motion speed of the bearing plane and pressure redistribution on a reference surface of a load is possible to reduce activity duration of orientation on 20... 35%.

Different constructional elements that are used in a packet creating machines of average productivity intensify operation, so for example: the bearing plane is executed in the form of the conical rollers located on the appropriate diagram; on pipelines set the special fixed planes; pressing elements and etc.

The specified measures sometimes are ineffective (especially in case of small values of speed of the bearing plane of the conveyor $V_c < 0,2$ m/s). In that case it is necessary to use combined option of force impact on a load, that is it is necessary to set in addition in the mechanism the active working organ, for example, push rod.On Fig. 3 the diagram of the mechanism of orientation of a tare load by an immovable emphasis with additional action on a load is provided push rod.

In this case, as well as in cases with passive working organs, operation of orientation can be given set of such characteristic stages:
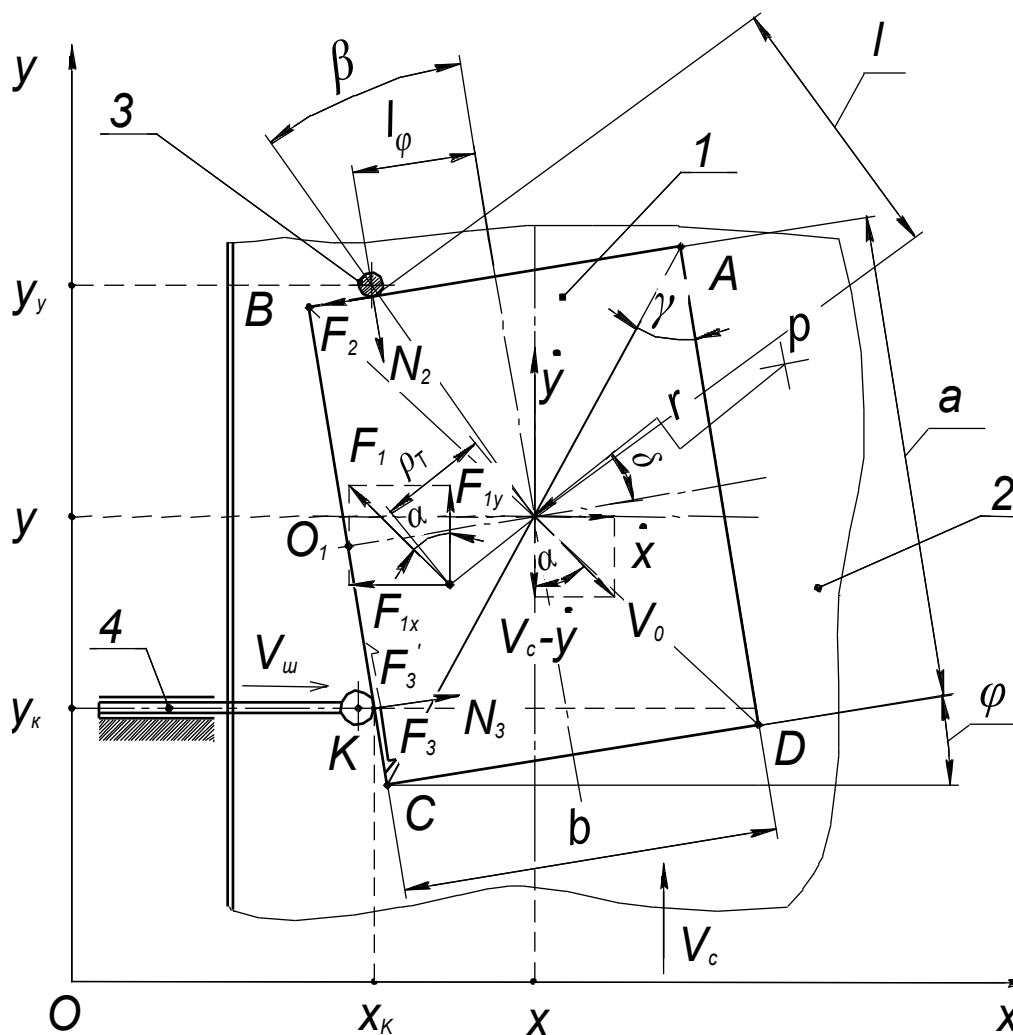
- direct noncentral shock of the load moving with a speed of V_c bearing planes of the conveyor, on fixed an emphasis [4];

- difficult plane movement of a load on the bearing plane of the pipeline in case of simultaneous sliding of its lateral surface on a surface of an emphasis and action of a pusher;

- difficult plane movement of a load on the bearing plane of the pipeline after its lift-off from an emphasis surface.

The main difference of mathematical simulation of movement of a tare load in such mechanism of orientation is the accounting of force impact on a load of a push rod.

In case of such design features of the mechanism of orientation the load is affected by normal components of responses N_2 and N_3 and tangents $F_2 = f_2 \cdot N_2$; $F_3 = f_3 \cdot N_3$, respectively from a fixed support and pucher and principal vector of sliding frictional forces F_1 reference surface of a load on the bearing plane of the conveyor.

Difficult plane movement of a load on the bearing plane under such circumstances can be described in the equations:

$$\frac{d^2x}{dt^2} = \frac{1}{m} \cdot (N_2 \cdot \sin\varphi - ...$$
$$... - F_2 \cdot \cos\varphi + N_3 \cdot \cos\varphi \pm ...$$
$$... \pm F_3 \cdot \sin\varphi - F_x);$$

$$\frac{d^2y}{dt^2} = \frac{1}{m} \cdot (F_y - N_2 \cdot \cos\varphi - ...$$
$$... - F_2 \cdot \sin\varphi + N_3 \cdot \sin\varphi \mp ... \qquad (7)$$
$$\mp F_3 \cdot \cos\varphi);$$

$$\frac{d^2\varphi}{dt^2} = \frac{12}{m \cdot c^2} (N_2 \cdot l \cdot \sin\beta + ...$$
$$... + F_2 \cdot 0,5 \cdot c \cdot \cos\gamma + ...$$
$$... + N_3 \cdot l_{0'K} \pm F_3 \cdot 0,5 \cdot c \cdot \sin\gamma - M_0);$$

Figure 3. *The diagram of interaction of forces in case of a turn of a tare load an immovable emphasis on the bearing plane of the conveyor a packet of the creating machine in simul taheus action of a pusher: 1- tare load; 2- the bearing plane of the pipeline, 3- fixed support, 4- pusher*

Equations (7) is used for the decision of system of equations :

$$\sin\varphi \cdot (y - y_k - 0,5 \cdot c \cdot \cos\gamma \cdot \sin\varphi + ...$$
$$... + 0,5 \cdot c \cdot \sin\gamma \cdot \cos\varphi) = V_{w} \cdot t;$$
$$y - y_y + 0,5 \cdot c \cdot \sin\gamma \cdot \cos\varphi - ...$$
$$..._{-}(x - x_y - 0,5 \cdot c \cdot \sin\gamma \cdot \sin\varphi) \cdot tg\varphi = 0,$$

(8)

also we will accept the following assumptions: initial contact of a pusher and load is shock-free; traverse speed of a pusher is a constant $V_{w}=const$; the direction of movement of a pusher is perpendicular to a velocity vector of the bearing plane.

The accepted assumptions simplify the solution of the task a little, along with it for full taking note of external factors pertinently to consider the possible direction of action of a pusher both under other angles and in case of variable speed of movement of a working organ of a pusher.

For beforehand accepted basic data and assumptions it is executed numerical calculations of system of equations (7). Graphic interpretation of results of calculation is given on a Fig. 4.

Results of numerical calculations of the mathematical models describing movement of a load in mechanisms of orientation, confirm a hypothesis of opportunity effectively to intensify operation of orientation of tare loads on the bearing plane of the pipeline a packet of the creating machine due to the correct selection of motion speeds of a working organ of a pusher movements of a working organ of a pusher and choice of its rational provision of rather lateral surface of a load.

In the modern packets the creating machines providing high performance of automated product lines, to orientation of loads widely apply mechanical devices of capture.

In case of use of such mechanisms, orientation can be carried out with a load lift-off from the

bearing plane and without lift-off apply mechanical devices of capture.

For high-quality orientation of a load it is important to justify scientifically a choice of drives and to provide rational parameters of movement of working organs of the mechanism of orientation.

Mechanisms of orientation of the first look are widely applied in different functional groups as packages, and other technological machines.

Therefore the technique of determination of rational force, kinematic and geometrical parameters of these mechanisms are developed rather fully. Slightly more difficult with scientific reasons for parameters of movement of loads in mechanisms of orientation of the second look.

The main complexity of calculations need to consider the moment of frictional forces of a reference surface in case of load deployment round center of masses. On Fig. 5 the estimated diagram of the mechanism of orientation with captures by working organs is provided.

The drive and the carriage are a part of such mechanism of orientation for horizontal relocation of elements of capture; the drive provides load deployment on the given angle; the drive providing a clip of elements of capture to a load.

In a case when the turn of a load is carried out on the bearing plane of the conveyor, the necessary effort of its clip can be determined by working organs by expression:

$$N_1 = k_1 \cdot \frac{m \cdot g \cdot f_2}{2 f_1}, \qquad (9)$$

where k_1 – the dimensionless coefficient considering non-uniformity of a clip of working organs to a load during its movement; m – load mass; f_1 – sliding friction coefficient of a reference surface of a load on the bearing plane; f_2 – load sliding friction coefficient on clamping working organs.

Duration of a kinematic cycle of operation of orientation is defined as the amount of dlitelnost of each stage of movement of working organs of the mechanism of orientation:

$$T_k = t_n + t_3 + t_o + t_{x.3.} + t_{x.n}, \qquad (10)$$

where t_n - duration of relocation approximate carts in an orientation zone; t_3 – action of capture process of load; t_o - duration of capture of a load; $t_{x.3.}$ - duration of leadout of fascinating elements in home position; $t_{x.n}$ – duration of relocation horizontal carts in home position.

Depending on construction of the mechanism of orientation the structure of a formula (10) can be a bit different. Along with it a mandatory component of a kinematic cycle is orientation duration.

In a general view movement of a load and working organs in case of orientation can be written:

$$\frac{d^2\varphi}{dt^2} = \frac{1}{I_{np}}(T - M_0), \qquad (11)$$

where: I_{np} - the given inertia moment of the bodies rotating together with a load; T – torsional moment on vertical to a shaft of the mechanism of orientation; M_0 - the moment of frictional forces of a reference surface of a load on the bearing plane of the conveyor in case of its deployment of rather geometrical center.
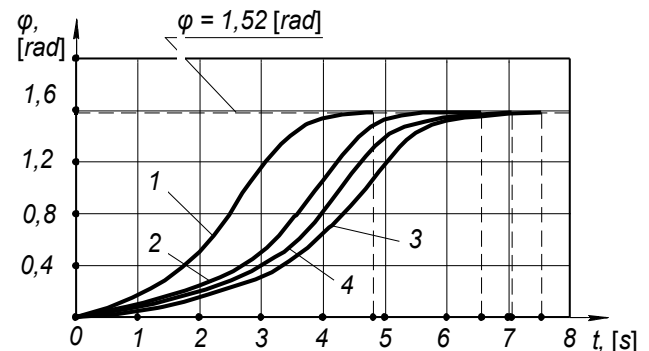
Figure 4. *The diagram of change of angular coordinate of a load during its turn an immovable emphasis and a pusher on the bearing plane:*
1- $V_{ш} = 0,1$ m/s; $l_{0'k} = 0,05$ m;
2- $V_{ш} = 0,1$ m/s; $l_{0'k} = 0,13$ m;
3- without pusher;
4- $V_{ш} = 0,3$ m/s; $l_{0'k} = 0,05$ m

Figure 5. *The orientation mechanism with captures:1- the carriage for horizontal relocation of the mechanism of orientation; 2- the drive of a turn of elements of capture with a load; 3- capture element*

Figure 6. *The mechanism of relocation of a tare load from a line item on a line item*

The moment of frictional forces of rather geometrical center of a load is determined by a formula.

$$M_0 = \int\limits_{-b/2}^{b/2} \int\limits_{-a/2}^{a/2} f_1 \cdot q(x,y)\sqrt{x^2 + y^2}\, dx dy . \quad (12)$$
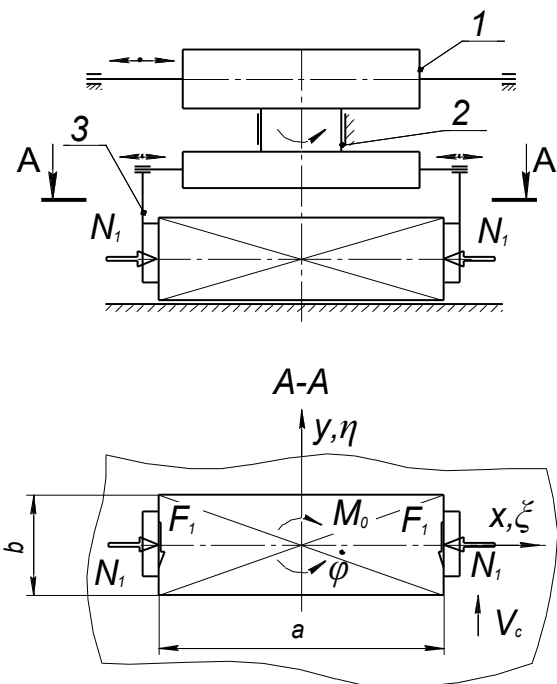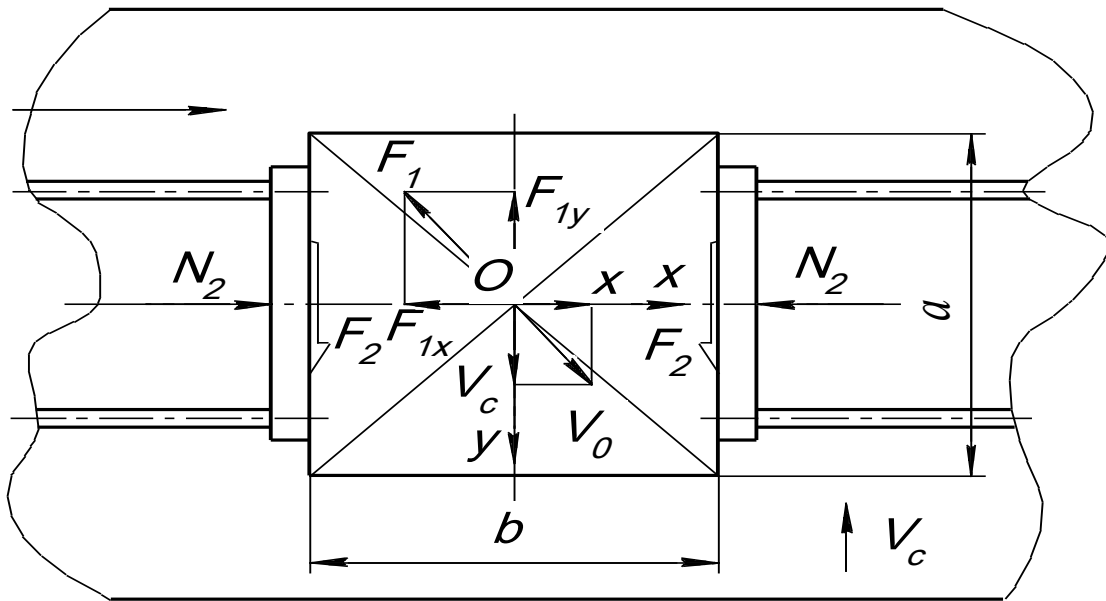
In case of uniform distribution of pressure on a reference surface the formula (12) will have an appearance:

$$M_0 = \frac{m \cdot g}{a \cdot b} \cdot f_1 \int\limits_{-b/2}^{b/2} \int\limits_{-a/2}^{a/2} \sqrt{x^2 + y^2}\, dx \; dy . \quad (13)$$

In case of constants of values I_{np}, T, M_0 and in case of basic data $t_n = 0$; $\varphi_n = 0$; $\frac{d\varphi}{dt} = 0$; $\varphi_\kappa = \pi/2$ we will receive:

$$\frac{d\varphi}{dt} = \frac{1}{I_{np}}(T - M_0) \cdot t , \quad (14)$$

$$\varphi = \frac{1}{I_{np}}(T - M_0) \cdot \frac{t^2}{2}. \quad (15)$$

Then duration of orientation can be determined from expression:

$$t_\kappa = \sqrt{\frac{\pi \cdot I_{np}}{T - M_0}}. \quad (16)$$

Similar design of the mechanism of orientation of this kind effectively apply to relocation of tare loads from one line item in another. The carriage of horizontal relocation and gripping elements is a part of such mechanism (Fig. 6). In certain cases mechanism construction, is given on Fig. 6, is the universal and can execute operations of a turn of a load on 90º and its relocation in other line item.

Clamping forces of a load can be defined from expression:

$$N_2 = \frac{m \cdot g \cdot f_1}{2 \cdot f_2} \cdot k_1 \cdot \frac{\dot{x}}{\sqrt{\dot{x}^2 + V_c^2}} , \quad (17)$$

where: $\dot{x}$ - traverse speed of a load in the direction of an axis OX; k_1 - the coefficient considering non-uniformity of effort of a clip of capturing of an element to a lateral surface of a load.

Having accepted a driving force of relocation of a load a constant of its motion equation it is possible to define having solved a non-linear differential equation:

$$\frac{d^2 x}{dt^2} = \frac{1}{m_{np}} \cdot \left(P_{pyu} - \frac{m \cdot g \cdot f_1 \cdot V_c}{\sqrt{\dot{x}^2 + V_c^2}} \right). \quad (18)$$

In a case when the drive of the horizontal carriage is executed on the basis of the electric drive, its estimated power can be determined:

$$N_{\partial s} = m_{np} \cdot \left(\frac{d^2 x}{dt^2} + \frac{g \cdot f_1 \cdot V_c}{\sqrt{\dot{x}^2 + V_c^2}} \right) \cdot \frac{\dot{x}}{\eta_0} , \quad (19)$$

where: m_{np} - the specified mass of mobile elements of the mechanism of orientation of a load; η_0 - performance coefficient of the drive of the carriage of horizontal relocation

IV. Conclusions

On the basis of the analysis of parameters influencing kinematics of movement of tare loads in orientation mechanisms the paketoformuyuchikh of

machines, the following ways of intensification of operation of orientation are set:

- redistributions of pressure and change of a field of the relative speed of a reference surface of a load in case of its contact with the bearing plane of the pipeline;

- application of combined working organs of the mechanism of orientation, for example - a fixed emphasis, a pusher;

- application of the active working organs of the mechanism of orientation, for example - gripping elements.

Scientific reasons for kinematic and force parameters of constructional executions of mechanisms of orientation and synthesis and the analysis of cycles of operation give the chance to provide the given or highest productivity the paketoformuyuchikh of machines.

References

[1] Gavva A. N. Metodika rascheta protsesa orientirovaniya shtuchnih gruzov nepodvizhnyim uporom. – Pischevaya promyishlenost. – 1999. – Vyipusk 40 – pp. 20 – 23.

[2] Gavva O. M., Bespalko A. P., Volchko A. I. Obladnannya dlya obrobki transportnih paketiv. – K. – Upakovka. – 2006 , p. 96.

[3] Gavva O. M., Volchko A. A., Goloporov I. V. RozpodIlennya tisku po opornIy poverhnI vantazhu (vpliv na kInematichnI parametri). – Upakovka. – 2006. – №3 – pp. 8 – 52.

[4] Gavva O. M., Krivoplyas-VolodIna L. O., Slyusarchuk A. V. Udarna vzaEmodIya tarnogo vantazhu z konstruktivnimi elementami pakuvalnogo obladnannya. – Upakovka.- 2006 – №5 – pp. 41 – 45.

[5] Krivoplyas A.P., Kukibnyiy A.A., Bespalko A.P. i dr. Paketoformiruyuschie mashinyi. – M.: Mashi-nostroenie, 1982, p. 239.

[6] Krivoplyas A. P. Razrabotka teoreticheskih osnov peremescheniya shtuchnih gruzov v potokovyih liniyah ukrupneniya gruzovyih edinits pischevyih proizvodstv i ih prakticheskoe prilozhenie. – Dis. dokt. tehn. nauk. – K. 1988, p. 500.

MAGNETIC FILTER INASTALATION WITH CONTROLLING POROSITY BY EXTERNAL MAGNETIC FIELD

I.A. Shorstkii

Kuban State Technological University

Abstract. *Magnetic filter baffle surfaces modeling with controlled porosity in range from 0,257 to 0,47. Filter nucleus description and its influence on porosity. Explore behavior of microscopic objects (spherical balls size 25-50 microns) in magnetic field, and developing method of laying spherical elements in dense structure.*

Also were conducted laboratory studies of physical properties and parameters of magnet. As a result of work prepare comparative table of the experimental and theoretical data of laboratory filter.

Kay words: Filtration, Controlling porosity, Ferromagnetic, Magnetic field, Dense structure

I. Introduction

Magnetic filtration processes are widely used in various fields of industry for fluids, gases purification. A large number of studies have been conducted with magnetic filters [1-4], but possibility of adjusting the porosity of the filter controlled by an external magnetic field has not been considered.

Using a magnetic field in the filtering process is deeply investigated in micro gravity condition G-MAFB [5] , allowing to apply these technologies in space. Process of influencing the stacking magnetic beads has been described in [2]. In our study, we considered constructing spherical body's model of flat figure, depending on the geometry of the core filter septum. Conducted laboratory experiments determined porosity of the filter septum, which is based on using spherical bodies, controlled by an external constant magnetic field.

Research objective is considering adjusting process of porosity on the filter walls, due to influence of external magnetic forces acting on the filter material, receipt and comparison of experimental and theoretical parameters of laboratory filter settings, and develop an effective mechanism for cleaning filter septum.

II.Materials and Methods

Materials. Laboratory magnetic filter was created and built in our laboratory (Kuban State Technological University). As the material of the experimental apparatus were used ferromagnetic spherical bodies company RICOH COMPANY (Iron Oxide 1317-61-9; Carbon Clack 1333-86-4), diameter of 25-30 mm and $\rho=2800$ kg/m^3 bulk density. As a source of constant magnetic field of the cylindrical magnet (N38), magnetic field strength 1200 μT .
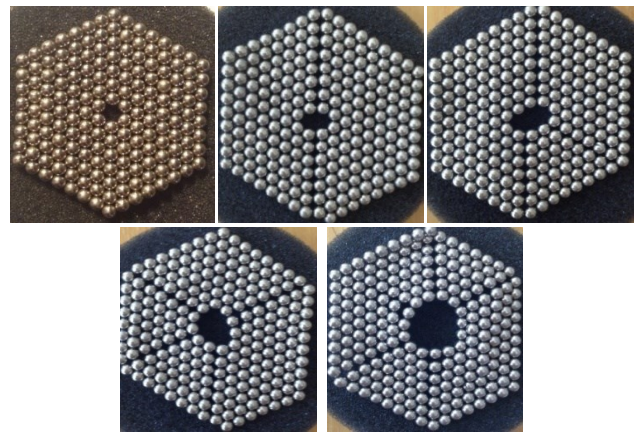
Figure 1. *Experimental value for the radial lines 6,8,10, 12 and 14 spherical bodies in the perimeter of the nucleus*

Filter layer modeling structure. Modeling of a single layer structure of the filter septum was performed using 216 neodymium magnets, diameter 3mm. In describing of ideal nucleus model was taken regular hexagon. This is a dense structure, tetrahedral stacking balls, with a porosity of 0,259.

During experimental pattern modeling was detected dependence of radial lines in structure model with number of the spherical bodies in the perimeter of the nucleus. Radial lines are in cubic packing structure with a porosity of 0,476.

Dependence of the number of radial lines expressed by equation:

$$N = B - (6 + m),\qquad(1)$$

where B is number of spherical bodies in the periphery of the nucleus, m 0.5 interval ratio from 0 to ∞ .

In this ideal size and shape depending, the possibility of the spherical bodies can has 100 % friable structure, while the amount of spherical bodies become 4006 in nucleus perimeter (Table 1).

Table 1. Nucleus percentage number of spherical bodies in friable structure in layer filters septum.

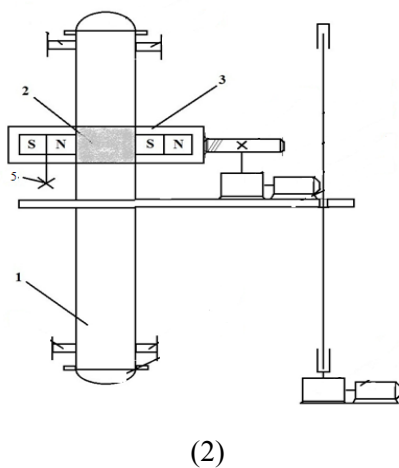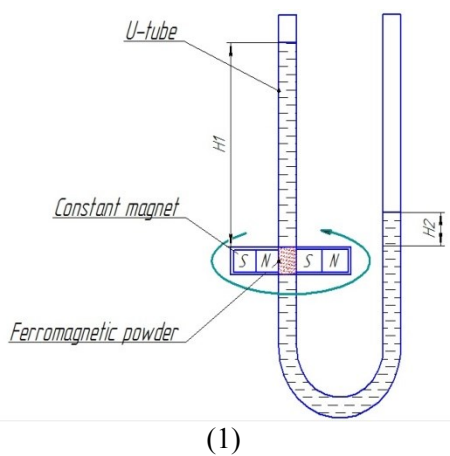| Number of spherical bodies in nucleus perimeter	Nucleus percentage number of spherical bodies in friable structure in layer filters septum, %
6	0
7	0,025
8	0,05
9	0,075
10	0,01
46	1
406	10
4006	100

(1)

(2)

Figure 2. *Laboratory filter: (1) model, (2) invention*

Magnetic filter with controllable porosity.

Ferromagnetic spherical bodies were placed in U-tube glass, 14 mm diameter. One side of the U-tube was connected to a hydraulic fluid column, with 1m height (H1). Another part of tube was open. Partition filter height was 15mm.
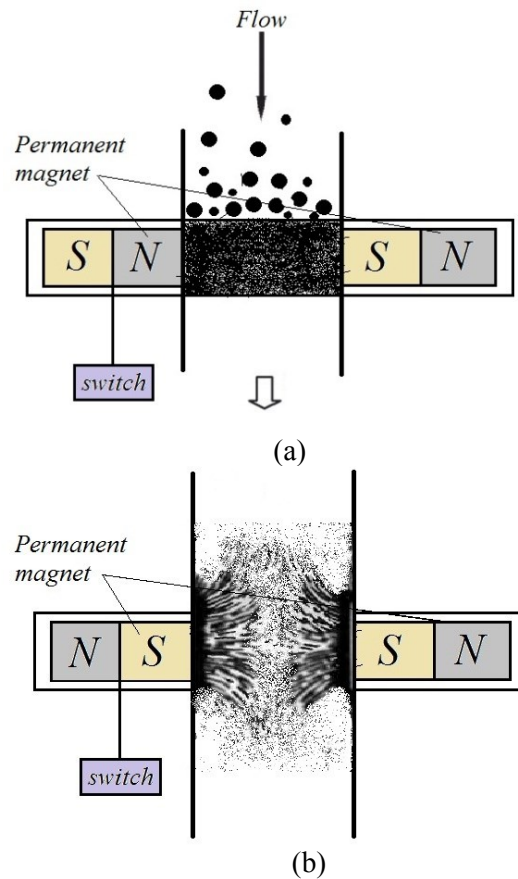

(a)

(b)

Figure 3. *Position of permanent magnets: operation N-S (a) and the cleaning process (reverse) S-S (b)*

Experiment time was 30 s. The experiment was repeated at least 3 times. As design was offered a patented invention [5]. Filtration device shown in Figure 3.

Ferromagnetic filter powder **2** poured into a dielectric vessel **1**. Vessel **1** has a cylindrical nozzle **4** with two permanent magnets **3**, transmitted by torque (Figure 4a). Dense (tetrahedral) structure filter material is forming. After filtering process, cleaning process is started.

Filter cleaning is a prerequisite filter process operation, and required periodicity of its execution. In our device cleaning principle is: The structure of the filter material is destroyed by a mechanical switch **5**. Magnetic powder holds by magnetic field lines of the permanent magnets, remains on the inner wall of the cylindrical vessel. Cylindrical nozzle make reciprocation motions along the vessel **1**. Washing water is supplied. After the cleaning process is finished, mechanical switch **5** is returned to its original position (Fig. 4b). The filtering process is repeated.

Dense structure filters formation under influence of the magnetic field. Under acting on ferromagnetic spherical bodies by external constant magnetic field, taken as a basis filter structuring
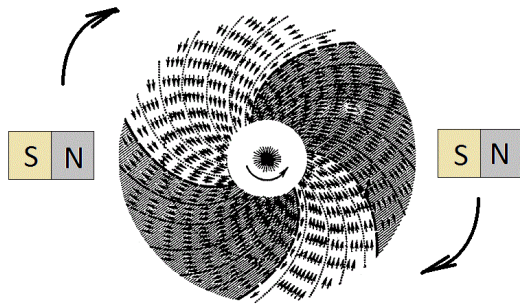
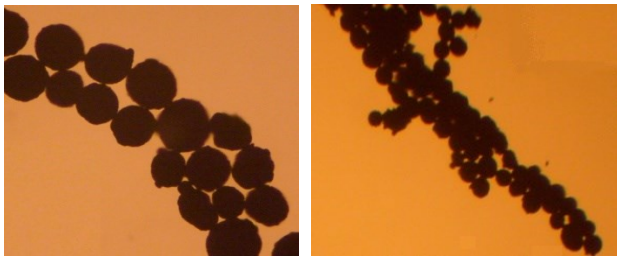**Figure 4**. *Filter structure in a rotational magnetic field*

Figure 5. *Fragments laying ferromagnetic beads: left represented cubic stacking balls not under the influence of the rotational magnetic field, right tetrahedral, under the influence of the rotational magnetic field (microscope ERGAWALL200fold, Germany).*
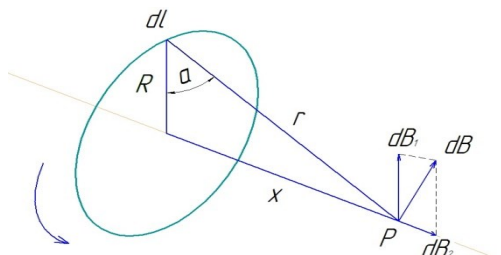

Figure 6. *A ring of radius R carrying a current i*

occurs along the magnetic field lines (Fig. 5). The magnetic field strength required for maintaining the structure of ferromagnetic filter partitions defined by the equation [7]:

$$\frac{\Delta P}{L} \approx \frac{2 \cdot F_M}{R} \qquad (2)$$

To construct tetrahedral dense stacking , it is necessary rotational movement ω of the magnetic field along the plane of the filter (Fig. 5) .

This formed structure resemble wrapped in a roll of paper. Ferromagnetic beads will seal dense packing form.

Depending of nature external magnetic field exposures (rotation or no rotation), various styling spherical bodies in the structure of the filter septum (Figure 3)

Table 2. Comparative characteristics of the filter parameters of equation (1), (2) for the theoretical data, and (3), (4) for experimental scientific work [4].

Data	Particle size, μm	Porosity coefficient, ε	coefficient of curvature , q	Linear speed of flow, u sm/s	filtration rate Q, m^3 / s
Theoretical	30	0,44	1,3	0,23	$3,07 \cdot 10^{-16}$
Experimental	25-30	-	-	0,3	$1,24 \cdot 10^{-16}$
Results [4]	22,5	0,46	1,43	-	-

Magnetic induction determination at distance x from center of magnet. For the current element shown in Fig.6 we have from the Biot-Savart Law [4],

$$dB = \frac{\mu_0 \cdot i \cdot \cos a \cdot dl}{4 \cdot \pi \cdot r^2} \qquad (3)$$

For our values with double permanent magnets with opposite arrangement , we have

$$B(x) = 2 \cdot \frac{\mu_0 \cdot i \cdot R^2}{2 \cdot (R^2 + x^2)^{3/2}}, \qquad (4)$$

For one permanent magnet, with magnet-power 1200 μT , with radius 5 mm and distance from center of magnet x 7 mm, have $B = 1464 \mu T$.

From Eq. (4) and (7) we can find maximal pressure, acting on filter without distraction.
$\Delta P = 0,3 MPa$

III.Results and Discussion

To determine the parameter of the filter walls, use the data [4]. Linear speed of flow u (cm/sec) at a differential pressure on both sides of the filter and viscosity of the liquid partitioning Pauzeyl obeys [4]:

$$u = \frac{a^2}{8 \cdot q \cdot L \cdot \eta} \cdot \Delta P \qquad (5)$$

where a is diameter of capillary, coefficient of curvature q, filter high L, permeable viscosity liquid η and differential pressure ΔP . For used liquid $u = 0,23 sm / s$

In this process, the filtration rate Q through a dense fine-grained (spherical) layer of material is described by Kozeny - Karman [4]:

$$Q = p \cdot S_M \cdot u \qquad (6)$$

where p is section coefficient, specific filter surface area S_M .

Experimental linear velocity calculation filter $Q_E = 0,23 m^3/s$ was performed by the formula:

$$Q_E = \frac{V}{t} \qquad (7)$$

where V is liquid volume of passing through the filter septum during time t.

The results obtained in scientific work, using as a basis the filter glass beads, size 22,5 mm [4] , compared with the experimental and theoretical data obtained in this research work. The comparison results are presented in Table 2.

IV.Conclusion

In the work carried out has been investigated regulation laying ferromagnetic spherical bodies of 0,476 cubic porosity in tetrahedral 0,259, under the influence of the torque constant magnetic field. A relationship was established radial lines cubic laying in the bed of the size of the filter kernel. The characteristics of the laboratory setup for flow rate, filtration rate, and porosity coefficient of curvature coinciding with the theoretical calculated data. The proposed mechanism of cleaning the filter element, which allows to reduce the time of the cleaning work to a minimum.

References

[1] Abbasov, T. \ Magnetic Filtration with magnetized granular beds: Basics principles and filter performance," China Particuology, Vol. 5, 7183, 2007

[2] Aerov M.E., Todes O.M., Thermal hydraulic basics of apprat with stationary and fluidized granular layer . Ed of "Chemistry", 1968 . , 512.

[3] Jordan Hristov \ Magnetic field assisted fluidization - a unified Approach Rev Chem Eng 2012 , 28 (4-6): 243-308.

[4] Holiday D., Resnick R.; Fundamental Phisics, 1976, 930.

[5] Moyer, C.A., M. Natenapit, and S. Arajs, \ Magnetic filtration particles in laminar flow throw a bed of spheres, "J. Magn. Mat., Vol. 44, 99 {104 , 1984 .

[6] Nakagami M. Physical Chemistry membranes : lane. Japanese . - New York: Wiley, 1991 . - 255.

[7] Richard R. Wheeler, Jr., And Goran N. JovanovicMagnetically Assisted Filtration for Solid Waste Separation and Concentration in Microgravity and Hypogravity Thana Sornchamni, James E. Atwater, James R. Akse, Ind. Eng. Chem. Res. 2005 , 44, 9199-9207

[8] Romankov P.G., Kurochkina M.I. Hidromechanical process of chemical technologies. – 3rd: Chemistry, 1982, 288.

[9] Shorstky I.A., Useful invention № RU 2013152099.

MANUFACTURE OF MEALS HIGH DEGREE READINESS AND SPECIAL REQUIREMENTS FOR PACKAGING MATERIALS

M.I. Botov, S.K. Oskolkov

Plekhanov Russian University of Economics

Abstract: *Industrial resource- and energy-saving technology of food raw materials processing for the production of semi-finished products based on the use of continuous mechanized and automated production lines. The mass food production and consumption of frozen food is growing rapidly. Freezing and storage of combined semis at low temperatures is a more complex process. The choice of packaging material determines the way of defrost and heating with minimum power. Microwave heating is popular, but this method also imposes additional special packaging requirements to design and technology. The ultrasonic irradiation of frozen semi-finished product allows to mitigate warming and to align volumetric heating of the product. Promising is application of frozen semi-finished and semi- permeable membrane, for packaging, allowing to harmonize heat- and mass exchange in the surface layers of thawed and warmed up semis.*

Kay words: packaging, packaging materials.

One of the factors limiting production of frozen semi-finished products of high readiness, combined dishes used for food service children in schools and preschools, is the lack of specialty packaging materials that can meet the demands of their storage, defrosting and reheating.

For semi-finished products manufacturing a resource-saving and energy-saving technology for the processing of food raw materials is actually applied, based on the usage of continuous mechanized and automated production lines, equally satisfying basic requirements in catering, and industry [2]. Culinary products processed under these conditions find their use in schools and other educational institutions, where semi-finished products of high readiness are widely common [3].The enterprises of mass production and consumption of food dishes in frozen form are sufficiently rapidly developing. The demand for frozen products due to their high quality and quite lengthy periods of storage grows [1]. However the disadvantages of this system are associated with a limited range of dishes, as well as the high cost of electricity and equipment for freezing, storage at temperatures below - 18 ° C and heating .Production of frozen or refrigerated semi-finished, semi-finished high degree of readiness as well as frozen or refrigerated foods requires special attention when choosing package and packaging materials.

Packaging material must meet the general, well-known requirements: it must be safe, clean and hygienic as long as possible to keep the original properties of prepared meals .However, in the case of semi-finished products of high readiness, these requirements for the packaging should be extended, as they should be performed:

- Cooling, freezing, including deep freeze and semi;

- Long-term storage at low temperatures;

When defrosting:

- On heating to a temperature of implementation.

The first two items of requirements for the use of film packaging materials in modern conditions virtually resolved, at least in part of homogeneous semis packing. Freezing and storage at low temperatures of combined semi-finished products, and in particular , the culinary specialties , as well as complexes of meals - breakfast , lunch and dinner, consisting of culinary products with the use of sauces , spices combined with the toppings – is a much more complicated process. We should take into account within this process the differences in the modes of freezing different products with different trophological properties. The same applies to their storage .

It is particularly difficult to carry out defrosting and heating of precooked and dishes in the package. Packing in this case should retain its strength and tightness and the desired ductility. Chemical changes in the packaging should not lead to the formation of toxic and other hazardous substances. The risk of such transformations is very high, as the chemical aggressiveness of many complex ingredients of semis increases dramatically at heating. For a proper choice of packaging material we should consider how the defrost and reheat is proposed for each semi-finished and allows to obtain a high quality product at the lowest cost of energy.

The most common ways of defrosting are:

- Slow surface heating at ambient temperature;

- Fast surface heating in a water or steam heating medium;

- Fast surface heating in a circulating steam-heatedmedium;

- Intensive volumetric heating in the microwave

field.

These methods of defrosting should be conducted in such a way that preserves the structure and initial biochemical and organoleptic properties of food products. Obviously, for products of animal and vegetable origin, with different water content, fat fraction and other differences, defrosting modes should also be different. General requirements for the heating mode should organically integrate the individual requirements. One of the general packaging requirements, operating in heating mode, is its water resistance. This is due to the fact that in the above-mentioned method of heating any culinary semi- shell packaging interacts with moisture or water vapor formed during the melting and evaporation of moisture from the surface layer. In most cases (except the microwave heating) a heating medium from the outside makes such an effect on packaging.

The microwave heating has become especially popular in recent years. However, this method also imposes additional special packaging requirements.

The first group of requirements is the constructive ones, which should include:

-power constraint defined by magnetron power, and as a consequence, the limit of the loading degree of chambers of the microwave devices ;

-limiting the thickness of the semi-finished product, which depends on the dielectric properties of defrosted product, included in the semis;

-and the inadmissibility metal or metal packaging materials that could cause a short circuit in the magnetron [3].

The second groups of requirements are technological and are associated with various technological requirements for heating mode.

While volumetric heating of food the microwave energy is absorbed unevenly, ie selectively. The most efficiently heated are the zones containing liquid water. However, upon irradiation of the crystalline material that is a frozen food product, a microwave field is practically not absorbed. The unintentionally occurring fusion centers become centers of heat flow and the uneven distribution of the volume can cause rupture of the tissues and significantly change the structure and distribution of moisture in the defrosted product, which can not but have a negative effect on its quality. At local boiling of water in the surface product layer adjacent to the packaging, it possibly occurs a pressure surge that can destroy the packaging envelope and change the structure of culinary products.

The shell itself should be transparent to the microwave field, otherwise the effect described above could be repeatedly reinforced. The ultrasonic irradiation of frozen semi-finished at the first initial stage of defrostation allows to soften heating and flatten the volumetric heating of the product. Ultrasonic treatment allows to shatter the crystal lattice of ice crystal structure and create a variety of fusion centers, uniformly distributed over the volume of the product.

The warming of annealed semi assumes a compliance with all packaging requirements set out for the warm-up mode, as well as a number of additional requirements. It should be noted that in some cases , e.g. in a combi oven for heating at a relatively low humidity of the heating medium , that the temperature of the package may exceed the boiling point , which could lead to its dehydration , and hence can lead to a very undesirable effect – the adhesion to the product. The necessity of increased thermal stability of the packaging material under the specified conditions should be noted. There are some nteresting proposals for the application of composite packaging materials, with special programmable optical properties with respect to the microwave field. It is possible to achieve the effect of heating outpacing the shell to the product using materials that are characterized by a dielectric loss tangent of a slightly larger one corresponding to the parameter of the food product, leading to additional volumetric surface heating and crust formation on the surface defining the organoleptics of a fried product.

One promising trend is the application of semi-permeable and permeable shells for the packing of frozen semi-finished products allowing to harmonize the heat- and mass-exchange in the surface layers of defrosted and warmed up semis and to maintain a high quality of culinary products . Minding the given above, it must be concluded that the choice of packaging for frozen semi-finished high degree of readiness and combined food products and dishes an integral influence on the properties of the packaging material parameters providing storage modes , defrosting and heating , as well as the processes used for this and technical means should be considered.

References

[1] Hanlon, J.F., R.J. Kelsey, and H.E. Forcinio. 1998. Handbook of Package Engineering, 3rd ed. Lancaster, PA: Technomic Publishing.

[2] Кирпичников В.П., Ботов М.И. «Оборудование предприятий общественного питания», Том 2 «Тепловое оборудование», Издательский центр «Академия», М., 2012 г., 390 с.

[3] Рогов И.А., Некрутман С.В., Лысов Г.В. «Техника сверхвысокочастотного нагрева пищевых продуктов», М., «Легкая и пищевая промышленность». 1981 г., 196 с.

MASS FLOW RATE UNDER EXTRUSION OF QUINOA AND GOJI BERRY

M. A. Dushkova, N. G. Toshkov, A. T. Simitchiev, A. Zh. Koleva, K. Balkanski

University of Food Technologies, Bulgaria

Abstract: *In the present investigation the effects of moisture and goji berry's content on the mass flow rate were studied. The increase in moisture content results in extrudates with higher mass flow rate. The increase in goji berry's content leads to a decrease in mass flow rate.*

Keywords: extrusion, mass flow rate, quinoa, goji berry

I. Introduction.

Phenolic plant compounds have been found to exert diverse biological and nutritional effects [11, 14].

In the nineties quinoa has been classified by NASA as an emerging crop with excellent nutritional properties for long term human space missions due to its high content in protein and unique amino acid composition in particular in what respects to lysine and sulfur amino-acids [17]. Quinoa also contains starch, minerals and oils and low amounts of several vitamins and antioxidants [13]. Quinoa leaves contain an ample amount of ash (3,3%), fiber (1,9%), nitrates (0.4%), vitamin E (2.9 mg a-TE/100 g) and Na (289 mg/100 g), vitamin C (1,2–2,3 g/kg) and 27–30 g/kg of proteins [5]. The investigations of Gawlik-Dziki et al. [12] indicate that phenolic ChL compounds of quinoa may exert a chemopreventive and anticarcinogenic effect on oxidative stress and ROS-dependent intracellular signaling via synergic effects. The relatively high potential bioaccessibility and bioavailability of the compounds probably responsible for these effects demonstrates the suitability of ChL for dietary supplementation.

Lycium barbarum L. (L. barbarum) is a Solanaceous defoliated shrubbery that grows in China, Tibet and other parts of Asia and its fruits are 1–2 cm-long, bright orange-red ellipsoid berries [1]. A ripe fruit has been used in Asian countries as a traditional herbal medicine and functional food [7]. Recent studies indicate that extracts from L. barbarum fruit and one of its active compounds, polysaccharides (LBP) possess a range of biological activities, including effects on aging, neuroprotection, anti-fatigue/endurance, increased metabolism, glucose control in diabetics, glaucoma, anti-oxidant properties, immunomodulation, anti-tumor activity and cytoprotection [16]. These were provided daily and changes in subjective ratings of feelings of general well-being, fatigue, stress, neurological/psychological traits, gastrointestinal and musculoskeletal complaints, cardiovascular effects (blood pressure and pulse rate), visual acuity [2], plasma levels of anti-oxidant factors [3], immune factors and any side effects [4] were determined at the end of the treatment period.

Extrusion cooking is used worldwide for the production of expanded snack foods, ready-to-eat breakfast cereals, confectionary and pet food products [8]. Despite increased use of extrusion processes in the food and feed industries, extrusion is still art that has yet to be fully understood with regard to processing variables, ingredient interactions and the effect of material modification on textural properties of the end-products [15].

The aim of this investigation was to study the mass flow rate under extrusion of quinoa meal and dried fruit from goji berry.

II. Materials and methods

Materials

The study was conducted with quinoa meal with an average particle size of 245.3 μm and dried fruit from Goji berry. The fruit was produced in the city Saedinenie, Bulgaria. For its drying, a convective oven at 100^0C was used. After drying, the fruit was milled using a laboratory mixer and mixed with the corn meal as a percentage ratio of 1, 3 and 5%.

Extrusion processing

Extrusion is carried out on a single-screw laboratory extruder Brabender20 DN, Germany [18], with: diameter of the nozzle 3 mm; compression ratio 3:1; speed of the feeding screw 30 min^{-1} and the extruder screw 200 min^{-1}; temperature zones in the extruder were 150, 160 and 170^0C.

Statistical analysis

The full factorial experimental design was used (N=2^2) with three complementary points in the centre of the planning to show interactions of the goji berry's content and the moisture content of the

mixture, in 7 runs (Table 1). All investigated points were obtained with three repetitions.

First-order polynomial model for mass flow rate was obtained using StatGraph v2.0 statistical software:

$$y = B_0 + \sum_{i=1}^{n} b_i X_i + \sum_{i=1}^{n} \sum_{j=1}^{n} b_{ij} X_i X_j \ . \quad (1)$$

Table 1. *Experimental design in natural and coded levels*

№	Natural levels		Coded levels	
	Goji berry's content, %	Moisture content, %	X_1	X_2
1	1	13	-1	-1
2	5	13	+1	-1
3	1	19	-1	+1
4	5	19	+1	+1
5	3	16	0	0
6	3	16	0	0
7	3	16	0	0

Measurement of mass flow rate

The mass flow rate was determined by collecting extrudate samples at 30 sec intervals and then weighing using an electronic balance.

III.   Results and discussion

Table 2 shows the mean values and standard deviation of the mass flow rate. The obtained results show that the mass flow rate varies between 2.58 and 3.03 kg/h.

**Table 2**. *Experimental results of mass flow rate*

№	O, kg/h
1	2,65±0,064
2	2,58±0,116
3	3,47±0,144
4	3,02±0,11
5	3,01±0,029
6	3,01±0,01
7	3,03±0,015

These results are similar with the investigations of Dogan et Karwe [10] under extrusion of quinoa seed using a twin-screw extruder. The following

adequate model at level of significance p=0.05 with significant coefficients was obtained:

$$Q = 2.966 - 0.129X_1 + 0.316X_2 - 0.096X_1X_2 \ . \quad (2)$$

The mass flow rate is main technico-economical parameter which characterizes the work of the extruder. In a single screw extruder it is dependent on the drag flow developed by the rotation of the screw and the pressure developed due to the restriction of the die [9]. The response surface figure shows that the goji berry's content negatively affects the mass flow rate and the moisture content affects it positively. Higher moisture content act like a lubricant and facilitate the flow of the material. The increase in density leads to an increase in mass flow rate. The increase in goji berry's content and the fat content respectively, leads to an increase in mass flow rate but the the complex of amylose and native lipids, which makes the structure more rigid, makes difficult the passage of the material in the extruder. This tendency is more pronounced at high levels of moisture content in comparison with low levels.
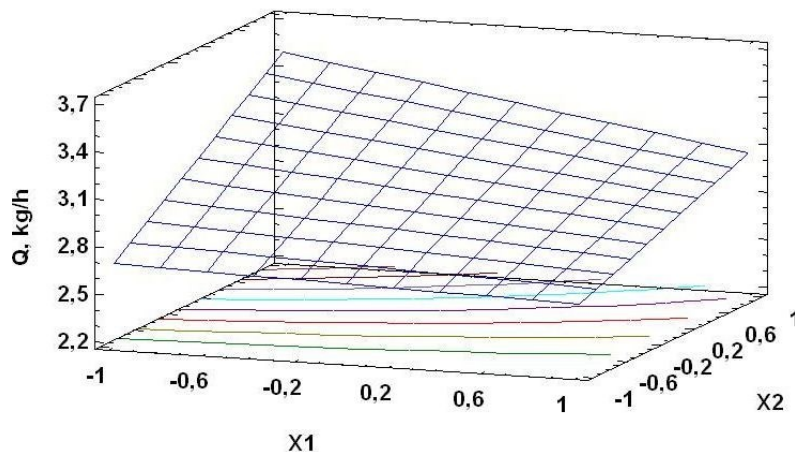
Figure 1. *Response surface for mass flow rate*

IV. Conclusions.

All effects are significant for the mass flow rate. Feed moisture has been found to be the main factor positively affecting the mass flow rate. The Goji berry's content negatively affects the mass flow rate.

References:

[1] Amagase, H., Farnsworth., N. A review of botanical characteristics, phytochemistry, clinical relevance in efficacy and safety of Lycium barbarum fruit (Goji). *Food Research International* 2011, pp. 1702-1717.

[2] Amagase, H., Hsu, C.H.P. Meta-analysis of the general effects of a standardized Lycium barbarum fruit juice shown in randomized, double-blind, placebo-controlled human clinical studies. *FASEB Journal* 2009, 23, pp. 711-716.

[3] Amagase, H., Sun, B., Borek, C. Lycium barbarum (goji) juice shows significant in vivo antioxidant effects in human serum in a randomized, double-blind, placebocontrolled clinical study. *Nutrition Research* 2009, 29, pp. 19−25.

[4] Amagase, H., Sun, B., Nance, M. Immunomodulatory effects of a standardized Lycium barbarum fruit juice in Chinese older healthy human subjects. *Journal of Medicinal Foods* 2009a, 12(5), pp. 1159−1165.

[5] Bhargava, A., Shukla, S., Ohri, D. Chenopodium quinoa—an Indian perspective. *Ind. Crop. Prod.* 2006, 23, pp. 73–87.

[6] Bhatnagar, S., Hanna, M. Amylose-lipid complex formation during single-screw extrusion of various corn starches. *Engineering and processing* 1994, 71(6), pp. 582-587.

[7] Bryan, J.K., D. Costa, N. Giese, K. Nummy, C. Rapp, E. Seamon, et al. Goji (Lycium spp) in natural standardmonograph.*Natural Standard Inc.* 2008.

[8] Burey, P., Bhandari, B.R., Rutgers, R.P.G., Halley, P.J., Torley, P.J. Confectionery gels: a review on formulation, rheological and structural aspects. *Int. J. Food Prop.* 2009, 12 (1), pp. 176–210.

[9] Chevanan, N., Rosentrater, K.A., Muthukumarappan, K. Effect of processing conditions on single-screw extrusion of feed ingredients containing DDGS. *Food Bioprocess Technology* 2010, pp. 111-120.

[10] Dogan, H., Karwe, M.V. Physicochemical properties of quinoa extrudates. *Food science and technology international* 2003, 9(2), pp. 101-114.

[11] Fang, Y.-Z., Yang, S., Wu, G. Free radicals, antioxidants, and nutrition. *Nutrition* 2002, 18 (10), pp. 872–879.

[12] Gawlik-Dziki U., Swieca, M., Sulkowski, M., Dziki, D., Baraniak, B., Czyz, J. Antioxidant and anticancer activities of *Chenopodium quinoa* leaves extracts – In vitro study. *Food and Chemical Toxicology* 2013, 57, pp. 154-160.

[13] Letelier, M.E., Rodriguez-Rojas, C., Sanchez-Jofre, S., Aracena-Parks, P. Surfactant and antioxidant properties of an extract from Chenopodium quinoa Willd. seed coats. *J. Cereal Sci.* 2011, 53, pp. 239–243.

[14] Liu, R.H. Potential synergy of phytochemicals in cancer prevention: mechanism of action. *J. Nutr.* 2004, 134, pp. 3479–3485.

[15] Pitts, K., Favaroa, J., Austinb, P., Day, L. Co-effect of salt and sugar on extrusion processing, rheology, structure and fracture mechanical properties of wheat–corn blend. *Journal of Food Engineering* 2014, pp. 58-66.

[16] Potterat, O. Goji (Lycium barbarum and L. chinense): Phytochemistry, pharmacology and safety in the perspective of traditional uses and recent popularity. *Planta Medica* 2010, 76(1), pp. 7−19.

[17] Schlick, G., & Bubenheim, D. L. Quinoa: An emerging ''New'' crop with potential for CELSS. NASA, Paper 3422, 1993.

[18] Toshkov, N. Investigation of the extrusion of fish feed. (2011). Thesis, UFT, Plovdiv.

MECHANICAL EXPANSION OF OIL SEEDS WITH CARBON DIOXIDE ASSISTED

Z.A. Meretukov, E.P. Koshevoy

Maykop State Technological University,Universitetskaya str. 191, Maykop, Russia;
zamer@radnet.ru;89064387438;
Kuban State Technological University,Moscowskaya str. 2, Krasnodar, Russia
koshevoi@kubstu.ru

Abstract: *The problems of increase of efficiency of extraction of components at processing various on properties of vegetative raw material connected with necessity the increases in depth of extraction caused of expansion range, increases of intensity of processes, decrease in material and power expenses and as development of clear technologies remain actual now.*

In the given work it is offered to pass to carbon dioxide – highly-flying, harmless, accessible and cheap solvent. Except for that carbon dioxide can be completely removed from an end-product that raises its ecological properties and value for the consumer.

In the offered scheme of manufacture of vegetable oil carbon dioxide is used on the closed cycle that provides decrease in expenses for output. It is necessary to note, that carbon dioxide can be applied during extraction of oil in the various phase condition defined by thermodynamic conditions. Thus processes of extraction pass at a low temperature level that increases quality of an end-product.

Keywords: mechanical expansion, oil seeds, extraction, carbon dioxide assisted.

I. Introduction.

The technology of extraction provides deep extraction of target components from the prepared vegetative raw material applying pressing and extraction. The basic problem in extraction of vegetable oils is use of hydrocarbon solvent - gasoline which not only the fire-dangerous and explosive, but also its rests in the taken oil do this product hazardous to health of consumers. In the given work it is offered to pass to carbon dioxide– highly-flying, harmless, accessible and cheap solvent. Except for that carbon dioxide can be completely removed from an end-product that raises its ecological properties and value for the consumer.

In the offered scheme of manufacture of vegetable oil carbon dioxide is used on the closed cycle that provides decrease in expenses for output. It is necessary to note, that carbon dioxide can be applied during extraction of oil in the various phase condition defined by thermodynamic conditions. Thus processes of extraction pass at a low temperature level that increases quality of an end-product.

The offered scheme of manufacture can effectively work at the small, average and large enterprises of reception of oils from vegetative raw material.

Use of dioxide of carbon as a working auxiliary component during extraction of vegetable oils helps to solve a universal problem on its recycling after catching from an atmosphere.

Solution of dioxide of carbon in oil.

Efficiency of the extraction technology of vegetable oils can be essentially increased if to use high solubility carbon dioxide in oil (much greater, than solubility of oil in CO_2), and don't create external volume of solvent, but having received a solution of vegetable oils in carbon dioxide in porous volume of a material and use pressing to its extraction. Such conducting process will sharply reduce quantity of used solvent and intensifies process.

At the first stage considered the questions of change of properties (first of all density and viscosity), a wrung out phase without submission of carbon dioxide and then with its submission.

Properties of density and viscosity of oils are presented by the equations depending on temperature:

$$\rho = \rho_0 - mT \ , \tag{1}$$

$$\mu = \mu_0 \exp(w/T) \ . \tag{2}$$

Experimental data of solubility at temperature 313K for different oils (palm-kernel, linen, cocoa) essentially differing on molecular weight, are presented in Figure 1 with concentration of carbon dioxide in the oils, expressed in mole rate (Stoldt and Brunner, 1998).
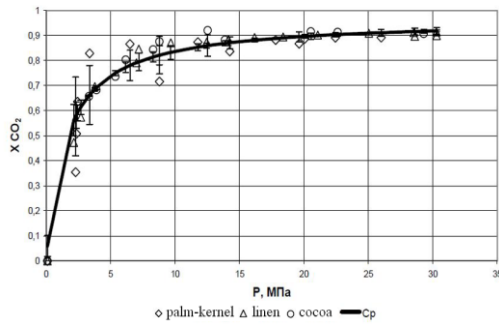
Figure 1: *Solubility CO$_2$ (mole rate) in vegetable oils at temperature 313K.*
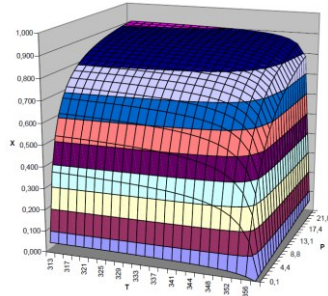
Figure 2: *Solubility CO$_2$ in vegetable oils depending on temperature and pressure.*

Figure 1 shows, that between various oils practically there is no difference on mole solubility in them of carbon dioxide. It is offered to describe this dependence by equation:

$$x(P, MПа)_{CO_2} = \frac{c}{a+b\cdot P} - \frac{c}{a} \qquad (3)$$

As modelling generalization it is used following regressive representation of dependence of solubility from pressure and temperatures:

$$x(P,T) = \frac{c(T)}{a(T)+b(T)\cdot P} - \frac{c(T)}{a(T)} \qquad (4)$$

Considering satisfactory concurrence mole solubilities CO$_2$ for various vegetable oils was modeled with use of dependence (4) concentration floor of mole solubilities CO$_2$ in vegetable oils in a wide range of temperatures and pressure (Figure 2). It is shows, that solubility grows with reduction of temperature and increase in pressure, the limit of growth is marked below 313K and above 20 MPa.

Simplified (without taking into account viscosity of pure carbon dioxide) and exact enough dependence of viscosity of a solution of carbon dioxide in oil looks like:

$$Ln[\mu_{mix}(T,P)] = Ln[\mu_{oil}(T,P_0)] + x_{co2}\cdot Aw_{12}(T,P) \qquad (5)$$

In Figure 3 calculation of change of viscosity of a binary solution from temperature and pressure is presented (on an example of oil of cocoa).

The superficial tension of oil with CO$_2$ defines capillary pressure in pore of a pressing out material, with its reduction capillary pressure which interferes with pressing decreases.
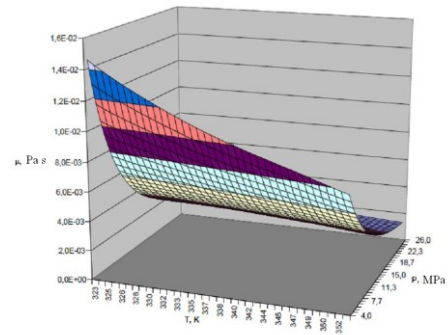
Figure 3: *Dependence of viscosity of a solution of carbon dioxide in oil from pressure and temperature.*

The generalized results of measurements of a superficial tension of oil (on an example of oil of corn germs) in CO$_2$ under various conditions (pressure up to 40 MPa and temperature from 40 up to 120°C) from density CO$_2$ are presented in Figure 4 and described by the equation:

$$\sigma(\rho_{CO_2}) = 27.37533\cdot\exp(-0.003685\cdot\rho_{CO_2}) \qquad (6)$$
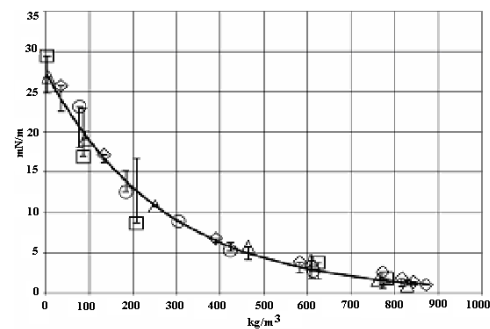
Figure 4: *Dependence of an interphase tension of oil in contact to CO$_2$ as function of density dioxide of carbon.*

We mark, that for a solution of oil with CO$_2$ at workers pressure and temperature the interphase tension decreases for the order.

II. Modeling of change of factor a pressure-conductivity from parameters of pressing.

For transition from normalized pressure, to consideration of change of pressure-conductivity factor in a real interval of pressure of process of the pressing, changing within the limits of an interval of pressure from «point of oil» which is defined as the minimal pressure u_{min}, necessary for occurrence of free oil on a surface of an olive material, up to the

maximal pressure in press $\mathbf{u}_{max}$ in view of presence of a moisture in a pressed out material that will allow to lower essentially expenses for pressing out oils from an oleaginous material, value of factor becomes:

$$c(u)=\frac{c_0}{1+\exp\left[-\left(a\cdot\dfrac{u-5.24\cdot\exp\left[0,0011(w_0^{2,4}+11,5)\right]}{u_{max}-5.24\cdot\exp\left[0,0011(w_0^{2,4}+11,5)\right]}-b\right)\right]} \quad .(7)$$

For carrying out of experimental researches filtrational and the compressional properties of an oleaginous material and definition of character of change of a degree of pressing out and limiting oleaginous from technological parameters, was used a known technique of pressing of a material in thermo-static metal cylinder established in the machine of compression.

The received set of factors is similar and corresponds to invariant change of dependence of pressure-conductivity factor from relative pressure (Figure 5) which defined on a parity:

$$U=1-\frac{u_0-\overline{u}(t)}{u_0-u_{pm}} \quad . \tag{8}$$
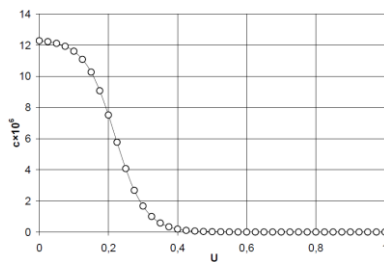
Figure 5: *Change of factor pressure-conductivity at use of the generalized vector of parameters of model*

Apparently from the presented data (Figure 6) process of pressing in these experiences is presented by three modes: initial with high pressure-conductivity factor, transitive and final with low factor pressure-conductivity.
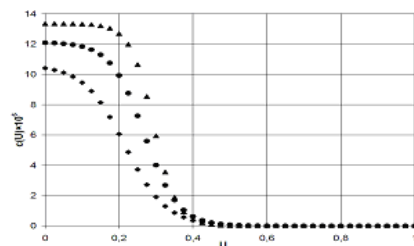
Figure 6: *Change of factor pressure-conductivity from pressure in parallel experiences of pressing of sunflower pressure 56MPa, temperature 105⁰C, humidity of 11,44 %, thickness of a layer of a material of 50 mm.*

It is obvious, that with a sufficient degree of approach it is possible to consider possible the description of this process in the form of two-zone models with corresponding step function of change of factor of permeability from pressure (Meretukov and Koshevoy, 2012).

Influence initial a material and decrease in humidity of an olive material has appeared complex. Obtained data have defined a conclusion, that variability of pressure-conductivity factor is rather great, therefore procedure of construction regress equations has been based on a tentative estimation of regress factors of dependences. As a result of identification of parameters of model it has been established, that the offered regress models adequately describe change of pressure-conductivity factor depending on olive of material, pressure, temperature, height of a layer of a material and its humidity.
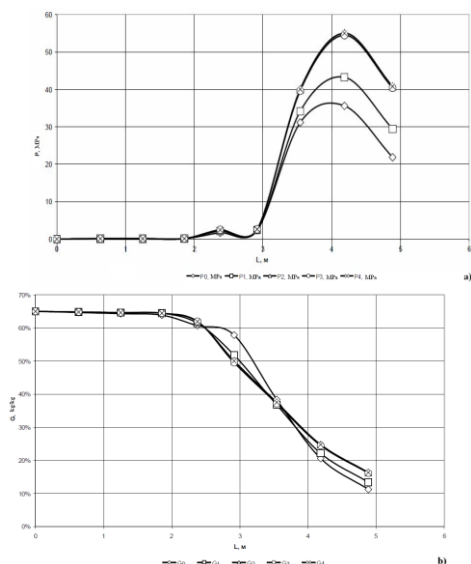
In the further the decision to increase extrapolation accuracy of parametrical model due to inclusion of data of pressing with dioxide of carbon was accepted, having received dependence for comparison purposes for clear pressing and pressing with preliminary saturation CO_2.

For construction of model of change of pressure-conductivity factor from parameters of process of pressing in view of saturation by dioxide of carbon the experimental data received at studying kinetics of pressing of an oleaginous material have been analysed (on an example of sesame, flax, rape, beans of cocoa, liquor of cocoa) from six key parameters - olive of material (Gbg=0,44÷0,56), pressure (Pbg=30÷60 MPa), temperatures (Tbg=40÷100 °C), heights of a layer of a material (Hbg=15÷45 mm), its humidity (Wbg=0,5÷8 %) and mole rate CO_2 (x_{CO2}=0÷0,9). As a result of carrying out of the regress analysis of these data have been received corresponding regress equations (Meretukov and Koshevoy, 2012):

$$(9)$$

$$(10)$$

$$Kp(Gbg, Pbg, Tbg, Hbg, Wbg) := \begin{vmatrix} kp \leftarrow \exp \left[\cdots \right] \cdot gY_2 \\ kr \leftarrow Kmin \ \text{if} \ kp < Kmin \\ kr \leftarrow Kmax \ \text{if} \ kp > Kmax \\ kr \leftarrow kp \ \text{if} \ [(kp \geq Kmin) \wedge (kp \leq Kmax)] \\ kr \end{vmatrix} \tag{11}$$

The received models have a high degree of adequacy, except for that these models have an initial appearance that raise the interpolation property of model.

Thus, the offered equations and the found parameters allow to predict change of pressure-conductivity factor an oleaginous material over a wide range of parameters of process of pressing with dioxide of carbon, and without use in a usual mode.

III. Modelling of process of pressing.

For modelling of process of pressing in the screw press we use the equation of process pressing oils (G_O) from an oleaginous material (G_X) average on a layer of this material (Lp) during pressing (τ):

$$G_0(\tau, a_P, b_P, K_P, L_P) = \frac{\int_0^{L_P} G_X(x, \tau, L_P, K_P, a_P, b_P)dx}{L_P} \tag{12}$$

The equation (12) includes parameters (K_p, a_p, b_p) dependences pressure-conductivity an oleaginous material during process of the pressing, defining kinetics this process and courses of this process depending on conditions. Definition of these parameters probably on generalized regress dependences, for process without use of carbon dioxide, and on corresponding dependences in case of its use.

The basic characteristic of work of the screw press alongside with residual oleaginous is productivity. The axial stream of the pressed material considered as non-Newton liquid, in the screw press on each separately taken coil was described by the equation:

$$Qx = \pi \cdot D \cdot W \cdot (H - \delta) \cdot N \cdot \cos(\theta) \cdot \frac{fd}{2} - \frac{H^3 \cdot W \cdot fpd \cdot fps}{12 \cdot n \cdot \mu s} \cdot \frac{dP}{dx} \tag{13}$$

During transportation inside in press there is a decrease olive of material, that essentially influences for it rheology. The defining parameter of current non-Newton liquids is speed of shift. For definition of speed of shift of a material on coils used following dependence:

$$\gamma_o(N, i) = \pi \cdot \frac{D_3(i) \cdot N \cdot \cos[\Theta_B(i)]}{H_B(i)} \tag{14}$$

This parameter is used for definition of effective viscosity of a transported oleaginous material:

$$\mu(G_m, T_m) = k_\mu \cdot [\gamma_o(N, i)]^{n_\mu - 1} \cdot \exp(-a_\mu \cdot G_m) \cdot \exp\left(\frac{b_\mu}{T_m}\right) \tag{15}$$

Current volumetric productivity can be certain on a difference between initial volumetric productivity on a pressed material (Q_H) and volumetric productivity on the wrung out oil (Q_K), that enables to define the pressure developed during pressing (P_K):

$$P_K(\tau, N, K_c, n_\mu, p_{BH}, p_{BK}, G_M, T_{m}, i) := \frac{Q_H(N, n_\mu, p_{BH}, p_{BK}, G_M, T_{m}, i) - Q_K(\tau, N, K_c, n_\mu, p_{BH}, p_{BK}, G_M, T_{m}, i)}{B_0(N, n_\mu, G_M, T_{m}, i)} \cdot L_{\Pi_i} \tag{16}$$

In connection with available distinctions in properties of different oleaginous materials, value absolute limiting olive and character of its change alongside with parameters of pressing will depend by nature pressed material.

Change of pressure and olive on length of the press channel at initial M_H=50 % is presented in Figure 7.

Figure 7: *Distribution on the press channel for 50 % of initial concentration of the olive phase. a) pressure; b) oleaginous.*

Similar calculations have been lead for model with addition to pressed material CO_2 and presented in figure 8 (Meretukov and Koshevoy, 2012).

It is possible to note an initial significant site of length screw shaft on which at submission CO_2 there is no rise of pressure and accordingly does not occur process of pressing. Then sharp rise of pressure with the subsequent pressure decrease in cone zone is marked.

Thus, at submission CO_2 in an oil phase with other equal, there is deeper pressing out an olive material, in view of removal CO_2, final oleaginous has decreased on 6÷12%.

Figure 8: *Distribution on the press channel for 65 % of initial concentration of the olive phase containing 0,9 mole CO_2. a) pressure; b) oleaginous.*

IV. Modelling of supercritical extraction of a vegetative oleaginous material.

At mathematical modelling supercritical extraction of a layer of a vegetative oleaginous material (sunflower) in view of features of dissolution of oil in carbon dioxide data on kinetics of extraction was used from which it is visible, that the initial stage is characterized by the constant speed defined by solubility and charge CO_2.

Each experimental curve E=q (t)/q_0 - dependence of the attitude of the current maintenance of oil in extraction material from time to its initial maintenance - can be presented by two sites - the period of constant speed and the period of falling speed. Thus, for the description kinetics of extraction it is possible to offer two-zone model (Meretukov Z. et al, 2012).

The generalized kinetic curve with the equations of two-zone model is presented in Figure 9. Accuracy of the equations is high.

$$E_1(t \cdot N) = 1 - 1,0115 \cdot (t \cdot N^{LIN}); \quad R^2 = 0,99872 \quad (19)$$

$$E_2(t \cdot N) = 0,96234 \cdot \exp[-1,38621(t \cdot N^{LIN})]; \quad R^2 = 0,97484 \quad (20)$$

The basic received result of application of preliminary pressing is an opportunity of reduction of duration of process of extraction.
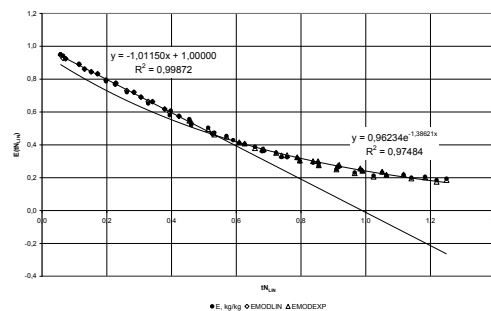
Figure 9: *Generalized kinetic curve with the equations of two-zone models by results of experiences.*

V. Conclusions

Technologies of extraction of vegetable oils with the carbon dioxide based on greater solubility in oil, than oils in carbon dioxide are perspective.

The density and viscosity of solutions of carbon dioxide in oil influence on pressing process. Volumetric expansion of a solution is connected with change of density and its greatest value (in particular 50%) is reached at high pressures (P=25MPa) and low temperatures (T=323 K). Thus the interphase tension decreases on the order. With growth of pressure and temperatures viscosity of solutions of carbon dioxide in oil decreases.

At pressing out vegetative materials the description of the phenomena of carry of pressure for small time intervals in the big interval of change of pressure, is connected with necessity of the account of dependence of pressure-conductivity factors from pressure.

At generalization of dependence on extraction kinetic from pressure and temperature the proved kinetic dependence with parameters of speed of complex extraction process an oleaginous material carbon dioxide the screw pre-extractor which is wringing out a material with impregnation by carbon dioxide is received.

References

[1] Stoldt J., Brunner G. Phase equilibrium measurements in complex systems of fats, fat compounds and supercritical carbon dioxide. Fluid phase equilibria, 1998, vol.146, pp.269-295.

[2] Meretukov Z., Koshevoy E. 2012, Physical-chemical mechanic of pressing of oleaginous materials. Russia, Krasnodar, Publishing House-South. (in Russian)

[3] Meretukov Z., Koshevoy E., Kosachev V. 2012, Mathematical model of mass transfer at supercritical extraction of oleaginous materials by dioxide of carbon. New technologies. № 3.-p. 39-44, (in Russian).

Nutrilab
food labelling

European Union

European Social Fund
Human Resources Development Operational Programme
Ministry of Education and Science
Investing in your future

European Social Fund

Journal of
FOOD and PACKAGING
Science, Technique and Technologies

National Academy of Packaging-Bulgaria